

MATERIALI IN TEHNOLOGIJE	LETNIK VOLUME	40	ŠTEV. NO.	6	STR. P.	225–285	LJUBLJANA SLOVENIJA	NOV.-DEC. 2006
-----------------------------	------------------	----	--------------	---	------------	---------	------------------------	-------------------

VSEBINA – CONTENTS**PREGLEDNI ZNANSTVENI ČLANKI – REVIEW ARTICLES****Plazemska sterilizacija bakterij s kisikovo plazmo**

Oxygen plasma sterilization of bacteria

D. Vujošević, Z. Vranica, A. Vesel, U. Cvelbar, M. Mozetič, A. Drenik, T. Mozetič, M. Klanjšek-Gunde, N. Hauptman 227

IZVIRNI ZNANSTVENI ČLANKI – ORIGINAL SCIENTIFIC ARTICLES**A comparison of experimental results and computations for cracked tubes subjected to internal pressure**

Primerjava eksperimentalnih rezultatov in izračuna za cevi z razpoko, ki so obremenjeni z notranjo razpoko

J. Capelle, I. Dmytrakh, J. Gilgert, Ph. Jodin, G. Pluviniage 233

Fatigue problems of transmission belts: a viscoelastic analysis of the strain-accumulation process

Problem utrujanja pogonskih jermenov: viskoelastična analiza procesa akumuliranja deformacije

I. Emri, J. Kramar, A. Nikonorov, U. Florjančič, A. Hribar 239

A micro-macro analysis of the tool damage in precision forming

Mikro-makroanaliza poškodb orodja za natančno kovanje

T. Rodič, J. Korelc, A. Pristovšek 243

The stability of cast alloys and CVD coatings in a simulated biomass-combustion atmosphere

Stabilnost zlitin in CVD-prevlek v simulirani atmosferi zgorevanja biomas

D. A. Skobir, M. Spiegel 247

Nastanek LaCrO₃ med zgorevalno sintezoLaCrO₃ formation during combustion synthesis

K. Zupan, M. Marinšek, S. Pejovnik, T. Hrobart 253

Dinamične mehanične lastnosti elastomernih kompozitov s polnili nanovelikosti

Dynamic mechanical properties of elastomeric composites with nano-scale fillers

Z. Šušterič, T. Kos, M. Šuštar 257

Fracture toughness of a high-strength low-alloy steel weldment

Žilavost loma zvara visokotrdnega malolegoranega jekla

J. Tuma, N. Gubeljak, B. Šuštaršič, B. Bundara 263

Solidification and fracture of an as-cast Ni alloy

Strjevanje in prelom lite nikljeve zlitine

M. Torkar 269

STROKOVNI ČLANKI – PROFESSIONAL ARTICLES**Laboratory accreditation – confidence in the activities of conformity assessment of products**

Laboratorijska akreditacija- zaupanje v aktivnost ocene ustreznosti proizvodov

A. Klobodanović, M. Oruč 273

LETNO KAZALO, LETNIK 40, 2006 – INDEX, VOLUME 40, 2006 277

PLAZEMSKA STERILIZACIJA BAKTERIJ S KISIKOVIM PLAZMO

OXYGEN PLASMA STERILIZATION OF BACTERIA

Danijela Vujošević¹, Zoran Vranica¹, Alenka Vesel², Uroš Cvelbar²,
Miran Mozetič², Aleksander Drenik², Tatjana Mozetič³, Marta Klanjšek-Gunde⁴,
Nina Hauptman⁴

¹Center za medicinsko mikrobiologijo, Inštitut za zdravje Crne gore, Ljubljanska bb, 8100 Podgorica, Črna gora

²Laboratorij za plazmo F4, Institut "Jožef Stefan", Jamova 39, 1000 Ljubljana, Slovenija

³Srednja zdravstvena šola, Poljanska 61, 1000 Ljubljana, Slovenija

⁴Kemijski inštitut, Hajdrihova 19, 1000 Ljubljana, Slovenija

alenka.vesel@ijs.si

Prejem rokopisa – received: 2006-08-16; sprejem za objavo – accepted for publication: 2006-11-13

Prikazane so osnovne značilnosti reaktivnih plazem in njihova uporabnost za sterilizacijo različnih materialov. Kisikova plazma uničuje in razgraje mikroorganizme (tj. bakterije) z UV-sevanjem, kemijsko razgradnjo in lokalnim ogrevanjem. V prispevku kratko opisemo vse tri načine delovanja plazme na mikroorganizme in ugotavljamo primernost različnih metod za sterilizacijo zraka in trdih materialov s poudarkom na sterilizaciji biokompatibilnih materialov. Pri uporabi sterilizacije s kisikovo plazmo se moramo zavedati nekaterih omejitev in težav, ki pri tem nastopajo.

Ključne besede: sterilizacija, plazma, kisik, bakterija, spore

The main reactive plasma characteristics are presented with their applications for sterilization of different materials. Oxygen plasma destroys and erodes microorganism with UV radiation, chemical reactions and local heating. Tree mechanisms of interaction with microorganism are described. Advantages of plasma sterilization for air sterilization and solid materials including biocompatible materials are discussed, baring in mind the limitations and disadvantages of the same method.

Key words: sterilization, plasma, oxygen, bacteria, spore

1 UVOD

Sterilizacija različnih materialov je eden od najstarejših problemov v medicini in biologiji. Zdravniki so že v starem veku ugotovili, da se rane celijo veliko hitreje, če obveze in podobni material pred uporabo izpostavijo sončnemu obsevanju. Mnogo pozneje so ugotovili, da komplikacije pri poškodbah povzročajo določeni mikroorganizmi. Ti so lahko plesni, bakterije in virusi. Za učinkovito zdravljenje poškodb bolezni in napak je treba zagotoviti sterilnost uporabljenih materialov. Tako kot je raslo znanje o povzročiteljih okužb, je raslo tudi znanje o preprečevanju okužb. Ugotovljeno je bilo, da je za preprečitev okužb ključnega pomena uničenje mikroorganizmov, ki okužbe povzročajo. Iz tega spoznanja se je rodila panoga, ki jo danes imenujemo sterilizacija. Sterilizacija pomeni popolno uničenje vseh mikroorganizmov, ki so ali bi lahko bili na določenem materialu. Ker prav vseh mikroorganizmov pogosto ni mogoče uničiti, danes velja nekoliko blažji standard: material je steriliziran, če je koncentracija mikroorganizmov na določenem materialu zmanjšana za faktor 10⁶. Sterilizacija je večni problem medicine, saj mnogih materialov preprosto ne moremo sterilizirati. Primer je npr. medicinska postelja. V zadnjem času je problem sterilizacije postal še posebej pereč ne le zaradi potencialnih groženj teroristov z biološkim orožjem, ampak tudi zaradi uvajanja novih materialov, ki niso primerni za sterilizacijo s klasičnimi postopki. Na tem

mestu omenjamo predvsem različne biokompatibilne materiale, ki se že danes uporabljajo v sodobni medicini, kot so različne proteze in implanti, in katerih uporaba se bo v naslednjih letih in desetletjih v razvitih državah še močno povečala.

Znanost o sterilizaciji je torej z novimi zahtevami in grožnjami dobila nove izzive, katerim se klasični postopki za sterilizacijo ne morejo postaviti po robu. Popolnoma jasno je, da bo treba razviti nove, učinkovite metode za sterilizacijo različnih trdnih materialov, pa tudi plinov, skupaj z zrakom.

Za sterilizacijo se sedaj največ uporablja termična in kemična metoda. Pri termični sterilizaciji izpostavimo vzorce visoki temperaturi – navadno za prenos topote uporabimo vodno paro, ki je segreta na okoli 130 °C. Voda je odličen medij za prenos topote, saj je izparilna toplota izredno visoka. Tekočo vodo s primernim grelnikom uparimo, pare pa se potem kondenzirajo na površini vzorcev, pri čemer se sprosti izparilna toplota. Tako je prenos topote bistveno hitrejši, kot če bi ogrevali vzorce s suhim zrakom. Pomanjkljivost metode je prav visoka temperatura – mnogi materiali je ne prenesejo. Predstavljam si samo, da bi poskusili s to metodo sterilizirati živila – vzorci bi se preprosto skuhalo. Prav tako metoda ni primerna za sterilizacijo velikih prezračevalnih sistemov, saj jih je praktično nemogoče ogreti na 130 °C.

Druga metoda je kemična. Vzorce izpostavimo zelo strupenemu plinu. Najboljši je etilen dioksid. Pri tem ni

treba vzorcev dodatno ogrevati, saj je plin izredno strupen in deluje že pri sobni temperaturi. Tudi ta metoda ni primerna za sterilizacijo prezračevalnih sistemov, ker bi poleg bakterij pomrla še vsa druga bitja, ki bi prišla v stik s plinom. Takšne nesreče so se že zgodile tudi v bolnišnicah.

Sterilizacijo lahko dosežemo tudi z različnimi sevanji. Na voljo so vsa sevanja, katerih osnovni kvanti imajo zadostno energijo – večjo od 4 eV. Pri elektromagnetnem sevanju lahko uporabimo UV-, X- in γ -žarke. V praksi se največ uporablja UV-sevanje, saj poznamo močne izvire: nizkotlačne plazme. Poleg elektromagnetnega sevanja lahko uporabimo tudi curke hitri delcev. Največ se uporablajo elektroni, pospešeni do energije okoli 1 MeV. Sterilizacijo s sevanjem največ uporabljajo v živilski industriji, medtem ko za uničevanje bakterij v večjih sistemih ni primerna, saj je s to metodo praktično nemogoče enakomerno obdelati velike površine.

V zadnjem času so raziskovalci ugotovili, da bi lahko prednosti termičnega, kemijskega in sevalnega načina sterilizacije združili tako, da bi kot sterilizacijski medij uporabili plazmo. Plazma je namreč močan izvir UV-sevanja, obenem pa v njej nastajajo z vidika mikroorganizmov zelo strupeni radikali, ki so bolj ali manj kratkoživi.

2 PLINSKA PLAZMA

Plinska plazma je stanje plina, v katerem v splošnem ne veljajo osnovni zakoni plinske termodinamike (**slika 1**). To pomeni,

- da temperatura kot termodinamska veličina sploh ni definirana;
- da je poprečna kinetična energija plinskih delcev ("kinetična temperatura") za različne delce v plinu različna;
- da je poprečna porazdelitev stanj plinskih delcev ("notranja temperatura") za različne delce v plinu različna.

Na Zemlji takšnega stanja plina ni najti, lahko pa ga ustvarimo v laboratorijih. Najpogostejša metoda za prehod plina v stanje plazme je električna plinska razelektritev. Plini pri navadnih pogojih sicer ne prevajajo električnega toka, pri določenih okoliščinah pa steče skozi plin tok, ki je posledica migracije elektronov in plinskih ionov med elektrodama. To se najpogosteje zgodi pri plinu pri nizkem tlaku med dvema elektrodama. V električnem polju med elektrodama se pospešujejo tako elektroni kot pozitivni ioni, vendar pa pozitivni ioni pri elastičnih trkih z molekulami plina izgubijo preveč energije, da bi lahko sodelovali pri vzdrževanju plazme. Pozitivni ioni v razelektritvi tako skrbijo le za prostorski naboj, ki preprečuje hitro difuzijo elektronov na stene posode, medtem ko elektroni pri trkih z molekulami povzročajo prehod plina v stanje plazme. Elektroni pri trkih z nevtralnimi molekulami povzročajo reakcije, ki so za primer kisika prikazane na tabeli 1.

Tabela 1: Prikaz najpomembnejših reakcij, ki potekajo v kisikovi plazmi

Table 1: Some most important reactions in the oxygen plasma

$O_2 + e^- \rightarrow O_2^+ + 2e^-$	$O + e^- \rightarrow O^+ + 2e^-$
$O_2 + e^- \rightarrow O^+ + O + 2e^-$	$O + e^- \rightarrow O^* + e^-$
$O_2 + e^- \rightarrow O^+ + O^+ + 3e^-$	$O^* + e^- \rightarrow O^+ + 2e^-$
$O_2^+ + e^- \rightarrow O^+ + O + e^-$	$O_2 + e^- \rightarrow O_2^* + e^-$
$O_2 + e^- \rightarrow O + O + e^-$	$O_2 + e^- \rightarrow O_2^- + 2e^-$
$O_2^+ + e^- \rightarrow O + O$	$O_2^+ + O_2^- \rightarrow O_3 + O$

Posledica prevajanja električnega toka skozi plin je torej vzbujanje molekul v visoka vzbujena stanja. Pogosto se zgodi, da v plazmi sploh niso prisotne plinske molekule, temveč prevladujejo disociirana (nascentni kisik) in ionizirana stanja. Plazme, v katerih je koncentracija navadnih molekul O_2 precej manjša od koncentracije vzbujenih delcev, imenujemo reaktivne plazme. Povprečna notranja energija plinskih delcev v reaktivnih plazmah pogosto dosega več elektron-voltov, kar ustreza povprečni notranji temperaturi delcev okoli 50.000 °C!

3 OSNOVNI MEHANIZMI STERILIZACIJE S PLAZMO

S plazemske sterilizacijo so se pričeli ukvarjati šele pred dobrim desetletjem¹. Prvi poskusi so bili opravljeni z vodikovim peroksidom. Očitno gre torej za mehak prestop iz čiste kemijske sterilizacije v kombinirano plazemske. Vodikov peroksid je močan oksidant in je že sam brez plazme dober sterilizant. Plazmo so uporabili predvsem za detoksifikacijo sistema po opravljeni sterilizaciji s peroksidom.

Kasneje so se raziskavam pridružili kemiki in fiziki, in plazemska sterilizacija je doživelva nov zagon. Za začetek so ugotovili, da lahko podobne ali boljše uspehe kot s peroksidom dosežejo z različnimi popolnoma netoksičnimi plini: voda, kisik, vodik, argon, helij, dušik. Ugotovili so, da je hitrost in učinkovitost sterilizacije močno odvisna od plazemskih parametrov, kot so temperatura elektronov, gostota pozitivnih in negativnih ionov, gostota metastabilnih atomov in molekul, vrsta in koncentracija radikalov...

Danes je plazemska sterilizacija ena najbolj intenzivnih raziskovalnih področij²⁻¹⁵. Oglejmo si osnovne mehanizme, ki omogočajo sterilizacijo v plazmi.

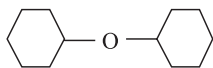
3.1 Radiacijske poškodbe. Plazma je močan izvir UV-sevanja. Absorpcija UV-žarkov v tkivu povzroča razpad kompleksnih organskih molekul in s tem počasno uničevanje živega tkiva. Z UV-obsevanjem pa je žal težko odstraniti razpadne produkte, ki so lahko tudi toksični. Radiacijske poškodbe povzroča tudi obstreljevanje vzorcev z energijskimi ioni, vendar pa je značilna kinetična energija ionov prenizka, da bi ioni prodrli skozi bakterijsko ovojico.

3.2 Kemijske poškodbe. Plazma je vir različnih vzbujenih molekul in radikalov, ki so kemijsko zelo aktivni.

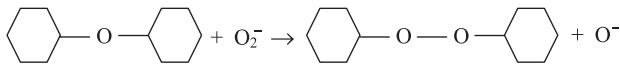
Kot primer si oglejmo kisikovo plazmo. V njej nastajajo pozitivni in negativni ioni, enoelktronsko vzbujene molekule, ozon in nevtralni kisikovi atomi. Nekateri delci (npr. negativni ioni) se kemijsko vežejo na kompleksne organske molekule in povzročajo njihov razpad na manjše molekule. Nevtralni kisikovi atomi se navadno ne vežejo na molekule, ampak povzročijo takojšnjo oksidacijo. Reakcijski produkt je CO ali H₂O, ki se v vakuumu desorbirata s površine. Proses je podoben gorenju, le da poteka oksidacija že pri sobni temperaturi.

3.3 Termične poškodbe. Mnogi plazemski delci imajo precejšnjo potencialno energijo. Pri relaksaciji delcev na površini se sprošča precejšnja energija. Druga, še pomembnejša metoda ogrevanja bakterije je oksidacija s kisikovimi atomi (glej zgornjo alinejo), ki je izredno eksotermska reakcija. Zato bakterija v reaktivni plazmi v hipu (pogosto manj kot v 1 s) preprosto zgori. Težje je ogreti bakterije v porah in na drugih nedostopnih mestih.

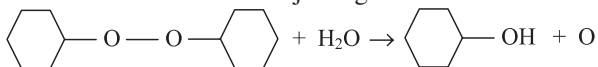
Podrobneje si oglejmo primer kemijskega jedkanja bakterijske ovojnici v kisikovi plazmi. V zunanjem ovoju endospor so ogljikovi obroči vezani s kisikovo vezjo:



Anionski radikal O₂⁻ iz plazme reagira s kisikovo vezjo:



Nastala struktura nadalje reagira z molekulo vode:



Kompleksna molekula tako razpade na dve manjši. Nastali kisikov atom lahko spet reagira z negativnim ionom, kar bi lahko pomenilo vzdrževanje cikla, dokler se atomi ne bi izgubili pri kakšni drugačni reakciji. Razmerje med številom razcepljenih vezi in adsorbičnih radikalov O₂⁻ naj bi bilo po trditvi nekaterih avtorjev (Ref 13) kar od 100 do 1000. Morebiti so avtorji spregledali še kakšno drugo možnost cepitve vezi, vsekakor pa opisani primer lepo ponazarja kemijsko plazemske razgradnjo celične stene mikrobov.

Oglejmo si še primer termičnega uničevanja mikrobov v plazmi. Temperatura plina je sobna, ogrevamo le bakterije. V prvem približku vzamemo bakterijo za oval, ki je nameščen na podlagi. V tem primeru je toplotni stik med bakterijo in podlago zanemarljiv. Bakterijo obdelajmo s plazmo, kakršno sicer uporabljamo za razmaščevanje elektronskih komponent in plazemske aktivacijo^{16,17}. Gre za visoko disociirano kisikovo plazmo, ki jo ustvarimo v radiofrekvenčni (RF) ali mikrovalovni (MW) razelektritvi. Gostota toka kisikovih atomov (*j*) na površino bakterije je reda 10²⁴ m⁻² s⁻¹. Verjetnost za

oksidacijo¹⁸ (reakciji C_{org} + O → CO in 2H_{org} + O → H₂O) je pri sobni temperaturi med 0,01 in 0,1. Z indeksom "org" smo označili organsko vezan ogljik in vodik. Reakciji sta eksotermski – energija, ki se sprosti, je skoraj 10 eV na kisikov atom. Gostota energijskega toka (*P*) je torej:

$$P = j \cdot \eta \cdot W$$

kjer je *j* gostota toka delcev na površino bakterije, *η* verjetnost za oksidacijo in *W* sproščena energija na atom, ki reagira na površini. Z vstavitvijo numeričnih vrednosti dobimo:

$$P = 10^{24} \text{ m}^{-2} \text{ s}^{-1} \times 0,01 \times 10^{-18} \text{ J} = 10^4 \text{ W m}^{-2}$$

Sprememba notranje energije bakterije je enaka produktu gostote energijskega toka in površine bakterije, enaka pa je tudi produktu mase, specifične toplotne kapacitete in sprememb temperature bakterije:

$$\Delta W = P \cdot S = m \cdot c_p \cdot \Delta T / \Delta t$$

Sprememba temperature bakterije v časovni enoti je torej:

$$\Delta T / \Delta t = (P \cdot S) / (m \cdot c_p) = 10^4 \text{ K/s}$$

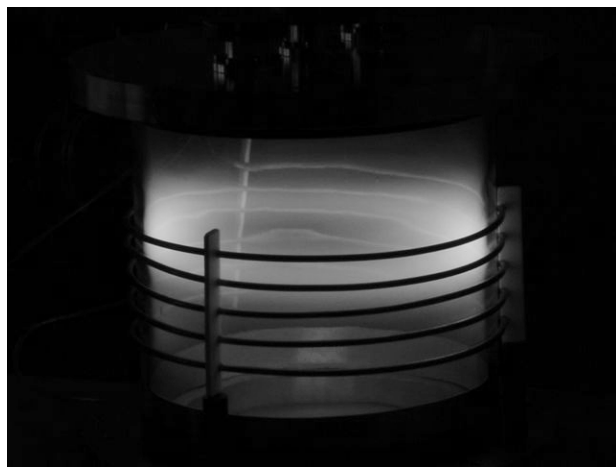
Pri tem smo vzeli za površino bakterije *S* = 1 μm², maso *m* = 10⁻¹⁵ kg in specifično toplotno kapaciteto *c_p* = 1000 J kg⁻¹ K⁻¹.

Izoliranim bakterijam na gladki podlagi se torej v kisikovi plazmi slabo piše. Bakterije, ki lebdijo v plinu, s plazmo uničimo že v nekaj stotinkah sekunde, za tiste na podlagi pa potrebujemo več časa. Pri zgornjem izračunu smo namreč predpostavili, da je bakterija toplotno izolirana, v resnici pa je površina, s katero se dotika podlage, vendarle končno velika. Termično uničevanje bakterij s kisikovo plazmo je torej odlična metoda, če so bakterije dobro izpostavljeni plazmi. Pri tem velja še enkrat omeniti, da je okolica na sobni temperaturi. Ogrevamo samo bakterije.

Žal se mnoge bakterije zadržujejo v režah, kjer je toplotni stik s podlago boljši, predvsem pa je v režah težko zagotoviti zadostno koncentracijo atomov kisika. Zaradi tega je značilni čas za sterilizacijo v kisikovi plazmi reda velikosti ene ure.

4 KRITIČNA OCENA PLAZEMSKA STERILIZACIJE

Sterilizacija biokompatibilnih materialov zaenkrat tehnološko še ni zadovoljivo rešena. Tudi raziskave s plazemske sterilizacijo teh materialov še niso privedle do komercializacije tega postopka. Bistvena težava je v tem, da je s plazemskega vidika biokompatibilni material zelo podoben mikroorganizmom, ki jih je treba uničiti. Če je plazma zadosti agresivna, da lahko jedka mikroorganizme, je navadno tudi dovolj agresivna, da jedka podlago. V tem smislu samo kemijsko jedkanje ne more prinesi zadovoljive sterilizacije. Tudi samo UV-sevanje ni posebej primerno za sterilizacijo biokompatibilnih materialov, saj poškoduje tudi podlago. Zaradi tega je sedaj večina raziskav za sterilizacijo biokompatibilnih

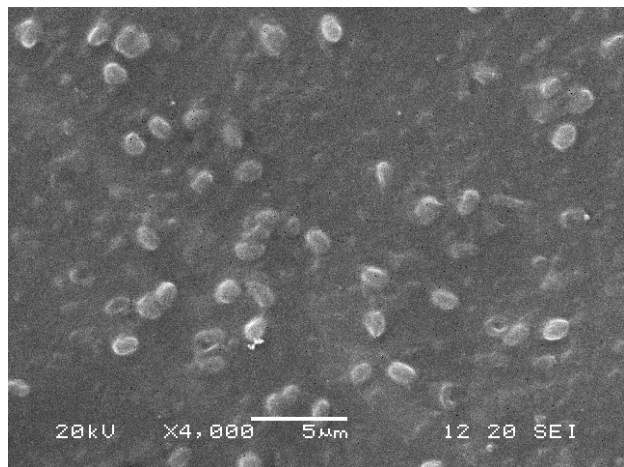


Slika 1: Primer kisikove plazme, ki nastane z radiofrekvenčnim vzbujanjem v steklenem reaktorju 30 l

Figure 1: An example of RF oxygen plasma created in a glass reactor with the volume of 30 l

materialov s plazmo osredinjena na kombinirano delovanje vseh treh bistvenih načinov sterilizacije s plazmo. Biokompatibilni materiali imajo pogosto dovolj gladko površino, da je termični stik med bakterijami in površino razmeroma slab (**slika 2**). Zaradi tega lahko v splošnem računamo, da je temperatura bakterije večja od podlage. Pri povišani temperaturi postane pomembno kemijo jedkanje. Znano je namreč, da je hitrost oksidacije organskih materialov z nekaterimi plinskim radikalim močno odvisna od temperature. Že nekoliko (reda nekaj 10 °C) povišana temperatura lahko povzroči porast verjetnosti za oksidacijo tudi za več velikostnih redov.

Sterilizacija biokompatibilnih materialov se zaplete, če imamo na površini tanko plast, na kateri so bakterije (**slika 3**). Neposredna hladna sterilizacija ni mogoča, saj se z jedkanjem bakterij na površini dogaja tudi erozija tanke plasti, ki je navadno bolj odporna proti eroziji z atomi. Posledice zelo kratke obdelave površine so

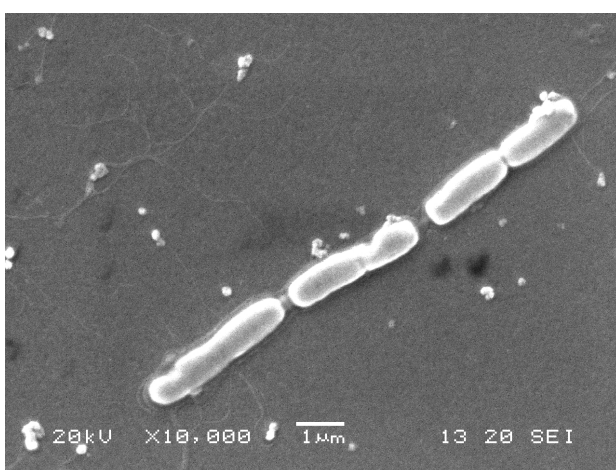


Slika 3: Spore "Bacillus subtilis" na podlagi v tanki plasti

Figure 3: Spores of *Bacillus subtilis* on the substrate

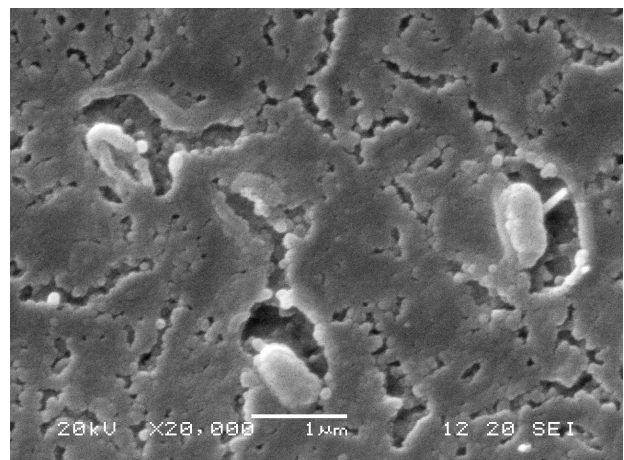
prikazane na **slikah 4** in **5**, kjer se poleg ovojnici bakterije prične degradacija plasti. Če je plast debelejša, se sorazmerno poveča dolžina obdelovanja, ki lahko traja tudi več ur. Razlog za to je izogibanje lokalnemu segrevanju, ki ga povzročajo rekombinacije delcev na površini. Ker temperatura za polimerne materiale, iz katerih so narejeni nekateri implantati, ne sme presegati temperature 100 °C, je treba reakcije omejevati s hlajenjem plinskega toka molekul, ki v vakuumski posodi odnašajo odvečno toploto s površine. Zaradi tega smo omejeni na pulzno delovanje, pri čemer hladimo vzorec v intervalih.

Plazemsko sterilizirani vzorci imajo po sterilizaciji povečano površinsko energijo, kjer so na površini nastale polarne in razcepljene vezi, ki so dovetne za vezavo katerega koli materiala. To je zelo ugodna lastnost za vezavo materiala z tkivi, ki se takšnega materiala bolje oprimejo.



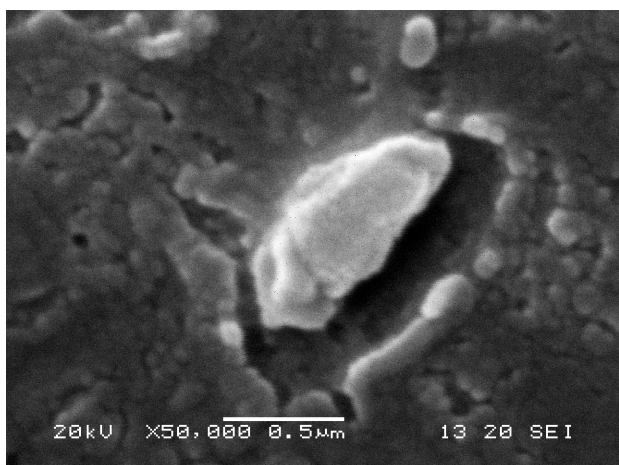
Slika 2: Aktivna bakterija *Bacillus subtilis* slikana z elektronskim mikroskopom (SEM) pri 10.000-kratni povečavi

Figure 2: SEM picture of an active bacteria *Bacillus subtilis*



Slika 4: Slika spor "Bacillus subtilis" po uničenju s kisikovo plazmo pri obdelavi s 5 pulzi po 10 s

Figure 4: SEM picture of the spores of *Bacillus subtilis* after being destroyed by the oxygen plasma treatment in 5 pulses for 10 s



Slika 5: Povečava spore, ki kaže učinkovitost kisikove plazme pri eroziji ovojnici spore, kjer jedkamo pretežno s kisikovimi atomi

Figure 5: SEM picture of one spore showing the efficiency of oxygen plasma treatment. The spore's protective layer is eroded by its etching mainly with the oxygen atoms created in the plasma

Bistvene raziskave, ki danes potekajo v svetu na temo plazemske sterilizacije, so namenjene ugotavljanju vpliva plazemskih parametrov na hitrost sterilizacije in na poškodovanje biokompatibilnih materialov. V idealnem primeru bi plazma popolnoma uničila bakterije, podlaga pa sploh ne bi bila poškodovana. Idealne rešitve verjetno ne bomo nikdar dosegli, lahko pa se idealu približamo s pravilno izbiro plazemskih parametrov. Pri tem mislimo predvsem na primerno koncentracijo različnih plazemskih radikalov. Znano je namreč, da različni radikali različno reagirajo z mikroorganizmi in podlagami. Težava je le v tem, da je na današnjem nivoju znanja zelo težko individualno spremenjati koncentracije radikalov. Če želimo npr. povišati koncentracijo ionov, se navadno poveča tudi koncentracija atomov in vzbujenih molekul.

Možna rešitev je posredna uporaba plazme. Namesto plazme, ki vsebuje različne radikale, uporabimo stanja plina po prehodu skozi plazmo. Splošni izraz za takšna stanja plina je "afterglow". Plin vodimo najprej skozi plazmo, da dosežemo visoko koncentracijo vseh radikalov. Pozneje pa s katalizo na izbranih površinah relaksiramo samo določene radikale, druge pa pustimo bolj ali manj nedotaknjene. Tako lahko v končni fazi pridobimo takšno stanje plina, v katerem imamo praktično samo eno vrsto radikalov. Žal je tudi poznanje selektivne relaksacije plazemskih radikalov na površinah še vedno izredno pomanjkljivo.

Pri sterilizaciji mikroorganizmov s plazmo nastopa še vrsta težav, ki se v literaturi redko omenja. Na tem mestu omenjamo samo najpomembnejše: (1) zagotavljanje enakomernosti plazme, (2) generiranje plazme v porah, (3) toksični plini v plazmi in (4) toksični plini kot reakcijski produkti.

Ker je hladna plazma neravnovesno stanje plina, je praktično nemogoče zagotoviti homogenost plazme v celotnem plazemskem reaktorju. Posledica tega je

neenakomernost sterilizacije. Področja, kjer je plazma močnejša (vsebuje več radikalov ali pa je energija radikalov povečana) se hitro sterilizirajo, področja, kjer je plazma šibkejša, pa se sterilizirajo počasneje. Tisti predeli, kjer je sterilizacija že potekla, so brez potrebe izpostavljeni radikalom, ki pogosto povzročajo neželene spremembe tudi na materialih, ki jih steriliziramo. Področja, izpostavljeni šibkejši plazmi, pa se sterilizirajo počasneje in lahko tudi po dolgotrajni izpostavi plazmi vsebujejo žive mikroorganizme ali vsaj spore. Problem nehomogenosti plazme je izredno pereč in sedaj še ni zadovoljive rešitve. Večina plinskih razelektritev, s katerimi je mogoče generirati plazme, namreč ustvarja nehomogeno plazmo ali pa plazmo z nezadovoljivo koncentracijo radikalov. To je posledica osnovnih procesov v plinskih razelektritvah, v katere se na tem mestu ne spuščamo. Da bi premostili problem nehomogenosti, so raziskovalci po svetu razvili različne razelektritve, ki omogočajo vsaj približno enakomernost plazme. Pri nizkih tlakih je plazma v marsikateri razelektritvi približno enakomerna, vendar pa vsebuje premajhno gostoto radikalov za uspešno sterilizacijo. Druga skrajnost je uporaba plazme pri navadnem zračnem tlaku, kjer je koncentracija radikalov zadostna, razmeroma hladno plazmo pa je sicer mogoče generirati z enosmerno ali nizkofrekvenčno razelektritvijo z dielektrično pregrado (angleško: dielectric-barrier glow discharge), vendar pa je takšna plazma pogosto nehomogena, vselej pa izrazito neizotropna in s tega vidika popolnoma neuporabna za sterilizacijo predmetov z zapleteno obliko. Večina raziskovalcev zato išče rešitve v uporabi razelektritev pri grobem vakuumu, kjer je plazma za silo izotropna in vsebuje zadostno koncentracijo radikalov. Ker plazma vselej vsebuje ionizirane delce, ki s prostorskim nabojem zastirajo električno polje, so za generiranje plazme z visoko koncentracijo radikalov pri grobem vakuumu najprimernejše visokofrekvenčne razelektritve, pri katerih je omogočeno približno enakomerno vzbujanje radikalov po celotnem volumnu. Sedaj je najbolj perspektivna radio-frekvenčna induktivno sklopljena razelektritev, ki jo uporabljam tudi v naših laboratorijih.

Generiranje plazme v porah ali ozkih režah je težava, na katero so opozorili fiziki, davno preden so se pojavile prve ideje o sterilizaciji materialov s plazmo. Plazma namreč slabo prodira v pore. Značilno se koncentracija radikalov hitro zmanjšuje z globino pore. Za to sta odgovorna dva procesa: majhna koncentracija energijskih radikalov v porah, kar vodi k zmanjšanju generiranja radikalov, in relaksaciji radikalov na notranjih stenah por. Prvi pojav je mogoče popolnoma izničiti z uporabo dodatne razelektritve, ki delujejo po principu votle katode: v pori, ki jo nabijemo negativno proti plazmi, se zaradi prostorskega naboja ustvari močan radialni gradient električnega polja, ki povzroči nihanje elektronov v pori. Posledica tega je lokalna ojačitev plazme, ki lahko izniči pojave, ki sicer preprečujejo normalno koncentracijo radikalov. Če so materiali, ki jih nameravamo sterilizirati, električno prevodni, lahko z

dodatno razelektritvijo z votlo katodo dosežemo odlične rezultate. Težava je v tem, da večina materialov, ki jih želimo sterilizirati s plazmo, ni električno prevodna. V teh primerih si z razelektritvijo z votlo katodo ne moremo prav nič pomagati. Delno lahko pojavi ojačitve plazme v porah izolatorjev nadomestimo z uporabo radiofrekvenčnega nabijanja materiala, kar pa je sedaj še vedno v fazi znanstvenih eksperimentov. Navadno radiofrekvenčno nabijanje ne vodi k pojavi ojačitve razelektritve v votli katodi.

Naslednja težava pri plazemski sterilizaciji je značilnost vseh plazem. V njih vselej nastajajo toksični plini. Vrsta takšnih plinov in njihova koncentracija je vselej odvisna od vrste plazme. V čisti kisikovi plazmi ne najdemo posebej toksičnih plinov. Izjema je ozon, katerega koncentracija je odvisna od vrste razelektritve. Koncentracija ozona v kisikovi plazmi lahko doseže prostorninski delež 10 %, kar je več velikostnih redov nad dovoljeno koncentracijo. V tehnikočkih procesih je navadno težko doseči obdelavo materialov s čistim kisikom. Četudi je zagotovljena laboratorijska čistota kisika iz jeklenke (več kot 99,999 %), je v procesni komori vselej residualna atmosfera, ki pogosto vsebuje dušik in vodno paro. V plazmi kisik reagira z obema plinoma in tvori dušikove okside in vodikov peroksid. Posebej to velja za razelektritve pri navadnem zračnem tlaku, kjer je vsaj delno mešanje kisika z zrakom običajen pojav.

Pri plazemski sterilizaciji poleg plinov, značilnih za plazmo v nečistem kisiku, nastajajo tudi drugi radikali, ki so lahko bistveno bolj toksični od ozona, dušikovih oksidov in vodikovega peroksidu. Interakcija kisika z ogljikovodiki (ki so pretežna sestavina živih bitij) je navadno nepopolna oksidacije: namesto CO₂ (ki je produkt popolne oksidacije) večinoma nastaja CO, ki je toksičen plin. Poleg obilice vodikovega peroksidu, ki je prav tako posledica nepopolne oksidacije ogljikovodikov, nastajajo med plazemsko oksidacijo organskih materialov tudi nekateri drugi toksični plini. Poleg dušikovih oksidov so to lahko bolj kompleksne molekule, kamor spada tudi vodikov cianid, poleg tega pa tudi žveplov oksid in podobni plini. Plazemska obdelava organskih snovi torej lahko vodi k sintezi različnih plinov, ki so večinoma toksični, vendar pomenijo nizek volumenski delež (manj od 10 %). Težava je še večja pri uporabi zraka za sterilizacijo. V tem primeru je koncentracija različnih (pogosto zelo toksičnih) plinskih molekul, ki vsebujejo C, N, H in druge elemente, lahko velika.

Plazemska sterilizacija torej kot večina plazemskih procesov vodi k sintezi različnih toksičnih plinov in radikalov. Le-ti se delno absorbirajo v vakuumski črpalki (če proces poteka v pri znižanem tlaku), v splošnem pa bi lahko postali resen problem. Z uporabo katalizatorjev za toksične pline je mogoče ta problem bistveno zmanjšati ali celo odpraviti¹⁹.

5 SKLEP

Opisali smo osnovne mehanizme sterilizacije s plazmo. Plazemska sterilizacija temelji na termičnih, kemijskih in radioloških efektih. V vsakem primeru lahko najdemo dovolj agresivno plazmo, s katero steriliziramo poljubne materiale. Težava nastopi tedaj, ko želimo sterilizirati temperaturno občutljive biokompatibilne materiale. V tem primeru je treba izbrati takšno plazmo, ki je dovolj reaktivna, da uniči bakterije, vendar še vedno dovolj nežna, da ne poškoduje podlage. Zaradi nasprotnosti obeh zahtev je takšno plazmo pogosto zelo težko generirati, in to je verjetno razlog, zaradi katerega plazemska sterilizacija še ni komercializirana.

Zahvala

Ta članek je rezultat skupnega dela slovenskih in črnogorskih raziskovalcev pri projektu BI-SCG/04-05-št. 28 v okviru SLO-CG znanstveno-tehničnega sodelovanja.

6 LITERATURA

- ¹ M. C. Krebs, P. Becasse, D. Verjat, J.C. Darbot, *Int. J. Pharm.*, 160 (1998), 75–81
- ² M. Mozetič, T. Mozetič, P. Panjan, *Vakuumist*, 21 (2001), 10–12
- ³ A. Vesel, M. Mozetič, *Vakuumist*, 23 (2003), 9–14
- ⁴ W. Bar, G. M. de Bar, A. Naumann, S. Rusch-Gerdes, *Amer. J. Infec. Contr.*, 29 (2001), 306–311
- ⁵ M. Moisan, J. Barbeau, S. Moreau, J. Pelletier, M. Tabrizian, L. H. Yahia, *Int. J. Pharm.*, 226 (2001), 1–21
- ⁶ S. D. Ferreira, W. S. Dernell, B. E. Powers, R. A. Schuchet, C. A. Kuntz, S. J. Withrow, R. M. Wilkins, *Clin. Orth. Rel. Res.*, 388 (2001), 233–239
- ⁷ M. Moisan, J. Barbeau, J. Pelletier, *Du Vide*, 56 (2001), 15–28
- ⁸ S. Cariou-Travers, J. C. Darbord, *Du Vide*, 56 (2001), 34–46
- ⁹ P. Koulik, S. Krapivina, A. Saitchenko, M. Samsonov, *Du Vide*, 56 (2001), 117–125
- ¹⁰ D. A. Mendis, *Physica Scripta T89* (2001), 173–175
- ¹¹ C. E. Holy, C. Chen, J. E. Davies, M. S. Shoichet, *Biomater.*, 22 (2001), 25–31
- ¹² R. Ben Gadri, J. R. Roth, T. C. Montie, K. Kelly-Wintenberg, P. P. Y. Tsai, D. J. Helfritch, P. Feldman, D. M. Sherman, F. Karakaya, Z. Y. Chen, *Surf. Coat. Technol.*, 131 (2000), 528–542
- ¹³ A. Kakligin, P. Koulik, S. Krapivina, G. Norman, E. Petrov, A. Ricard, M. Samsonov, *Proc. 13th Int. Coll. Plasma Processes*, (2001), 28–32
- ¹⁴ T. K. Subramanyam, R. Schwefel, P. Awakowitz, *Proc. 13th Int. Coll. Plasma Processes*, (2001), 33–36
- ¹⁵ M. Moisan, J. Barbeau, J. Pelletier, N. Philip, B. Saoudi, *Proc. 13th Int. Coll. Plasma Processes*, (2001), 12–18
- ¹⁶ A. Vesel, M. Mozetič, *Vacuum*, 61 (2001), 373–377
- ¹⁷ D. Babič, I. Poberaj, M. Mozetič, *Rev. Sci. Instr.*, 72 (2001), 4110–4114
- ¹⁸ M. Mozetič, A. Zalar, P. Panjan, M. Bele, S. Pejovnik, R. Grmek, *Thin Solid Films*, 376 (2000), 5–8
- ¹⁹ M. Mozetič, G. A. Evangelakis, U. Cvelbar, *Plazemska sterilizacija pretočnega zraka*, SI21448. Urad za intelektualno lastnino Republike Slovenije (2004)

A COMPARISON OF EXPERIMENTAL RESULTS AND COMPUTATIONS FOR CRACKED TUBES SUBJECTED TO INTERNAL PRESSURE

PRIMERJAVA EKSPERIMENTALNIH REZULTATOV IN IZRAČUNA ZA CEVI Z RAZPOKO, KI SO OBREMENJENI Z NOTRANJO RAZPOKO

Julien Capelle¹, Igor Dmytrakh², Joseph Gilgert¹, Philippe Jodin¹, Guy Pluvinage¹

¹Laboratoire de Fiabilité Mécanique, ENIM & Université de Metz, Île du Saulcy F-57045 Metz cedex, France

²Karpenko Physico-Mechanical Institute of National Academy of Sciences of Ukraine, (KPhMI), Department of Physical Fundamentals of Fracture and Strength of Materials, Lviv, Ukraine
jodin@univ-metz.fr

A cylindrical pipe that is used for gas transportation is mainly submitted to stresses originating from internal pressure. Other stresses are due to weight and the unexpected movements of supports and/or the ground. The first give rise to circumferential stresses, the second to longitudinal bending stresses. Here, we study the case of pipes that are joined by welding. This weld is an eventual source of defects, where cracks can originate. But there are other kinds of defects that can come from corrosion pits or accidental notches caused by diving machines, or in the case of work on the pipe. In this last case, the notch corresponds to a reduction of the section, which is enhanced by the stress-concentration factor. The objective of this work is to compare the prediction of finite-element computations with fracture experiments on such notched pipes. The results are given in terms of stress-concentration factors and show some discrepancy with the experimental results. As the mechanical properties have been measured on standard plane specimens, a transfer problem to curved structures is suspected to be at the origin of the difference, because with the dimensions of the pipe it is not possible to have standard and curved specimens in the same direction of rolling, and the mechanical properties of this pipe are different in the circumferential and transverse directions.

Key words: pressure pipe, notch fracture mechanics, transferability

V valjasti cevi za pretok plina so napetosti zaradi notranjega pritiska. Druge napetosti nastanejo zaradi gravitacije in nepričakovanih premikov podpor ali zemljišča. Prve napetosti so obodne, druge pa podolžne in upogibne. V tem delu obravnavamo primer cevi, ki so povezane z varjenjem. Zvar je eventualni vir napak, na katerih nastanejo razpoke. Druge vrste napak lahko nastanejo zaradi koroziskih zajed ali odrgnin, ki jih povzročijo gradbeni stroji ali nastanejo že pri izdelavi cevi. V tem primeru zarezta ustrezajo zmanjšanju prereza, napetost pa je povečana zaradi zarezne koncentracije napetosti. Cilj tega dela je primerjava napovedi na podlagi izračuna z metodo končnih elementov s preizkusi preloma cevi z napako. Rezultati izračunov, ki so predstavljeni v obliki faktorja intenzitete napetosti, se ne ujemajo popolnoma z rezultati preizkusov. Ker se mehanske lastnosti določijo pri standardnih ravninskih preizkušancih, predpostavljamo, da je vzrok za razliko prenos na ukrivljeno strukturo. Zaradi izmer cevi ni mogoče izdelati standardnih in ukrivljenih preizkušancev v enaki smeri valjanja in so mehanske lastnosti cevi drugačne v obodni kot v prečni smeri.

Ključne besede: cev pod pritiskom, mehanika loma, prenos

1 INTRODUCTION

The computation of circumferential stress, also called hoop stress, in cylindrical pipes subjected to internal pressure is well known, and the general relationship is given as follows:

$$\sigma_{\theta} = \frac{p_i \cdot r}{t} \quad (1)$$

where σ_{θ} is the hoop stress, p_i is the internal pressure, r is the radius of the tube and t is the thickness of the tube. This relationship is valid if $t \leq r/10$, in other cases the relationship (1) is corrected as:

$$\sigma_{\theta} = \frac{a^2 \cdot p_i}{(b^2 - a^2)} \cdot \left[1 + \left(\frac{b^2}{r^2} \right) \right] \quad (2)$$

where a is the internal radius, b is the external radius, r is the radius of the computed point in the cylinder wall and p_i is the internal pressure.

These relationships are accurate enough to design pressure pipes if no defect is present in the tube. But, if the tube is realized by welding, misalignment or lack of penetration can occur, or if there are corrosion pits, or if the diving equipment causes damage to the external envelope of the tube, a reduction of section occurs and the stress is increased as a consequence. However, the reduction of section is not the only effect that causes a stress increase, and the notch-concentration-factor effect brings the majority of the increase. The objective of this work was to compute the actual hoop stress when an external notch is present and to compare with a fracture test under gas pressure that was made with the three coded methods, i.e., the ASME B31 G, the modified ASME B31 G and the DNV RP-F101. This work is based on a study of the pipeline and has resulted in several publications and presentations at international congresses ^{1,2}.

2 CODED METHODS

2.1 ASME B31 G³

This is a code for evaluating the remnant strength of corroded pipelines. It is a supplement of the ASME B31 code for pressure piping. The code was developed in the late nineteen-sixties and early seventies at the Battelle Memorial Institute and provides a semi-empirical procedure for the assessment of corroded pipes. Based on an extensive series of full-scale tests on corroded pipe sections, it was concluded that line pipe steels have an adequate toughness and that the toughness is not a significant factor. The failure of blunt corrosion flaws is controlled by their size and the flow stress or yield stress of the material. The input parameters include the pipe's outer diameter (D_{ext}) and the wall thickness (t), the specified minimum yield strength (SMYS), the maximum allowable operating pressure (MAOP), the longitudinal extent of corrosion ($2c$) and the defect depth (a). According to this code, a failure equation for the corroded pipelines is proposed by means of the data from a bursting experiment and expressed by considering the two conditions below:

- First, the maximum hoop stress cannot exceed the yield strength of the material.
- Second, short corrosion defects are projected with a parabolic shape, and long corrosion defects are projected with a rectangular shape on the shape of a rectangular one (**Figure 1 and 2**).

The failure pressure equation for a corroded pipeline with a parabolic defect is:

$$\sqrt{0.8 \left(\frac{2c}{D_{ext}} \right)^2 \left(\frac{D_{ext}}{t} \right)} \leq 4 \quad (3)$$

$$P_{ult} = \frac{2 \cdot (1.1\sigma_y) \cdot t}{D_{ext}} \cdot \left[\frac{1 - 0.66(a/t)}{1 - 0.66(a/t)/M} \right] \quad (4)$$

with $M = \sqrt{1 + 0.8 \left(\frac{2c}{D_{ext}} \right)^2 \left(\frac{D_{ext}}{t} \right)}$ (5)

M is the so-called bulging factor.

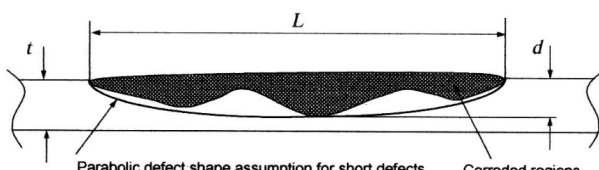


Figure 1: Corrosion defects projected with a parabolic shape
Slika 1: Koroziske poškodbe, predstavljene s parabolično obliko

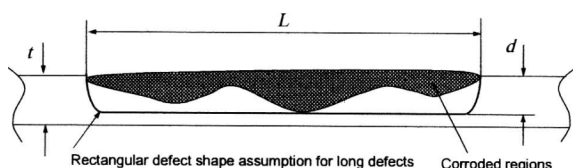


Figure 2: Corrosion defects projected with a rectangular shape
Slika 2: Koroziske poškodbe, predstavljene s pravokotno obliko

2.2 Modified ASME B31 G

This includes the modified flow stress and the bulging factor. The flow stress σ_{ult} is taken as:

$$\sigma_{ult} / \text{MPa} = 1.1\sigma_y + 69 \quad (6)$$

where σ_y is the yield strength.

Two cases are considered:

$$\text{Case 1} \quad \left(\frac{2c}{D_{ext}} \right)^2 \left(\frac{D_{ext}}{t} \right) \leq 50 \quad (7)$$

$$P_{ult} = \frac{2 \cdot (1.1\sigma_y + 69) \cdot t}{D_{ext}} \cdot \left[\frac{1 - 0.85(a/t)}{1 - 0.85(a/t)/M} \right] \quad (8)$$

The bulging factor is equal to:

$$M = \sqrt{1 + 0.6275 \left(\frac{2c}{D_{ext}} \right)^2 \left(\frac{D_{ext}}{t} \right)} - 0.003375 \left(\frac{2c}{D_{ext}} \right)^4 \left(\frac{D_{ext}}{t} \right)^2 \quad (9)$$

$$\text{Case 2} \quad \left(\frac{2c}{D_{ext}} \right)^2 \left(\frac{D_{ext}}{t} \right) > 50 \quad (10)$$

$$P_{ult} = \frac{2 \cdot (\sigma_{ult}) \cdot t}{D_{ext} - t} \cdot \left[\frac{1 - (a/t)}{1 - (a/t)/Q} \right] \quad (11)$$

The bulging factor is equal to:

$$M = 3.3 + 0.032 \left(\frac{2c}{D_{ext}} \right)^2 \left(\frac{D_{ext}}{t} \right) \quad (12)$$

It is necessary to recall that the ASME B31G is limited to low stress-concentration factors and internal pressure loading conditions.

The assessment procedure considers the maximum depth and the longitudinal extent of the corroded area, but ignores the circumferential extent and the actual profile. If the corroded region is found to be unacceptable, B31G allows the use of a more rigorous analysis or a hydrostatic pressure test in order to determine the pipe's remaining strength. Alternatively, a lower maximum allowable operating pressure may be imposed.

2.3 DNV RP-F101⁴

This is the first comprehensive and extensive code on pipeline-corrosion defect assessment. It prepares guidance on the pipeline under internal pressure and combined loading. Furthermore, it provides a codified formulation for pressure and bending and area depth. DNV RP-101 proposes two methods to find the failure pressure.

The first method is named the partial safety factor, and the second is classified as the allowable stress design. The allowable-stress-design method that considers non-interacting defects is discussed here. To pursue the design procedure via DNV RP-101 it is necessary to determine the loading type (pressure only

and combined loading), and consequently the failure pressure can be obtained as:

$$P_{\text{ult}} = \frac{2\sigma_{\text{ult}}t}{D_{\text{ext}} - t} \cdot \left[\frac{1 - (a/t)}{1 - (a/t)/Q} \right] \quad (13)$$

where Q is the correction factor:

$$Q = \sqrt{1 + 0.31 \left(\frac{1}{\sqrt{D_{\text{ext}}t}} \right)} \quad (14)$$

According to this code, the failure pressure should not exceed the maximum allowable stress design operating pressure (MAOP); otherwise, the corroded pipe will have to be repaired or replaced before returning to service.

3 FINITE-ELEMENT COMPUTATION

3.1 Meshing the model

The model tube is a rolled steel cylindrical pipe with an external diameter of 219.1 mm and a thickness of 6.1 mm. A quasi-semi-ellipsoidal notch represents an accidental external defect. The major axis of the ellipsoid is parallel to the axis of the tube and the length of the notch is 30.5 mm.

The depth of the notch is 3.05 mm and the width is also 3.05 mm. The radius of the notch tip is 0.15 mm, as shown in **Figures 3 and 4**.

As the defect has two perpendicular planes of symmetry, only a quarter of the whole structure was meshed. A schematic view of the notched tube is given in **Figure 4**. For our computations, the CAST3M pro-

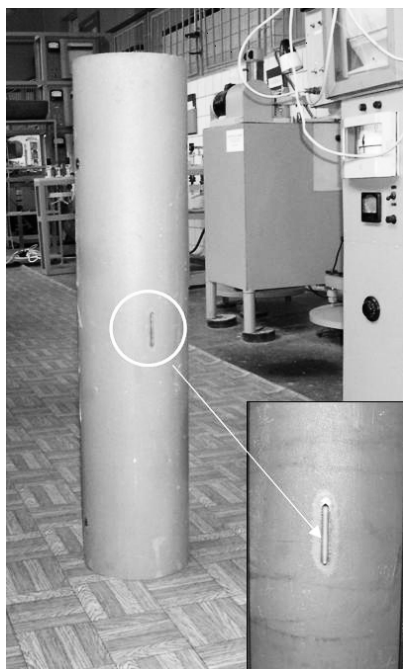


Figure 3: Notch on the pipe

Slika 3: Zareza na cevi

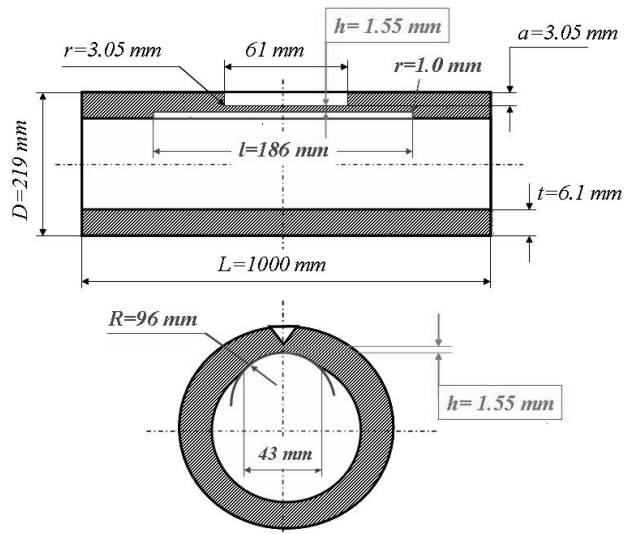


Figure 4: Plan of the grinding part

Slika 4: Načrt brušenja

gramme was used. Such a structure is not very easy to model exactly, as the very small notch-tip radius implies very strong geometrical constraints.

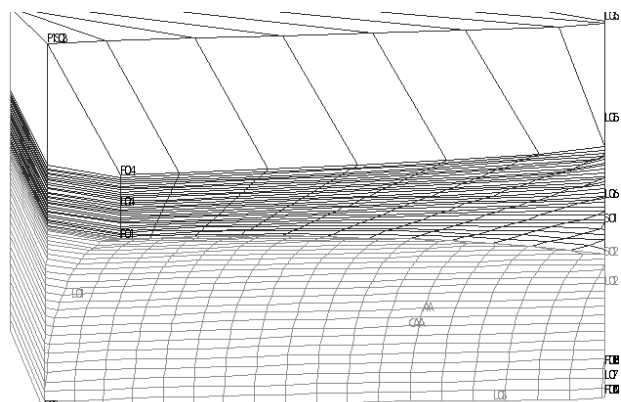
Figure 5 shows the mesh of an ellipsoidal notch with the approximate notch radius. Due to the program's constraints, simple linear elements were used.

3.2 Boundary conditions and loading

As the model represents a quarter of the whole structure, and no pressure effect on the ends is assumed, symmetrical boundary conditions were applied on each section of the models. The loading is applied as a 15 MPa uniform pressure on the internal face of the tube.

3.3 Material behaviour and properties

The material constituting the tube is rolled steel. A Young's modulus of 203000 MPa was deduced from previous tests on a "Roman-tiles-type" specimen ⁵.



The yield strength was estimated to be 528 MPa. The Ludwik's law will make it possible to introduce the actual behaviour of the steel into its plastic range, where the hardening parameter is $n = 0.0446$, and the resistance coefficient is $K = 587.3$ MPa.

$$\sigma = K \varepsilon_p^n \quad (15)$$

3.4 Post-processing of results

The results of the computations were given in terms of the hoop stress distribution on the ligament surface between the notch tip and the inner surface of the tube. The figures were obtained with the help of the home-made SCILAB® programme.

4 RESULTS

4.1 Finite-element computations

The results are shown in **Figure 6**. The hoop stress field is represented over the mesh where it is computed. The hottest point is on the small axis of the ellipsoid. But the hoop stress does not take into account the degree of triaxiality, when the ligament is reduced, just under the small axis of the ellipse. Consequently, the Von Mises stress was computed and represented in **Figure 7**. It is clear that if the stress level far from the notch is about the same as the hoop stress at the same place, the stress along the notch tip and, particularly at the deepest point of the notch, is much higher.

For comparison, the hoop stress is computed using the relationships (1) and (2). The results are the following:

- (1): hoop stress at mid thickness: 174.6 MPa
- (2): hoop stress at inner face: 174.7 MPa
- (2): hoop stress at outer face: 164.7 MPa

From the FE computation (**Figure 8**) we can extract the values of the hoop stress on the outer face, far from the notch, 148.5 MPa, and on the inner face, 189.9 MPa. The value at the mid thickness is, therefore, 169.2 MPa. This value is quite similar to that obtained for the usual

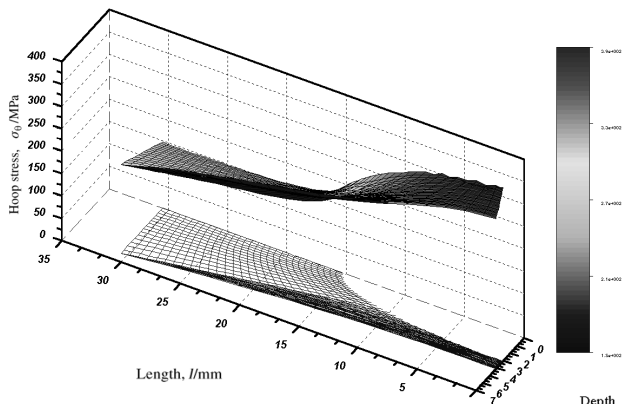


Figure 6: Variation of the hoop stress on the surface of the ligament
Slika 6: Variacija hoop-napetosti na površini ligamenta

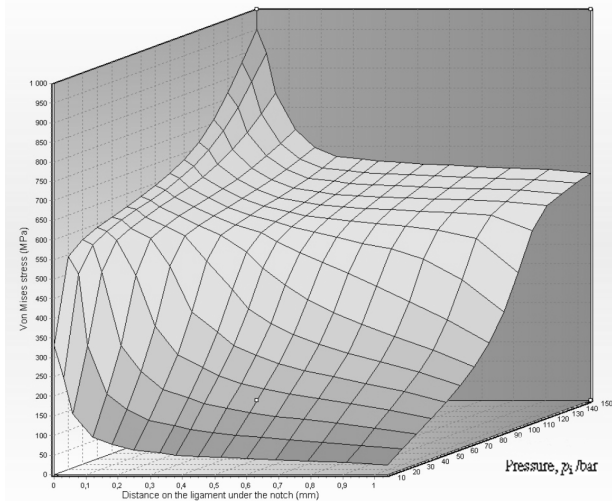


Figure 7: Von Mises stress on the ligament under the notch for different pressures
Slika 7: Von Misesova napetost v ligamentu pod zarezo pri različnem pritisku

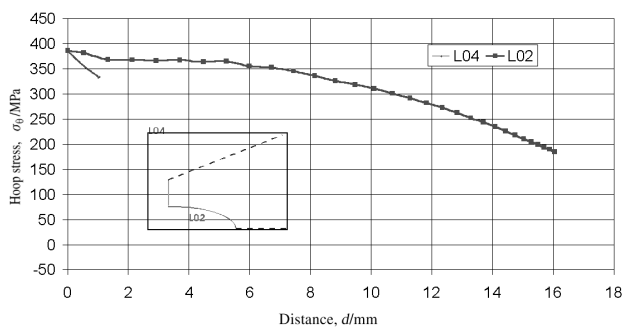


Figure 8: The variation of the hoop stress around the notch. L04 is the ligament line prolonging the small axis of the ellipse, L02 is the notch front line
Slika 8: Variacija hoop-napetosti okoli zareze. L04 je črta ligamenta podaljšek male osi elipse, L02 je čelna črta zareze

analytical relationships of cylindrical tubes (174.6 MPa). This validates the FE computation.

For this particular notch we have estimated the stress-concentration factor using the relationship:

$$K_{ep} = \frac{\sigma_{max, pl}}{\sigma_{G, pl}} \quad (16)$$

In this case, we obtain:

$$K_{ep} = \frac{386}{186} = 2.07 \quad (17)$$

4.2. Experimental results

Some tubes containing a notch with the dimensions given here were loaded with a gas up to failure. With the ground tubes the fracture occurs under a pressure of about 12 MPa. Only two results are available, but they give fracture pressures that are close together. These results seem to be in agreement with the tests carried out by a South Korean team⁶, although these tests used a

pipe in X65 with different dimensions. Moreover, this type of burst test with gas is rare, as are papers on this subject. So it is very difficult to properly compare our results.

5 COMPARISON OF RESULTS

If we consider the hoop stress, it appears that the computation gives a maximum value that is less than the yield strength. The hoop stress acts along the circular direction of the tube, but the stress in a perpendicular direction acts in the longitudinal direction of the tube, and the strains in this direction are constrained by the great length of the tube. Consequently, a triaxiality effect is induced, and the stress to be observed is the Von Mises stress (**Figure 7**). This triaxiality effect induces an over stress to obtain the yield of the material. Here, the overstress factor is $t = \sigma_{VM}/\sigma_Y = 760/528 = 1.44$. The maximum value is about 760 MPa for an internal pressure of 12 MPa.

Calculated codes give other results:

Table 1: Different ultimate pressure

Tabela 1: Različne končne napetosti

	P_{ult} /MPa	Error compared between experimental result (%)
ASME B31 G	11.3	5.8
Modified ASME B31 G	10.8	10
DNV RP-F101	6.6	45

To take account of the grinding in these calculations, we reduced the value of the ligament under the notch to 2 mm. According to the experimental result, it seems

that the ASME B31G code is the closest. The DNV RP-F101 is the most conservative code.

6 CONCLUSION

It has been shown in this paper that the construction of a meshed structure that conveniently represents a notched pressure pipe is quite difficult. However, the results of the FE computations give consistent results with respect to the experimental data.

To improve the prediction of fracture of the notched pressure pipes it is necessary now to improve the meshing of the notch. Moreover, experiments provided different data that will be compared with further FE computation predictions.

7 REFERENCES

- ¹ J. Capelle, J. Gilgert, G. Pluvinage, Ch. Schmitt: Calcul du facteur de sécurité associé à la ténacité d'un tuyau de faible épaisseur, Paper presented at the conference IFCAM01, (2006)
- ² J. Capelle, M. Lebienvenu, G. Pluvinage: Hydrogen effect on fatigue life of a pipe steel, Paper presented at the conference ICMFM XIII, (2006)
- ³ ASME B31G-1991: Manual for determining the remaining strength of corroded pipelines, The American Society of Mechanical Engineers, New York, USA, (1991)
- ⁴ DNV-RP-F101: Corroded pipelines, Det Norske Veritas, 1999
- ⁵ G. Pluvinage, J. Capelle: Etude d'un dimensionnement de conduite de gaz basée sur la mécanique de rupture et l'analyse limite, Paper presented at the 5^{ème} Journée de Mécanique de l'Ecole Militaire Polytechnique, 2006
- ⁶ J. B. Choi, B. K. Goo, J. C. Kim, Y. J. Kim, W. S. Kim: Development of limit load solutions for corroded gas pipelines, International Journal of Pressure Vessels and Piping 80 (2003), 121–128

FATIGUE PROBLEMS OF TRANSMISSION BELTS: a viscoelastic analysis of the strain-accumulation process

PROBLEM UTRUJANJA POGONSKIH JERMOV: viskoelastična analiza procesa akumuliranja deformacije

Igor Emri, Janez Kramar, Anatolij Nikonor, Urška Florjančič, Anton Hribar

University of Ljubljana, Faculty of Mechanical Engineering, Aškerčeva 6, 1000 Ljubljana, Slovenia
igor.emri@fs.uni-lj.si

Prejem rokopisa – received: 2006-05-17; sprejem za objavo – accepted for publication: 2006-10-09

We performed an analysis of the time-dependent behaviour of drive belts under the loading conditions to which they are exposed during normal operation. They are dynamically loaded with a tooth-like periodic (cyclic) load. Within each loading cycle the elastomeric material undergoes a combination of creep and retardation processes. Under certain conditions, the retardation process between two loadings cannot be fully completed. Thus, the material enters the second phase of loading with a residual strain state. Consequently, the strain state starts to accumulate, which leads to hardening of the material, crack formation, and ultimately to the failure of the belt.

We recognized that drive belts exhibit the accumulation of strain when exposed to normal operation at certain critical angular velocities. The strain accumulated in each consecutive cycle depends on the geometry of the belt, the angular velocity of the pulleys, the number of completed cycles, and the retardation spectrum of the material. In this paper we discuss the effect of the number of loading cycles to which the material is exposed in the strain-accumulation process. For a given belt geometry the critical angular velocity increases with the number of loading cycles. At the same time the magnitude of the accumulated strain decreases non-linearly as the number of loading cycles increases. Hence, the strain-accumulation process slows down with the increasing number of loading cycles. However, if the belt operates at, or in the close vicinity of, its critical angular velocity, it will almost certainly fail. Since the critical angular velocity is directly related to the retardation time of the material, and the magnitude of the accumulated strain depends on the strength of the corresponding discrete spectrum lines, we can conclude that the time-dependent mechanical properties of the elastomeric material from which the belt is constructed are the most critical parameters for predicting the durability of drive belts and other dynamically loaded elastomeric products.

Key words: time-dependent constitutive modelling, power transmission belts, synchronous belts, failure, viscoelastic analysis, strain accumulation, elastomers, time-dependent behaviour, mechanical spectrum

V delu predstavljamo viskoelastično analizo časovnega vedenja pogonskih jermenov, ki so med obratovanjem motorja dinamično obremenjeni s koračno spremembou. V času enega obremenitvenega cikla je posamezna viskoelastična komponenta jermena izpostavljena kombiniranemu procesu lezenja in relaksacije. Pri določenih pogojih, ki jih opredeljujeta geometrija jermena in kotna hitrost jermenice, se proces retardacije med dvema obremenitvenima cikloma ne zaključi. To pomeni, da material vstopi v naslednjo obremenitveno fazo s preostalo deformacijo. Postopoma se začne deformacija akumulirati, kar vodi do utrjevanja materiala, nastanka razpoke in posledično do propada jermena.

Analiza pokaže, da se akumulacija deformacije v jermenu pojavi pri določenih kritičnih vrednostih kotne hitrosti. Proses akumuliranja deformacije v vsakem zaporednem obremenitvenem ciklu je odvisen od geometrije jermena, kotne hitrosti jermenice, števila zaključenih obremenitvenih ciklov in retardacijskega spektra materiala, iz katerega je narejen jermen. Predstavljeno delo obravnava vpliv števila obremenitvenih ciklov na proces akumuliranja deformacije v pogonskem jermenu med obratovanjem motorja. Pri dani geometriji jermena kritična kotna hitrost narašča s povečevanjem števila obremenitvenih ciklov, medtem ko velikost akumulirane deformacije nelinearno pojema, kar kaže, da se z naraščanjem števila ciklov obremenjevanja proces akumuliranja deformacije upočasni. Rezultati kažejo, da bo jermen med obratovanjem pri kritični kotni hitrosti (oz. v njeni bližini) zelo verjetno odpovedal. Z ozirom na to, da je kritična kotna hitrost povezana z retardacijskim časom materiala in je velikost akumulirane deformacije odvisna od jakosti pripadajoče diskretne spektralne linije, lahko sklepamo, da so časovno odvisne mehanske lastnosti elastomernega materiala, iz katerega je narejen jermen, kritični parameter za napoved trajnosti jermenov in drugih dinamično obremenjenih elastomernih produktov.

Ključne besede: časovno odvisno konstitutivno modeliranje, pogonski jermen, utrujanje, propad jermena, viskoelastična analiza, akumulacija deformacije, elastomeri, časovno odvisno vedenje, mehanski spekter

1 THE LOADING CONDITIONS OF A SYNCHRONOUS BELT

The loading conditions of a synchronous belt were determined with the commercial FEM program called ANSYS, assuming the elastic behaviour of all belt components. The belt was pre-stressed with a force F and loaded with a desired torque M so that the pre-stressing force was adequately divided into the strand on the tension side, F_1 , and the strand on the slack side F_2 , as schematically shown in **Figure 1**. The distance between the two pulleys is indicated as l , the radius of

both pulleys is R , and the times t_1 and t_2 indicate when the belt enters and leaves the driving pulley.

The driving pulley and the driven pulley were then rotated such that a selected point on the belt would return to its initial position. Such a movement we designated as a complete loading cycle of the belt. For a further analysis of the strain accumulation, we selected the location on the tooth where the shear stress state within the loading cycle, calculated with the FEM program, has the form of an impulse function. This location is indicated as point A in **Figure 2a**. The corresponding

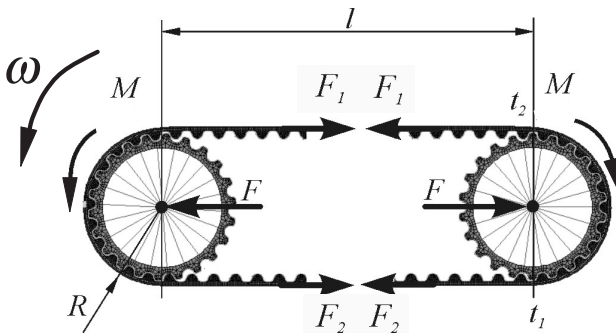


Figure 1: Schematic diagram of the belt-loading conditions and the geometry

Slika 1: Shematičen prikaz obremenjevanja jermenja in njegove geometrije

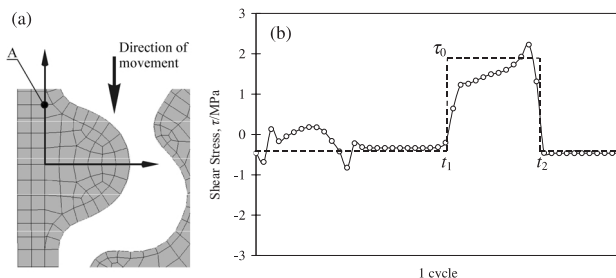


Figure 2: Shear stresses at point A within a complete loading cycle
Slika 2: Spreminjanje stržne napetosti v točki A v enem obremenitvenem ciklu

calculated time-dependent evolution of the stress state is shown in **Figure 2b**.

As a first approximation the shear stress may be modelled as the difference between two step functions with the shear stress intensity τ_0 . Hence,

$$\tau(t) = \tau(0)h(t) + \sum_{n=1}^{N-1} \{\tau_0[h[t-t_1-(n-1)\xi] - h[t-t_2-(n-1)\xi]]\} \quad (1)$$

The times t_1 and t_2 and the duration of one loading cycle ξ are functions of the geometry and the angular velocity of the belt drive, ω . Here, N is the number of cycles to which the belt has been exposed, and $\tau(0)$ is the shear stress at $t = 0$. Hence, $t_1 = (l+\pi R)/(\omega R)$, $t_2 = (l+2\pi R)/(\omega R)$, and $\xi = (2l+\pi R)/(\omega R)$.

2 ANALYSIS OF THE STRAIN ACCUMULATION

The time-dependent strain response of a rubber material can be expressed as¹,

$$\gamma(t) = \tau(0)J(t) + \int_0^t J(t-s) \frac{d\tau(s)}{ds} ds \quad (2)$$

where $J(t)$ is the shear creep compliance. Assuming the material is simple and can be modelled with a single

spectrum line, the material function is expressed as $J(t) = J_g + L_1 e^{-t/\lambda_1}$, where J_g denotes the glassy compliance and λ_1 is the retardation time where the corresponding spectrum line $L_1 = (\lambda_1)$ is located.

Let us analyse the accumulated strain at the end of N completed cycles at $t = t_N = N\xi$. Substituting Equation (1) into Equation (2), and considering the geometry of the drive belt as $l/R = \pi$, we obtain

$$\gamma(N) = \tau(0)J\left(\frac{4\pi N}{\omega}\right) + \Gamma_N(N), \quad \Gamma_N(N) = \sum_{n=1}^N \Delta\Gamma_n(n) \quad (3)$$

where

$$\Delta\Gamma_n(n) = \tau_0 L_1 \exp\left(\frac{\pi(4n-3)}{\omega\lambda_1}\right) \left[1 - \exp\left(-\frac{\pi}{\omega\lambda_1}\right)\right] \quad (4)$$

denotes the strain accumulation for each consecutive cycle. Equation (3) describes the time-dependent evolution of the strain field in the material when exposed to cyclic loading. **Figure 3** shows the strain accumulation in each consecutive cycle, expressed by Equation (4), as a function of $\lg \omega$ for different numbers of completed cycles. From **Figure 3** it is clear that the strain accumulation has its maximum at a certain critical angular velocity.

The location of the critical angular velocity, $\omega_{CR}(n)$, can be obtained by equating the two last terms in Equation (4),

$$1 - \exp(-\pi/\omega_{CR}(n)\lambda_1) = \exp[\pi(4n-3)/\omega_{CR}(n)\lambda_1] \quad (5)$$

The critical angular velocity at which the accumulated strain has a peak magnitude is a close form solution of Equation (5) and can be expressed as

$$\omega_{CR}(n) = \frac{\pi}{\lambda_1 \ln \frac{4n-2}{4n-3}} \quad (6)$$

It is important to note that the critical angular velocity is directly related to the retardation time of the

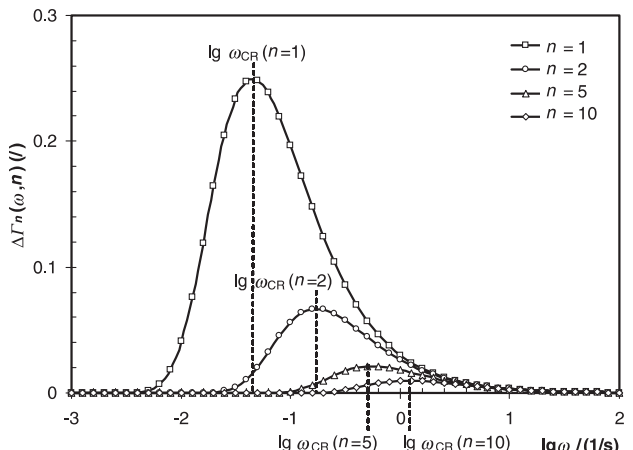


Figure 3: The effect of different numbers of loading cycles on the strain accumulated in the material

Slika 3: Vpliv števila obremenitvenih ciklov na akumulacijo deformacije v materialu

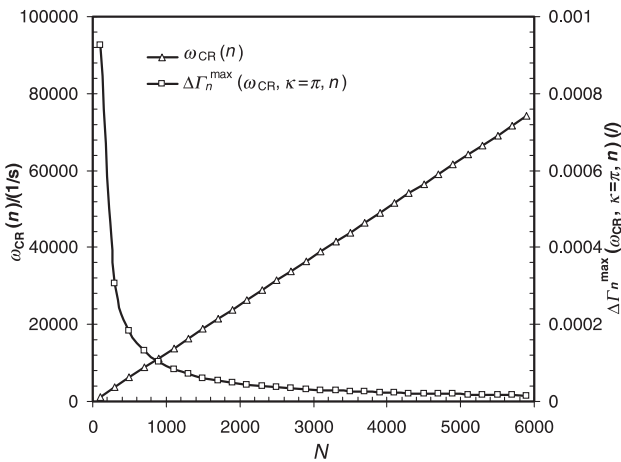


Figure 4: The critical angular velocity and the maximum strain accumulation as a function of the number of loading cycles

Slika 4: Kritična kotna hitrost in največja akumulirana deformacija v odvisnosti od števila obremenitvenih ciklov

material, which clearly emphasizes the importance of the material's time-dependent properties. By combining Equations (3) and (6) we obtain the corresponding peak value of the accumulated strain in each loading cycle,

$$\Delta\Gamma_n^{\max}(\omega_{\text{CR}}, n) = \tau_0 L_1 \frac{1}{4n-2} \left(\frac{4n-3}{4n-2} \right)^{(4n-3)}; \\ n = 1, 2, 3 \dots, N \quad (7)$$

The critical angular velocity and the corresponding peak value of the accumulated strain in each loading cycle as a function of n for $\lambda_1 = 100 \text{ s}^{-2}$ are shown in **Figure 4**. From the figure we can clearly see that the critical angular velocity shifts towards higher frequencies for each consecutive loading cycle, and that the relation is almost linear. At the same time the corresponding accumulated strain decreases for each consecutive cycle.

Providing the drive belt can operate at the critical angular velocity at all times, the maximum strain that could be accumulated over N cycles would be,

$$\Gamma_n^{\max}(\omega_{\text{CR}}, n) = \sum_{n=1}^{N=n} \Delta\Gamma_n^{\max}(\omega_{\text{CR}}, n) = \tau_0 L_1 \sum_{n=1}^{N=n} \frac{1}{4n-2} \left(\frac{4n-3}{4n-2} \right)^{(4n-3)} \quad (8)$$

It is important to stress that

$$\lim_{n \rightarrow \infty} \Delta\Gamma_n^{\max}(\omega_{\text{CR}}, \kappa = \pi, n) = \lim_{n \rightarrow \infty} \tau_0 L_1 \frac{1}{4n-2} \left(\frac{4n-3}{4n-2} \right)^{(4n-3)} = 0 \quad (9)$$

which means that the strain accumulated during each cycle will tend towards zero value as $n \rightarrow \infty$. However

$$\lim_{n \rightarrow \infty} \Delta\Gamma_n^{\max}(\omega_{\text{CR}}, N) = \lim_{n \rightarrow \infty} \tau_0 L_1 \sum_{n=1}^{N=N} \frac{1}{4n-2} \left(\frac{4n-3}{4n-2} \right)^{(4n-3)} = \infty \quad (10)$$

which means that if a belt were to operate all the time at the critical angular velocity it would always fail.

The total accumulated strain, expressed by Equation (8), as function of the cumulative number of loading cycles is shown in **Figure 5**.

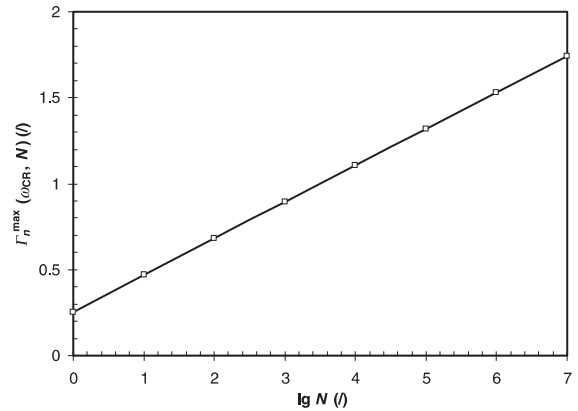


Figure 5: The total accumulated strain as a function of the cumulative number of loading cycles

Slika 5: Celotna akumulirana deformacija v odvisnosti od kumulativnega števila obremenitvenih ciklov

3 CONCLUSIONS

From the presented analysis we can conclude that drive belts will exhibit the accumulation of strain when exposed to normal operation at certain angular velocities. For a given belt geometry the critical angular velocity increases with the number of loading cycles. At the same time the magnitude of the accumulated strain decreases non-linearly as the number of loading cycles increases. Hence, the strain-accumulation process slows down with the increasing number of loading cycles, and will be negligible after a certain number of loading cycles, as shown in **Figure 4**.

However, if the belt operates at, or in the close vicinity of, its critical angular velocity, it will almost certainly fail. The critical angular velocity depends on the material's retardation time (i.e., the location of the mechanical spectrum), while the magnitude of the accumulated strain depends on the strength of the corresponding discrete spectrum lines. Thus, the time-dependent mechanical properties of the elastomeric material from which the belt is constructed are the most critical parameters for predicting the durability of drive belts and other dynamically loaded elastomeric products.

ACKNOWLEDGEMENTS

We would like to acknowledge the support provided by the Slovenian Research Agency under the contract L2-66000-0782. The contribution to the numerical calculations, data processing and the preparation of the figures by R. Cvelbar is greatly appreciated.

4 REFERENCES

- 1 N. W. Tschoegl, The phenomenological theory of linear viscoelastic behavior: an introduction, Springer-Verlag, Berlin Heidelberg, 1989
- 2 I. Emri, T. Prodan, A measuring system for bulk and shear characterization of polymers, *Experimental Mechanics* 46 (2004), 429–439

A MICRO-MACRO ANALYSIS OF THE TOOL DAMAGE IN PRECISION FORMING

MIKRO-MAKROANALIZA POŠKODB ORODJA ZA NATANČNO KOVANJE

Tomaž Rodič^{1,3}, Jože Korelc², Anton Pristovšek³

¹Naravoslovnotehniška fakulteta, Oddelek za materiale in metalurgijo, Aškerčeva 12, 1000 Ljubljana, Slovenia

²Fakulteta za gradbeništvo in geodezijo, Jamova 2, Ljubljana, Slovenia

³C3M, d. o. o., Vandotova 55, 1000 Ljubljana, Slovenia

tomasz.rodic@c3m.si

Prejem rokopisa – received: 2006-05-17; sprejem za objavo – accepted for publication: 2006-10-05

A micro-macro finite-element model for predicting the cyclic stress-strain response and damage evolution in tool-steel materials is presented. The elasto-plastic constitutive model at the macro-scale combines isotropic and kinematic hardening with continuum damage. This permits relatively precise modelling of the critical regions in the tooling systems over a large number of loading cycles. The macroscopic stress-strain fields are coupled with representative volume elements at the micro-level, where interactions between the primary carbides (M_6C , MC , V_8C_7) and the martensitic matrix are evaluated. This provides a detailed insight into the stress-strain fields at the micro-level and reveals the damage mechanisms at the micro-scale. The performance of the model is demonstrated on an industrial example of a tool for the cold precision forming of metals.

Key words: damage, micro-macro, finite element method, tool steels, precision forming of metals

Predstavljen je numerični model za analizo cikličnih napetostno-deformacijskih odzivov in razvoja poškodb orodnih jekel na različnih dimenzijskih skalah po metodi končnih elementov. Makroskopski elasto-plastični konstitutivni model povezuje izotropno in kinematično utrjevanje s poškodbami kontinuma. To omogoča razmeroma natančno modeliranje kritičnih območij v sistemu orodij za veliko število obremenitvenih ciklov. Makroskopska napetostno-deformacijska polja so povezana z reprezentativnimi volumenskimi elementi na mikroravnini, kjer analiziramo medsebojne vplive med primarnimi karbidi (M_6C , MC , V_8C_7) in martenitno osnovo. S tem dobimo podrobnejši vpogled v napetostno-deformacijska polja in poškodbene mehanizme na mikroravnini. Uporabnost mikro-makromodela je prikazana na industrijskem primeru orodja za natančno preoblikovanje kovin v hladnem.

Ključne besede: poškodbe, mikro-makro, metoda končnih elementov, orodna jekla, natančno preoblikovanje kovin

1 INTRODUCTION

The tooling systems applied in production of cold forged components are repetitively subjected to very high loads. Despite of the high strength materials and prestressing applied to die inserts, these loads often cause local plastic deformation of the dies. Even though the plastic deformations caused by each forming cycle are relatively small they accumulate during the production and can eventually lead to the initiation of fatigue cracks. Once a fatigue crack is initiated it can grow and lead to the failure of tooling system. Statistical investigations show that more than eighty percent of cold forging tools fail in this way.

The designers are therefore interested in identifying and optimising those design parameters that have strong impact on the fatigue response of tooling systems. In this work the response is modeled by an elasto-plastic constitutive model, which combines isotropic and kinematic hardening with continuum damage. This permits relatively precise modelling of stress/strain response of tool steels over large number of loading cycles and estimation of accumulated damage. A method for evaluating the sensitivity¹ of damage to material parameters and optimisation² can be combined with this approach.

2 CONSTITUTIVE MODEL

The elasto-plastic material model developed by Pedersen³ is considered. This model takes into account simultaneous evolution of isotropic and kinematic hardening and damage. Since the strains in the tool are expected to be small (<1) an additive decomposition of the strain tensor ε_{ij} into elastic and plastic parts is assumed;

$$\varepsilon_{ij} = \varepsilon_{ij}^e + \varepsilon_{ij}^p \quad (1)$$

The elastic stress strain relationship is given by

$$\sigma_{ij} = L_{ijkl} \cdot \varepsilon_{kl}^e \quad (2)$$

where L_{ijkl} is the tensor of elastic moduli. The summation convention is adopted for repeated indices. It is noted that experimental investigations of tool steel materials do not reveal significant effect of damage on their elastic response. The rate of plastic strain is derived from the normality rule

$$\dot{\varepsilon}^p = \lambda \frac{\partial f}{\partial \sigma_{ij}} \quad (3)$$

where f is the yield surface and λ is the plastic multiplier derived from the consistency condition, $\dot{f} = 0$. The flow rule implicitly comprises damage D as follows:

$$f = \tilde{\sigma}_e - (R + k) = 0 \quad (4)$$

where

$$\tilde{\sigma}_e = \sqrt{\frac{3}{2} \tilde{s}_{ij} \tilde{s}_{ij}} \quad (5)$$

$$\tilde{s}_{ij} = \tilde{\sigma}_{ij} - \frac{1}{3} \delta_{ij} \tilde{\sigma}_{kk} \quad (6)$$

$$\tilde{\sigma}_{ij} = \frac{\sigma_{ij}}{1-D} - X_{ij} \quad (7)$$

$$\dot{f} = \frac{\partial f}{\partial \sigma_{ij}} \dot{\sigma}_{ij} + \frac{\partial f}{\partial X_{ij}} \dot{X}_{ij} + \frac{\partial f}{\partial R} \dot{R} + \frac{\partial f}{\partial D} \dot{D} \quad (8)$$

In the above equations X_{ij} is represents kinematic hardening while the scalars R and k describe isotropic hardening.

2.1 Kinematic hardening

The back stress tensor X_{ij} is the centre of the yield surface in stress space, it is defined by the following evolution equations

$$X_{ij} = \sum_{n=1}^3 X_{ij}^{(n)} \quad (9)$$

$$\dot{X}_{ij}^{(n)} = \frac{2}{3} \gamma^{(n)} X_{mn}^{(n)} (1-D) \dot{\epsilon}_{ij}^{pl,c} - \left(\frac{X_e^{(n)}}{X_\infty^{(n)}} \right)^{m_n} X_{ij}^{(n)} \gamma^{(n)} \dot{\lambda} \quad \text{and} \quad (10)$$

$$X_e^{(n)} = \sqrt{\frac{2}{3} X_{pq}^{(n)} X_{pq}^{(n)}} \quad (11)$$

2.2 Nonlinear isotropic hardening

The scalar k is assumed to be constant while evolution equation for R is defined by

$$\dot{R} = b(R_\infty(\Lambda, q) - R)\dot{\lambda} \quad (12)$$

where b is a material parameter and $R_\infty(\Lambda, q)$ represents the limit of isotropic hardening or softening.

2.3 Continuum damage

Many different evolution equations have been proposed in the literature to describe irreversible damage development. For the industrial example described in this paper the following equation has been applied

$$\dot{D} = \frac{\sigma_e^2 \left(\frac{2}{3}(1+\nu) + 3(1-2\nu) \left(\frac{\sigma_{kk}}{3\sigma_e} \right)^2 \right)}{2 \cdot S \cdot E (1-D)^2} \dot{p} \cdot \alpha(p) \quad (13)$$

where

$$\alpha(p) = \begin{cases} 1, & \text{za } p \geq p_d \\ 0, & \text{za } p < p_d \end{cases} \quad (14)$$

$$\dot{p} = \frac{\dot{\lambda}}{1-D} \quad (15)$$

$$p_d = \text{Max}(p_{(D=0)}) \quad (16)$$

$$D_c = \text{Max}(D_{(p)}) \quad (17)$$

3 COMPUTER IMPLEMENTATION

The material model has been implemented into a specialised commercial finite element system ⁴ by using the code development concept ⁴⁻⁶ shown in **Figure 1**.

The symbolic system ^{5,6} for automatic code generation is based on the *Mathematica* package and allows constitutive models, element formulations and response functionals to be described on a highly abstract level. The formulations are automatically processed by computer, to derive consistently linearised element stiffness matrices, loading vectors and sensitivity terms for either direct differentiation method or adjoint method. From these expressions the computer code is automatically generated for different languages including C and FORTRAN; this code can then be integrated into a finite element environment which performs both direct and sensitivity analyses on a global structural level. An optimisation shell is also build around the finite element software to allow automatic optimisation of design parameters. The interactions between the symbolic system, the finite element environment and the optimisation shell are indicated in **Figure 1**.

4 INDUSTRIAL APPLICATION

The computational model has been applied to multi-scale damage analysis an industrial tool (**Figure 2a**) for production of an automotive precision part ⁷. In the first step the macro-mechanical tool loads have been

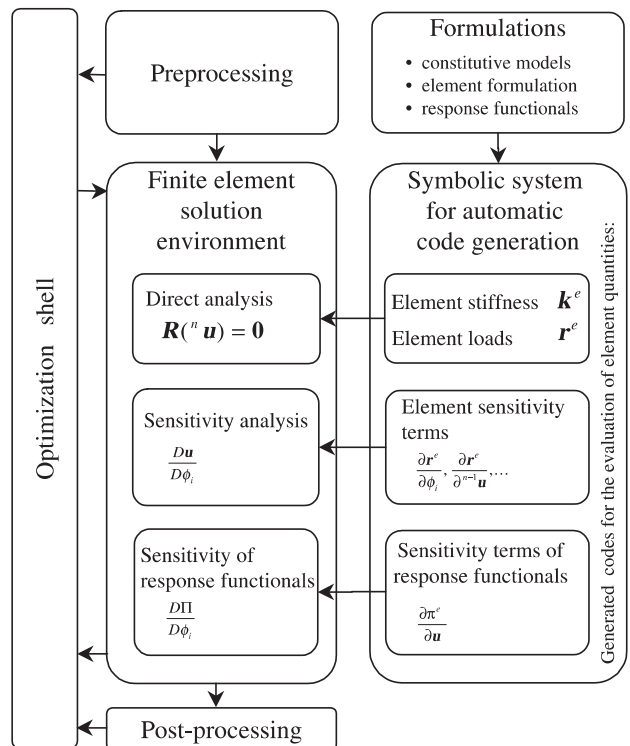


Figure 1: Code development concept
Slika 1: Koncept za razvoj programske kode

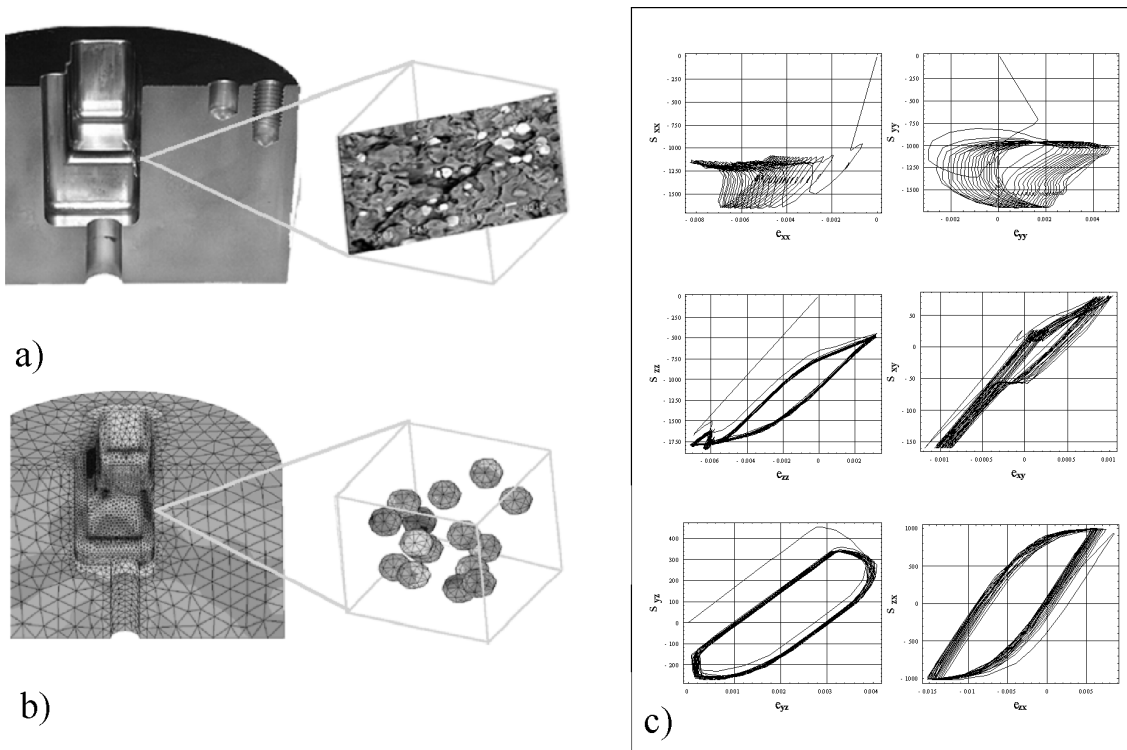


Figure 2: Micro-macro analysis of an industrial tool for cold precision forming of metals: (a) real macro-micro problem; (b) stress fields in virtual FE model at macro and micro levels; (c) cyclic stress-strain response of RVE of tool steel.

Slika 2: Mikro-makroanaliza industrijskega orodja za natančno preoblikovanje kovin v hladnem: (a) relni makro-mikroproblem; (b) napetostno polje v virtualnem MKE-modelu na makro- in mikroravnini; (c) ciklični napetostno-deformacijski odziv RVE orodnega jekla

evaluated by the finite element simulation of the forming process. These loads were then repetitively applied to the working surface of the prestressed die insert. In **Figure 2c** the macroscopic stress-strain response of the tool at the most critical location is shown for the first fifty forming cycles. These loading cycles were then mapped to the representative volume element (RVE) of a high strength powder metallurgical tool steel in order to evaluate stress-strain fields at the micro level where interactions between spherical primary carbides (M_6C , MC, V_8C_7) and martensitic matrix occur. In **Figure 2b** the stress levels in carbides are shown. The model⁸ can be extended to tribological problems where damage and wear of tool surfaces can be evaluated by taking into account stress concentrations due to surface roughness, temperature changes due to dissipation of plastic work and friction, internal stresses at the microstructure due to different thermal expansion of the carbides and the martensitic matrix as well as cooling effects due to the presence of lubricants.

5 REFERENCES

- ¹ S. Stupkiewicz, J. Korelc, M. Dutko, T. Rodič: Shape sensitivity analysis of large deformation frictional contact problems. *Comput. methods appl. mech. eng.* 191 (2002) 33, 3555–3581
- ² Doltsinis I. St., Rodic T.: Process design and sensitivity analysis in metal forming processes: Computational methods and applications, *International Journal for Numerical Methods in Engineering* 45 (1999), 661–692
- ³ Pedersen T. O.: Cyclic plasticity and low cycle fatigue in tool materials. Ph. D. Thesis. DCAMM, Report No. S 82, November 1998
- ⁴ www.c3m.si
- ⁵ Korelc J.; Automatic generation of finite-element code by simultaneous optimization of expressions, *Theoretical Computer Science*, 187 (1997a), 231–248
- ⁶ Korelc J.; Automatic generation of numerical codes with introduction to AceGen 4.0 symbolic code generator, www.fgg.uni-lj.si/Symech/
- ⁷ Grønbæk J., Hinsel C.: The importance of optimized prestressing with regard to the tool performance in precision forging (Keynote Paper). Kuzman, K. (Edtr.): 3rd International Conference on Industrial Tools, ICIT 2001, Rogaska Slatina, April 22–26, 2001
- ⁸ A. Ibrahimbegović, I. Grešovnik, D. Marković, S. Melnyk, T. Rodič: Shape optimization of two-phase material with microstructure, *Engineering Computations: International Journal for Computer-Aided Engineering and Software*, 22 (2005) 5/6, 1108

THE STABILITY OF CAST ALLOYS AND CVD COATINGS IN A SIMULATED BIOMASS-COMBUSTION ATMOSPHERE

STABILNOST ZLITIN IN CVD-PREVLEK V SIMULIRANI ATMOSFERI ZGOREVANJA BIOMAS

Danijela A. Skobir¹, Michael Spiegel²

¹Institute of Metals and Technology, Lepi pot 11, SI-1000 Ljubljana, Slovenia

²Max-Planck-Institut für Eisenforschung GmbH, Max-Planck-Straße 1, D-40237 Düsseldorf, Germany
danijela.skobir@imt.si

Prejem rokopisa – received: 2006-09-29; sprejem za objavo – accepted for publication: 2006-10-13

The corrosion resistance in a biomass-combustion environment was studied for the following materials: cast alloys (Alloy 800, Inconel 617, 1.4910, HCM 12 and P91), Fe-9 % Cr model alloys with and without additions of Al, Si and Mo, and cast alloys coated using the pack-cementation process with Al and Al-Si. The simulated atmosphere for the biomass-combustion environment contained 200 µg/g HCl, volume fractions 13 % CO₂, 22 % H₂O and 5 % O₂. The samples were covered with a salt mixture of mass fractions of 52.4 % KCl and 47.6 % K₂SO₄ in order to simulate the corrosion beneath the deposits. The specimens were exposed for 1000 h at the test temperature of 550 °C.

Keywords: hot corrosion, biomass combustion, CVD-coatings, deposits

S korozijskimi preizkusi v simulirani atmosferi za zgorevanje biomas smo raziskovali korozisko obstojnost naslednjih materialov: lite zlitine (zlitina 800, Inconel 617, 1.4910, HCM 12 in P91), modelne zlitine Fe-9 % Cr z dodatki Al, Si in Mo in brez njih ter lite zlitine, na katere je bila s CVD-postopkom nanesena plast Al oziroma Al-Si. Simulirana atmosfera za zgorevanje biomas je vsebovala 200 µg/g HCl in prostorninske deleže: 13 % CO₂, 22 % H₂O in 5 % O₂. Vzorci so bili prekriti s solno mešanicu z masnim deležem 52,4 % KCl in 47,6 % K₂SO₄ za simulacijo korozije pod depoziti. Preizkusi so potekali pri temperaturi 550 °C, čas trajanja preizkusov pa je bil 1000 h.

Ključne besede: visokotemperaturna korozija, zgorevanje biomas, CVD-prevleke, depoziti

1 INTRODUCTION

One of the most important problems of modern society is the removal of waste and biomass, stemming mainly from the production of highly developed industrial products. An effective and useful way of removing biomass is combustion, connected with the production of steam used for the production of electrical energy. Nowadays, approximately 23 % of the total amount of waste in Europe is burned; the rest is deposited in landfills^{1,2}. In Western Europe, nearly 600 combustion plants are in operation, and the number is still increasing. Until 2010 an increase in the total amount of energy from renewable sources, from 6 % to 12 %, is expected, as well as a substantial increase in the efficiency of thermal power plants.

Corrosion is a major issue concerning the limited lifetime of tube materials and the plant efficiency in biomass- and waste-incineration plants. In biomass-fired plants, high contents of potassium and chlorine are present in the combustion environment, causing early failure of the thermal components, such as superheater tubes^{3,4}. Solid and/or liquid chloride salts, together with their vapours, can destroy the protective surface oxide scales of high-temperature materials, even at temperatures well below the melting points of the salts^{2, 5-7}. Rapid corrosion results from the complicated chemical

reactions between tube materials and the gaseous species (HCl, SO₂, etc.) and, especially, the low melting point of the eutectic salts of heavy metals (Sn, Pb, Zn) and alkali-metal (K, Na) chlorides, as well as sulfates^{2, 8-10}. The most corrosive species in the flue gas is HCl. There is generally more HCl than SO₂; however, the HCl/SO₂ ratio strongly depends on the waste being burned. A generally accepted model for chlorine-induced corrosion in waste- and biomass-fired boilers is the 'active oxidation' mechanism, first observed and described by Lee and McNallan¹¹. The chlorine is produced by the catalytic oxidation of HCl according to Deacon reaction (Eq. 1) as well as by the reaction of the salt with the oxide scale of the pre-oxidized metal, according to Eq. 2 and 3:



The chlorine diffuses through the cracks and pores of the oxide scale to the metal/scale interface, reacting to form FeCl₂(s):



As the vapor pressure of the chloride is 10⁻⁴ bar at 500 °C, it evaporates and the volatile chloride diffuses

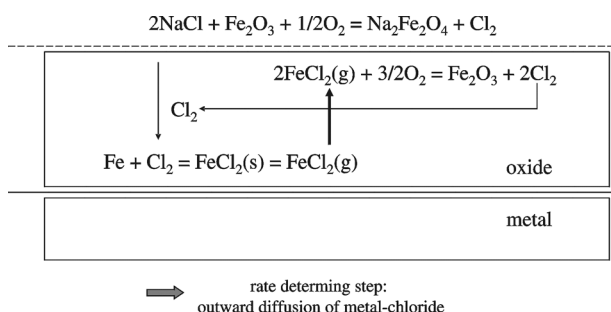
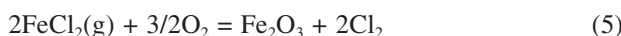


Figure 1: Schematic model of the mechanism of "active oxidation"
Slika 1: Shematski prikaz modela "aktivne oksidacije"

outwards through the oxide scale. At the oxide/gas interface the reaction to Fe_2O_3 takes place, releasing chlorine again:



The growth of the Fe_2O_3 in the cracks and pores of the oxide destroys the scale and the corrosive gas can react with the unprotected metal. Hence, a scale is produced on the metal substrate, which is not passivating and, for this reason, the mechanism was nominated as active oxidation. The mechanism of this oxidation is schematically presented in **Figure 1**. The chlorine plays a catalytic role in this corrosion process because it is not consumed. In-depth thermogravimetric studies on the mechanism of active oxidation were carried out by Reese and Grabke¹², showing that the evaporation of $\text{FeCl}_2(\text{g})$ from the metal/scale interface is the rate-determining step in NaCl -induced corrosion. In order to increase the efficiency of combustion plants it is necessary to develop effective protective coatings for vital components in hostile combustion environments.

2 EXPERIMENTAL

In this study, bare metals, CVD coatings and model alloys were tested in a simulated biomass-combustion

atmosphere. The chemical composition of the cast alloys is presented in **Table 1**. All of these alloys are based on iron, except for Inconel 617, which is a nickel-based alloy.

With the goal to decrease the surface degradation that occurs on exposure to high temperatures and corrosive atmospheres the cast alloys were coated using the pack-cementation process. The results of the exposure tests of uncoated as well as coated alloys were compared.

The pack-cementation process is essentially an *in-situ* chemical vapour deposition (CVD) process, which is used to deposit Al or some other elements (Al-Si, Al-Cr and Al-B) onto metal substrates to form aluminide diffusion coatings.

The substrates to be coated were placed in a sealed or semi-sealed container together with a powder mixture that consists of metal elements to be deposited (diffusion element), a halide activator (NH_4Cl) and an inert filler (Al_2O_3). The substrates can be buried in, or placed above, the powder mixture. The sealed container is heated under a protective atmosphere of Ar to a temperature between 650–1200 °C and held there for a specified time. At these coating temperatures the halide activators react with the metal elements in the powder mixture and form a series of metal-halide vapour species such as AlCl , AlCl_2 , AlCl_3 and Al_2Cl_6 ¹³. The coating is formed via reduction reactions of the metal-halide vapours at the substrate surface and subsequent solid-state diffusion between the metal elements and the substrate. For this reason, the coatings produced by using this process are also termed diffusion coatings.

Additionally, Fe-9 % Cr model alloys with and without additions of Al, Si and Mo were tested under the same conditions. The chemical composition of the model alloys is presented in **Table 2**.

All the materials were machined into specimens with dimensions of about (10 × 10 × 2) mm, then ground with 400 # and 600 # SiC paper, cleaned in a ultrasonic bath

Table 1: Chemical composition of the cast alloys (w/%)

Tabela 1: Kemijkska sestava litih zlitin (w/%)

Alloy	Cr	Ni	Fe	Mn	Mo	Al	Co	Si	V
Alloy 800	19–23	30–34	bal	<1.5	-	0.1–0.6	-	0.5	-
Inconel 617	20–24	bal	max 3	max 1	8–10	-	10–15	max 1	-
1.4910	16–18	12–14	bal	<2	2–2.5	-	-	<0.75	-
HCM 12	11.2	0.66	bal	0.50	0.86	-	-	-	0.25
P 91	8.6	0.26	bal	0.41	0.93	-	-	0.3	0.21

Table 2: Chemical composition of the model alloys (w/%)

Tabela 2: Kemijkska sestava modelnih zlitin (w/%)

Alloy	Fe	Cr	Mo	Al	Si
VI811	bal	9	-	2.5	2.5
VI813	bal	9	10	-	-
VI814	bal	9	10	2.5	2.5
VI815	bal	9	5	2.5	2.5

of acetone and weighed. After drying, each sample was covered with a salt mixture of mass fractions 52.4 % KCl and 47.6 % K₂SO₄ to simulate the corrosion beneath deposits.

The exposure experiments were performed in a flue-gas, using a horizontal furnace equipped with a quartz working tube. The furnace was connected to gas-mixing equipment; however, the N₂-5 % O₂-200 µg/g HCl mixture was supplied as a premixed commercial gas. The gas was dried by passing it through columns filled with P₂O₅ before entering the furnace. Because of the large constant-temperature zone it was possible to test 20 samples at the same time. The exposure experiments were carried out at 550 °C. The extent of the corrosion was determined by measuring the mass loss after 1000 h of reaction after the removal of the corrosion products by chemically etching in a KMnO₄-NaOH solution at 80 °C. After exposure, metallographic cross-sections were prepared by dry grinding the samples in order to prevent the dissolution of the chloride products from the scale. Scanning electron microscopy (SEM) and energy-dispersive X-ray analysis (EDX) were used to study the morphology and the chemical composition of the corrosion products.

3 RESULTS AND DISCUSSION

Figure 2 shows the extent of the corrosion on the investigated alloys, expressed in terms of mass change in mg/cm². The model alloys, VI814 and VI815, show a relatively small mass loss for the samples in the biomass-combustion environment due to their high content of Al, Si and Mo. The corrosion layer on the SEM micrograph of a cross-section of the VI815 alloy (**Figure 3a**) is very thin, about 52 µm. The corrosion layer consists of an Fe-rich layer and closer to the metal there is a scale interface, with an increasing amount of Cr, Al, Si and Mo being detected. The inner part is a Cr-rich layer with a large amount of Cl (**Figure 3b**).

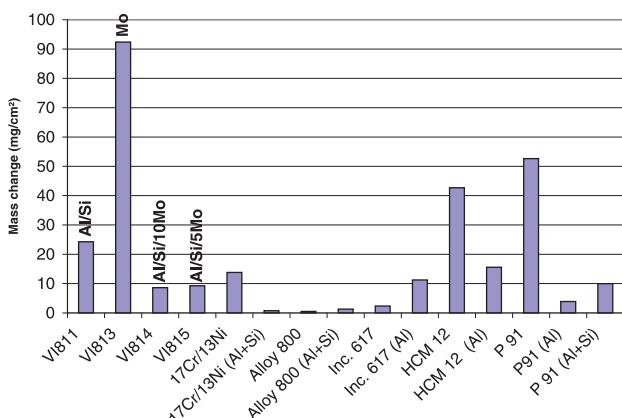


Figure 2: Mass loss of the materials exposed in a flue gas for 1000 h at 550 °C and covered with the KCl-K₂SO₄ salt mixture

Slika 2: Sprememba mase preizkušancev po 1000-urnem korozijskem preizkusu na 550 °C pod depozitom solne mešanice KCl-K₂SO₄

Slightly worse corrosion behavior was shown by the VI811 alloy, whereas the VI813 alloy with a high Mo content was almost completely corroded. The analysis of the deposited layer of the VI813 alloy shows that the corrosion layer consists of two sublayers and is very thick, about 622 µm (**Figure 4a**). In the upper layer is the remainder of the salt on the top, and below an Fe-oxide was formed, where no chromium was found. The underneath layer is the layer of the inner corrosion products. **Figure 4b** shows a detailed view of the internal oxidation zone, which is relatively deep and therefore responsible for the large mass loss. The outer part of the scale of inner corrosion products is an Fe-rich layer, and towards the metal-scale interface an increasing content of Cr, Cl and Mo and no sulphur were detected.

From **Figure 2** it can also be seen that the corrosive attack on the nickel-based Inconel 617 alloy and on the 800 alloy with the high Ni content is much smaller than on the iron-based cast alloys. From **Figure 5a** it is clear that the corrosion layer on the exposed Inconel 617 is extremely thin, only about 3.6 µm, which shows that this alloy is just slightly corroded. The corrosion layer consists of two layers (**Figure 5b**): the first layer is the Ni-rich layer, and the second is the Cr-rich layer below. No chlorides were detected in this layer.

The corrosion layer for the cast P91 alloy (**Figure 6a**), which has the lowest corrosion resistance among the

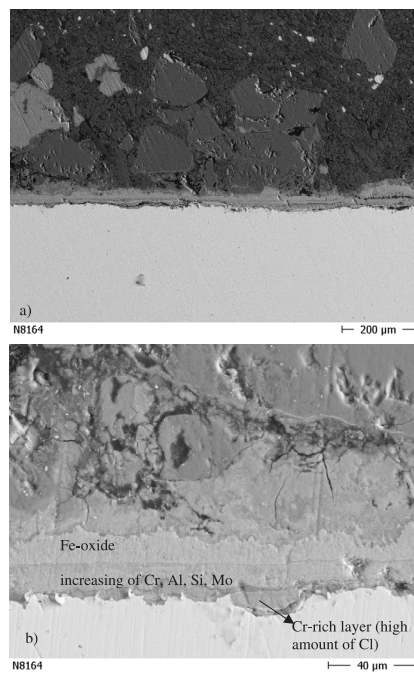


Figure 3: SEM micrograph from a metallographic cross-section of the VI815 model alloy after corrosion beneath the KCl-K₂SO₄ salt mixture in N₂-5 % O₂-200 µg/g HCl at 550 °C for 1000 h. (a) overview image; (b) detailed image of the internal part of the corrosion layer

Slika 3: SEM-posnetek metalografskega prereza za modelno zlitino VI815 po koroziji pod solno mešanico KCl-K₂SO₄ v N₂-5 % O₂-200 µg/g HCl pri 550 °C in po 1000 h. (a) pregledna slika; (b) detaljna slika notranjega dela korozjske plasti

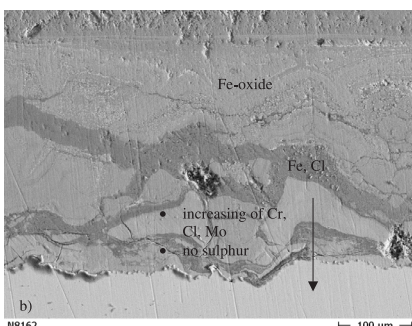
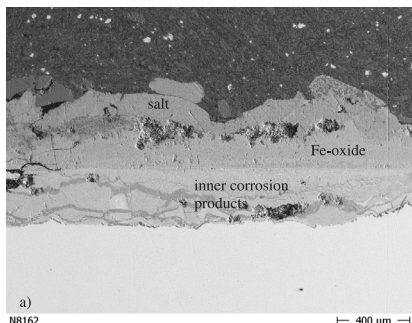


Figure 4: SEM micrograph from a metallographic cross-section of the VI813 model alloy after corrosion beneath the KCl-K₂SO₄ salt mixture in N₂-5 % O₂-200 µg/g HCl at 550 °C for 1000 h. (a) overview image; (b) detailed image of the internal part of the corrosion layer

Slika 4: SEM-posnetek metalografskega prereza za modelno zlitino VI813 po koroziji pod solno mešanico KCl-K₂SO₄ v N₂-5 % O₂-200 µg/g HCl pri 550 °C in po 1000 h. (a) pregledna slika; (b) detajljna slika notranjega dela korozjske plasti

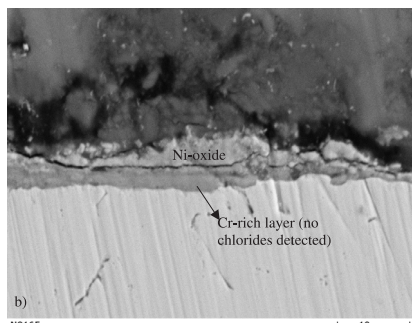
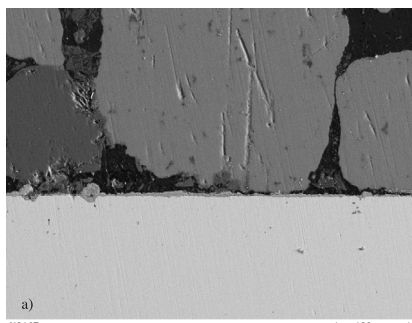


Figure 5: SEM micrograph from a metallographic cross-section of the Inconel 617 alloy after corrosion beneath the KCl-K₂SO₄ salt mixture in N₂-5 % O₂-200 µg/g HCl at 550 °C for 1000 h. (a) overview image; (b) detailed image of the internal part of the corrosion layer

Slika 5: SEM-posnetek metalografskega prereza za zlitino Inconel 617 po koroziji pod solno mešanico KCl-K₂SO₄ v N₂-5 % O₂-200 µg/g HCl pri 550 °C in po 1000 h. (a) pregledna slika; (b) detajljna slika notranjega dela korozjske plasti

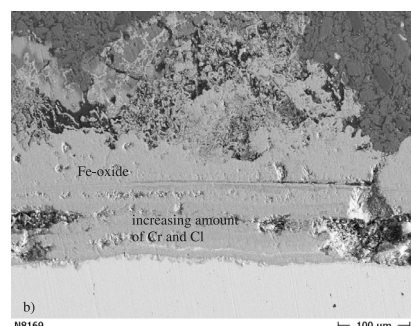
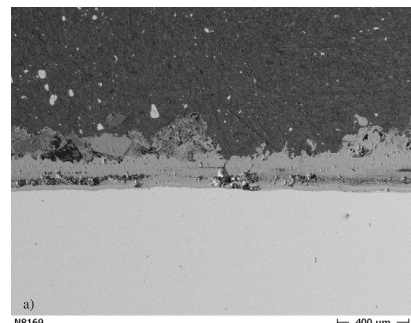


Figure 6: SEM micrograph from a metallographic cross-section of the P91 alloy after corrosion beneath the KCl-K₂SO₄ salt mixture in N₂-5 % O₂-200 µg/g HCl at 550 °C for 1000 h. (a) overview image; (b) detailed image of the internal part of the corrosion layer

Slika 6: SEM-posnetek metalografskega prereza za zlitino P91 po koroziji pod solno mešanico KCl-K₂SO₄ v N₂-5 % O₂-200 µg/g HCl pri 550 °C in po 1000 h. (a) pregledna slika; (b) detajljna slika notranjega dela korozjske plasti

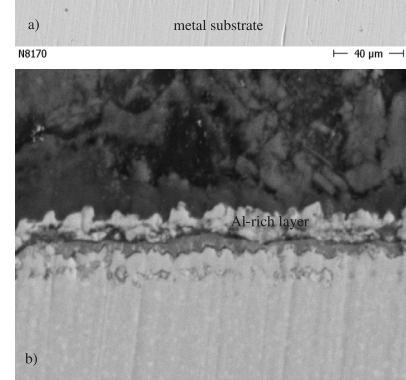
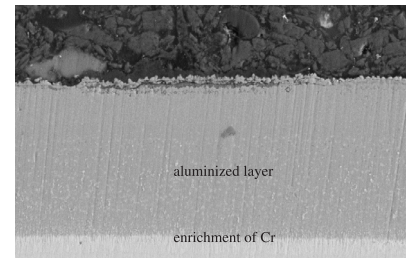


Figure 7: SEM micrograph from a metallographic cross-section of Al-coated Inconel 617 alloy after corrosion beneath the KCl-K₂SO₄ salt mixture in N₂-5 % O₂-200 µg/g HCl at 550 °C for 1000 h. (a) overview image; (b) detailed image of the internal part of the corrosion layer

Slika 7: SEM-posnetek metalografskega prereza za zlitino Inconel 617, prevlečeno z Al po koroziji pod solno mešanico KCl-K₂SO₄ v N₂-5 % O₂-200 µg/g HCl pri 550 °C in po 1000 h. (a) pregledna slika; (b) detajljna slika notranjega dela korozjske plasti

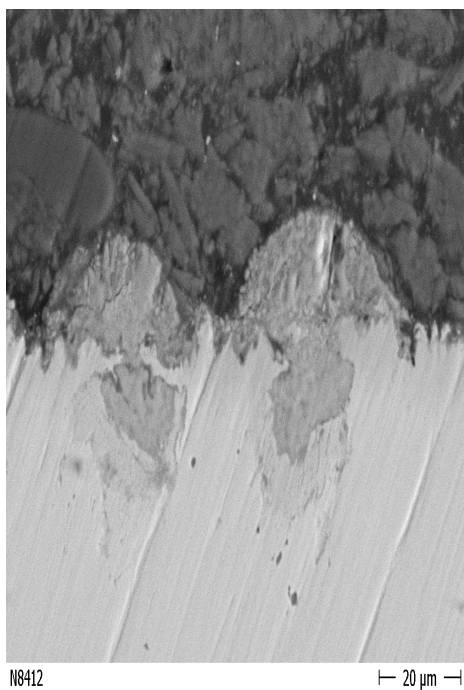


Figure 8: SEM micrograph from a metallographic cross-section of the P91 alloy, coated with Al-Si after corrosion beneath the KCl-K₂SO₄ salt mixture in N₂-5 % O₂-200 µg/g HCl at 550 °C for 1000 h. (a) overview image; (b) detailed image of the internal part of the corrosion layer

Slika 8: SEM-posnetek metalografskega prereza za zlitino P91, prevlečeno z Al-Si po koroziji pod solno mešanico KCl-K₂SO₄ v N₂-5 % O₂-200 µg/g HCl pri 550 °C in po 1000 h. (a) pregledna slika; (b) detajljna slika notranjega dela korozjske plasti

cast alloys, is much thicker (244 µm) than that on the Inconel 617. On the SEM micrograph, again an Fe-rich layer was detected on the top, and an increasing amount of Cr and Cl was detected towards the metal-scale interface (**Figure 6b**).

The exposure tests of Al-coated Inconel 617 and Al-Si-coated 800 alloy did not show any improvement in corrosion resistance compared to the uncoated material (**Figure 2**). In the case of the Inconel 617, coated with Al, there is almost no corrosion layer formed (**Figure 7a**). The aluminised layer (**Figure 7b**) has the chemical composition 36.2 % Al, 35.4 % Ni, 13.7 % Cr, 7.3 % Co, 6.6 % Mo and 0.77 % Fe. Just below this layer an enrichment of Cr was detected. The chemical composition of this layer is 33.9 % Cr, 4.6 % Al, 27.6 % Ni, 11.6 % Co and 19.1 % Mo. Below this layer is the metal substrate.

For all the other coated cast alloys an improvement in the corrosion resistance was observed (**Figure 2**). **Figures 8a and b** show the corrosion layer of the P91 alloy, coated with Al-Si.

In spite the fact that the Al-Si coatings were not as thick as the Al coatings (the Al coatings were about 80 µm and Al-Si about 30–40 µm) no significant differences in the corrosion resistance were observed.

4 CONCLUSIONS

Exposure tests were carried out to compare the corrosion resistance of several iron- and nickel-based alloys, as well as the same alloys coated with Al, Al-Si and Fe-9 % Cr model alloys beneath a salt mixture of KCl and K₂SO₄ in N₂-5 % O₂ atmosphere with the addition of 200 µg/g HCl. In this atmosphere, which is typical for a biomass-combustion environment, active oxidation by the HCl and alkali-chlorides plays a major role in the corrosion of this material. The results showed that among the model alloys (Fe-9Cr) the most corrosion-resistant are the VI814 and VI815 alloys, due to their large amount of Al, Si and Mo. In the group of cast alloys, the Inconel 617 nickel-based alloy has the best corrosion resistance, followed by the 800 alloy, which also contains quite large amounts of Ni. The Inconel 617 alloy coated with Al, and the 800 alloy coated with Al-Si do not show any improvement in corrosion resistance compared to the uncoated alloys. It can therefore be summarized that the alloying elements Ni, Mo, Al and Si have a beneficial effect on the corrosion resistance of the model and cast alloys. The coatings on the alloys that do not include these alloying elements do not improve the corrosion resistance. The formation of deposits significantly contributes to the corrosion by solid and liquid salts (i.e., chlorides and sulphates).

ACKNOWLEDGEMENTS

This work was carried out within the SUNASPO-Research Training Network at the Department of Interface Chemistry and Surface Engineering of the Max-Planck-Institut für Eisenforschung GmbH, Düsseldorf, Germany. The author would like to thank PD Dr. Michael Spiegel for the opportunity of working in the field of High Temperature Corrosion, and especially for his support. The financial support of the European Commission is gratefully acknowledged.

5 REFERENCES

- ¹ Statistisches Bundesamt Wiesbaden (1992), Statistik der öffentlichen Abfallbeseitigung von 1990
- ² Spiegel M.: Materials and Corrosion 50 (1999), 373–393
- ³ Sander B.: Biomass and Bioenergy 122 (1997), 177
- ⁴ Nielsen H. P., Frandsen F. J., Dam-Johansen K. and Baxter L. L.: Prog Energy Combust Sci. 26 (2000), 283
- ⁵ Grabke H. J.: Incinerating municipal and industrial waste in Bryers (ed.), Hemisphere Publ. Corp., (1991), 161–176
- ⁶ Li Y. S., Niu Y. and Wu W. T.: Mater. Sci. Eng A345 (2003), 64
- ⁷ Shinata Y.: Oxid. Met. 27 (1987), 315
- ⁸ Montgomery M. and Karlsson A.: Materials and Corrosion 50 (1999), 579
- ⁹ Miller P. D. and Krouse H. H.: Corrosion 28 (1972), 274
- ¹⁰ Grabke H. J., Reese E. and Spiegel M.: Corros. Sci. 37 (1995), 1023
- ¹¹ Lee Y. Y., McNallan M. J.: Metallurg. Trans. 18A (1987), 1099
- ¹² Reese E., Grabke H. J.: Materials and Corrosion 43 (1992), 547
- ¹³ Xiang Z. D., Burnell-Gray J. S. and Datta P. K.: Journal of Material Science 36 (2001), 5673

NASTANEK LaCrO₃ MED ZGOREVALNO SINTEZO

LaCrO₃ FORMATION DURING COMBUSTION SYNTHESIS

Klementina Zupan, Marjan Marinšek, Stane Pejovnik, Teja Hrobat

Univerza v Ljubljani, Fakulteta za kemijo in kemijsko tehnologijo, Aškerčeva 5, 1000 Ljubljana, Slovenija
klementina.zupan@fkkt.uni-lj.si

Prejem rokopisa – received: 2006-01-23; sprejem za objavo – accepted for publication: 2006-10-09

Med vrsto postopkov mokre kemije, s katerimi poskušajo zagotoviti v produktu večjo homogenost na atomskem nivoju, večjo čistost ter večjo aktivnost prahov, je zgorevalna sinteza iz raztopin tista metoda, ki v zadnjem času hitro pridobiva na pomenu. Pri zgorevalni sintezi lantanovega kromita lahko izhajamo iz kovinskih nitratov, izbiramo pa lahko med različnimi reducenti (tetraformaltrisazin-TFTA, urea, glicin citronska kislina). V prispevku primerjamo nastanek lantanovega kromita med kalcinacijskim postopkom in v procesu zgorevalne sinteze iz citratno-nitratnega gela. Pri obeh postopkih smo pogoje za pripravo intermediarov izbrali na osnovi razultatov termične analize reakcijskih zmesi. Sestavo faz ter morfologijo vmesnih in končnih produktov smo določali z rentgensko praškovno in SEM-analizo.

Ključne besede: zgorevalna sinteza, lantanov kromit, nastanek

Several methods for the low-temperature synthesis of LaCrO₃ have been developed to achieve the compositional homogeneity, purity and activity of powders including combustion synthesis from the solutions. The reaction mixtures usually employ metal nitrates and different reducing agents, e.g., TFTA (teraformal trisazine), urea, glycine, and citric acid. In the present work the formation of LaCrO₃ in the calcining and in the combustion process was compared. In both procedures, intermediate formation temperatures were determined by thermal analysis. The intermediates and the final products were characterized by X-ray powder diffraction and by scanning electron microscopy.

Key words: combustion synthesis, lanthanum chromite, formation

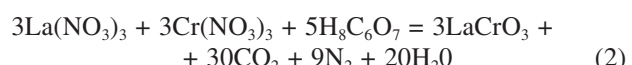
1 UVOD

Lantanov kromit spada zaradi svojih dobrih lastnosti (obstojnost pri visokih temperaturah, električna prevodnost) med spojine za pripravo materialov za elektrodo ali vmesnik v visokotemperurnih gorivnih celicah s trdnim elektrolitom. Vmesnik med seboj povezuje posamezne dele gorivne celice (katoda / trdni elektrolit / anoda). Uporablajo ga tudi kot grelni element ali obloga v visokotemperurnih pečeh¹.

Materiale na osnovi lantanovega kromita navadno pripravljamo s kalcinacijsko metodo iz oksidov, hidroksidov in karbonatov s ponavljanjem operacij mletja in žganja. Hitrost reakcij v trdnem je omejena z difuzijo, zato v novejšem času za pripravo teh materialov preizkušajo in uvajajo t. i. metode mokre kemije, npr. sol-gel-postopki², koprecipitacijska metoda³, metoda trdnih raztopin prekurzorjev⁴, zgorevalna sinteza⁵ in druge metode.

V primerjavi z enostavno reakcijo zgorevalne sinteze v trdnem je potek zgorevalne sinteze iz raztopin veliko bolj kompleksen. Kljub številnim raziskavam in enostavemu osnovnemu principu pogosto ostane nepojasnjen. Pri reakciji (enačba 1) trdnih komponent A in B v trdno komponento AB z dovolj visokim tališčem se reakcijska toplota redoks reakcije porabi izključno za nastanek enofaznega produkta in njegovo segrevanje. Pri zgorevalni sintezi iz raztopin pa se reakcijska toplota ne porablja le za nastanek in segrevanje končnih produktov (enačba 2), ampak tudi za vse transformacije in fazne

spremembe, ki v sistemu potekajo. Med zgorevalno sintezo iz citratno-nitratnega gela lahko poteka več zaporednih ali vzporednih reakcij⁶, čeprav jih med samo sintezo ne ločimo zaradi eksotermnosti in avtokatalitske narave procesa. Predvsem pa nanje pokaže analiza vmesnih in končnih produktov. Pri tovrstnih sintezah moramo računati tudi s toplotnimi izgubami ter temperaturnimi gradienti v reakcijski zmesi



Da bi razjasnili potek sinteze lantanovega kromita iz citratno-nitratnega gela, je bilo smiselno, da raziskave izvajamo v nedopiranem sistemu (LaCrO₃), kjer je število kristalnih faz, ki med reakcijo nastajajo, čim manjše. Nastanek lantanovega kromita smo poskušali pojasniti z analizo vmesnih produktov reakcije. Za primerjavo smo lantanov kromit sintetizirali s kalcinacijo iz lantanovega hidroksida in kromovega oksida.

2 EKSPERIMENTALNO DELO

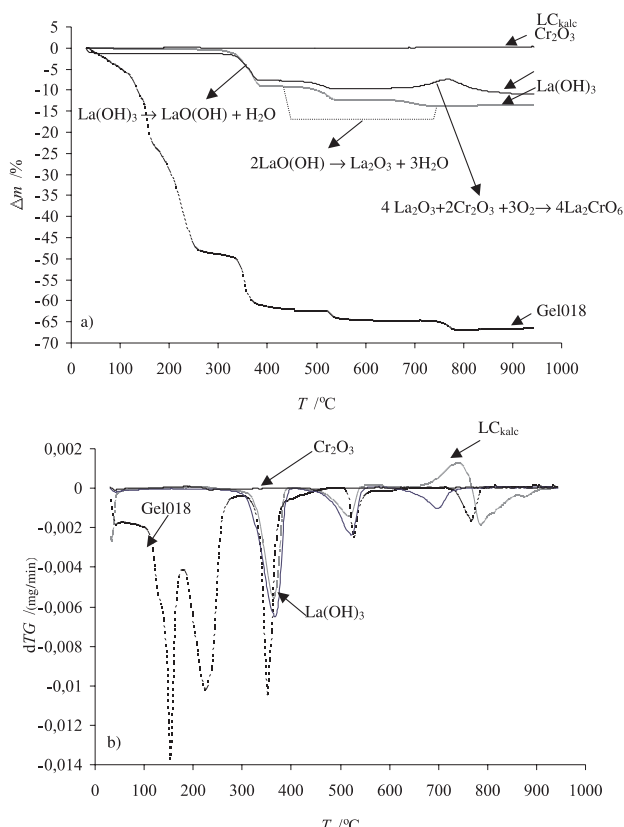
Gele, intermediate ter končni produkt smo pripravili iz citratno-nitratnih začetnih snovi. Reakcijske zmesi smo pripravili tako, da smo kovinske nitratre lantana in kroma raztopili v minimalni količini vode ter dodali vodno raztopino citronske kislino. Molsko razmerje med citronsko kislino in nitratnimi ioni je bilo 0,18. Reakcijsko zmes smo prenesli v 500-mililitrsko bučko ter jo

sušili pri temperaturi 60 °C in nižjem tlaku (vodna črpalka 2,7 kPa). Po sušenju smo citratno-nitratni gel uporabili za pripravo vmesnih produktov. Segrevali smo miligramske količine gelov do izbranih temperatur (170 °C, 310 °C, 380 °C, 600 °C in 800 °C) ter tako preprečili, da bi reakcija potekla avtokatalitsko do konca. Lantanov kromit smo pripravili tudi po kalcinacijskem postopku iz lantanovega hidroksida in kromovega oksida. Obe komponenti smo zatehtali v ustrezem mol-skem razmerju ter zmes ob dodatku etanola homogenizirali v ahatni ferilnici. Nato smo reakcijsko zmes stisnili v tablete (60 MPa, $\Phi = 6$ mm) ter jih žgali 4 h pri izbranih temperaturah (600 °C, 800 °C, 1000 °C).

Lastnosti reaktantov ter reakcijskih zmesi smo spremljali s termično analizo s termoanalizatorjem Mettler 3000. Rentgensko praškovno analizo vzorcev smo izvedli z difraktometrom tipa D4 ENDEAVOR X-ray Diffractometer (Bruker). Morfologijo vmesnih in končnih produktov smo spremljali z vrstičnim elektronskim mikroskopom JEOL T300.

3 REZULTATI IN DISKUSIJA

TG/DTG-analizo smo uporabili za določanje termičnih lastnosti reakcijskih zmesi za kalcinacijski postopek in za zgorevalno sintezo. V primeru kalcinacij-



Slika 1: a) TG- in b)DTG-analize Cr₂O₃, La(OH)₃ in reakcijskih zmesi LC_{kalc} ter Gel018 v zraku

Figure 1: a) TG and b) DTG curves of Cr₂O₃, La(OH)₃ and reaction mixtures LC_{kalc} and Gel018 in air

skega postopka smo analizirali tudi izhodni komponenti lantanov hidroksid ter kromov oksid (**Slika 1**).

Pri segrevanju kromovega oksida v izbranem temperaturnem območju med 20 °C in 950 °C pričakovano ni opaziti sprememb mase, nasprotno od lantanovega hidroksida, ki izgublja maso v več stopnjah. V prvi se pretvorji oksid v hidroksid. Dejanska izguba mase je 9,3 % in je v skladu s teoretično izračunano vrednostjo 9,5 %. Druga stopnja naj bi ustrezala nastanku lantanovega oksida,⁷ vendar v našem primeru ta reakcija poteče v temperaturnem intervalu med 440 °C in 740 °C, ko se izguba mase 4,6 % dobro ujema s teoretično izgubo 4,7 %. V reakcijski zmesi LC_{kalc} je potek do temperature 600 °C enak kot pri lantanovem hidroksidu, ko prične masa naraščati. Nastaja z lantanom bogata faza La₂CrO₆ pri reakciji oksidov s kisikom. Nad temperaturo 750 °C vzorec ponovno izgublja maso, kar pripisujemo reakciji La₂CrO₆ s Cr₂O₃. Po podatkih Kikkawe in soavtorjev⁸ lantanov kromit pri kalcinacijskem postopku nastaja nad temperaturo 900 °C, pri hidrazinskem postopku pa v temperaturnem intervalu med 780 °C in 840 °C. Pri naši sintezi iz hidroksida in oksida je temperatura nastanka nižja, kar je lahko posledica razlik v začetni stopnji priprave reakcijske zmesi in s tem nekoliko spremenjenega mehanizma nastanka perovskitne faze.

Citatno-nitratni gel prav tako izgublja maso v več stopnjah. Prvi dve sta posledica reakcije med nitratnimi ioni in citronsko kislino, tretja pa je gorenje organskega ostanka z zrakom, kar smo že obravnavali v pretklih raziskavah⁹. Pri temperaturi 530 °C kristalizira lantanov kromat (LaCrO₄). Nad temperaturo 744 °C poteka reakcija razpada lantanovega kromata po reakciji:



Z rentgensko struktурno analizo vmesnih in končnih produktov smo določili zaporedje nastanka faz pri obeh sinteznih postopkih. Pri vzorcu LC_{kalc} smo sestavo kristalnih faz določili po kalcinaciji pri 600 °C, saj pri temperaturah, nižjih od te, najprej poteče pretvorba lantanovega hidroksida v oksid. Vzorec je slabo kristaliziran in vsebuje z lantanom bogato fazo La₂CrO₆ ter Cr₂O₃ ter LaCrO₄. Po kalcinaciji pri 800 °C je v vzorcu le perovskitna modifikacija. Citratno-nitratni geli (Gel018) so po segrevanju do 170 °C, 310 °C in 380 °C amorfni, po segrevanju do 600 °C pa je v njih le LaCrO₄ v monoklinski modifikaciji. Po segrevanju do 800 °C vzorec Gel018 vsebuje le perovskitno modifikacijo lantanovega kromita. Rezultati rentgenske praškovne analize so skladni s termično analizo in kažejo na razliko v mehanizmu nastanka lantanovega kromita pri obeh uporabljenih sinteznih metodah. LaCrO₄ v vzorcu LC_{kalc} po kalcinaciji pri 600 °C dopušča možnost, da lantanov kromit nastaja po dveh mehanizmih. Po prvem nastaja lantanov kromit v reakciji faze, bogate z lantanom (La₂CrO₆), s kromovim oksidom, v drugi pa z razpadom LaCrO₄. Po podatkih iz literature v reakciji lantanovega hidroksida z amornim kromovim oksidom prevladuje

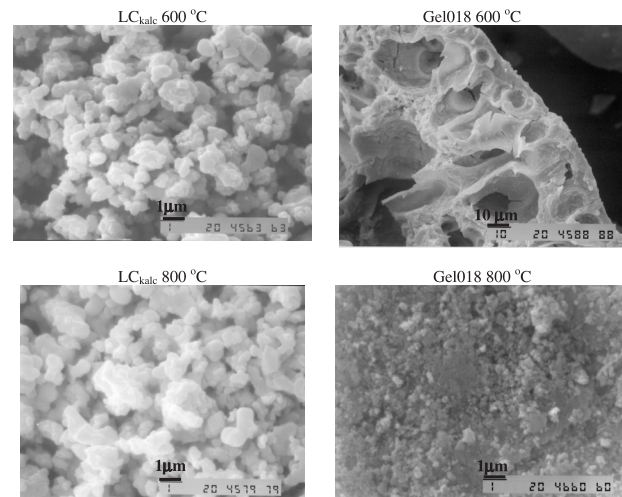
prvi mehanizem⁸. Navzočnost LaCrO₄ v produktih, pripravljenih s kalcinacijo, je možna zaradi uporabe etanola pri pripravi reakcijske zmesi. Reducent preprečuje oksidacijo kroma iz 3+ v 6+ ter s tem preprečuje nastanek lantanovega kromita izključno preko vmesnega La₂CrO₆. Pri zgorevalni sintezi blizu stehiometrijskega citratno-nitratnega razmerja je mehanizem nastanka lantanovega kromita vezan na reakcijo razpada lantanovega kromata (enačba 3). V predhodnih raziskavah smo perovskitno fazo potrdili v vseh vzorcih, pripravljenih z zgorevalno sintezo za citratno nitratna razmerja c/n od 0,18 do 0,28¹⁰. Druge faze pa so bile vezane na obliko reakcijske zmesi pri zgorevalni sintezi. Pri sintezi v plasti je stik med delci gela nepopoln, v produktu je podobno kot pri kalcinacijskem postopku navzoč tudi La₂CrO₆, ki lahko nastane zaradi temperaturnih gradientov in zaradi kratkih časov pri temperaturi sinteze.

Tabela 1: Kristalne faze v intermediatih, pripravljenih s kalcinacijskim postopkom in z citratno-nitratnega gela

Table 1: Crystallographic modifications in intermediates prepared by calcining and citrate-nitrate

Vzorec	T _{kalcinacije} °C	Glavne kristalne faze
Gel018	170	amorfen
Gel018	310	amorfen
Gel018	380	amorfen
Gel018	600	LaCrO ₄
Gel018	800	LaCrO ₃
LC _{kalc}	600	La ₂ CrO ₆ , Cr ₂ O ₃ , LaCrO ₄
LC _{kalc}	800	LaCrO ₃

Slika 3 prikazuje vzorca LC_{kalc} in Gel018 po topotni obdelavi pri temperaturah 600 °C in 800 °C. Vzorec LC_{kalc}, kalciniran pri 600 °C, je v obliki mikrometrskih zrn, ki se deloma povezujejo v aglomerate, medtem ko je vzorec LC_{kalc} po kalcinaciji pri 800 °C sestavljen



Slika 3: Posnetki vzorcev LC_{kalc} in Gel018 po različni topotni obdelavi

Figure 3: SEM micrographs samples LC_{kalc} in Gel018 after different thermal treatment

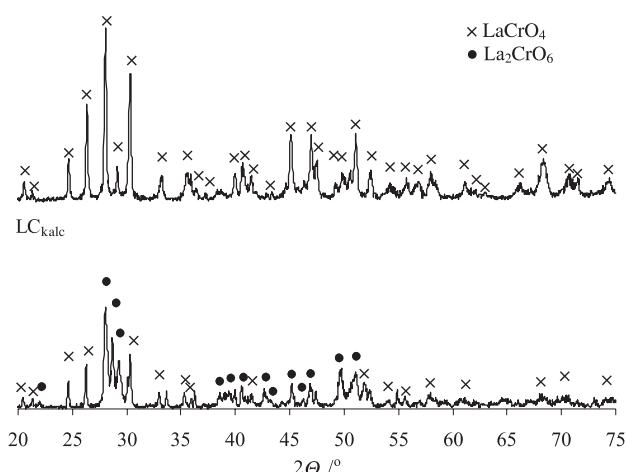
pretežno iz aglomeratov, večjih od 2 µm. V temperaturnem intervalu od 600 °C do 800 °C se La₂CrO₆ in LaCrO₄ pretvorita v perovskitno modifikacijo, kar pa se ne izraža v spremembji morfologije. Vzorec Gel018, segret do 600 °C, ima značilno cevasto zgradbo voluminoznih aglomeratov, ni pa opaziti izrazitejše zrnate strukture. Pri segrevanju vzorca Gel018 do 800 °C enako kot pri kalcinacijskem postopku nastane perovskitna modifikacija, ki jo spremlja očitna sprememba morfologije vzorca. Vzorec sestavlja zrna velika do 0,5 µm, ki niso povezana v aglomerate. Skladno z drugimi metodami karakterizacije se razlika v mehanizmu nastanka lantanovega kromita pri kalcinacijskem postopku in pri zgorevalni sintezi izraža tudi pri morfologiji.

4 SKLEP

Nastanek lantanovega kromita pri zgorevalni sintezi iz citratno-nitratnega gela smo poskušali pojasniti z analizo vmesnih produktov reakcije. Za primerjavo smo lantanov kromit sintetizirali s kalcinacijo iz lantanovega hidroksida in kromovega oksida.

V reakcijski zmesi kalcinacijskega postopka so termične lastnosti do temperature 600 °C enake kot pri lantanovem hidroksidu, ki v tem temperaturnem intervalu izgublja vodo. Naraščanje mase, ki sledi, je povezano z nastankom z lantanom bogate faze La₂CrO₆ pri reakciji kovinskih oksidov s kisikom. Nad temperaturo 750 °C vzorec ponovno izgublja maso, kar pripisujemo reakciji La₂CrO₆ s Cr₂O₃. Temperatura nastanka lantanovega kromita je v našem primeru nižja od pričakovane, kar je lahko posledica razlik v pripravi reakcijske zmesi pri kalcinacijskem postopku.

V citratno-nitratnih gelih pri segrevanju sledi več stopenj. V prvih dveh tečeta reakciji med nitratnimi ioni in citronsko kislino, tretja pa je gorenje organskega



Slika 2: Praškovni posnetki LC_{kalc} in gela018 po kalcinaciji pri 600 °C

Figure 2: Phase development of samples LC_{kalc} and Gela018 during thermal treatment at 600 °C

ostanka z zrakom. Kromatna faza kristalizira pri temperaturi 530 °C, nad temperaturo 744 °C pa razpada do kromita.

Mehanizem nastanka lantanovega kromita se pri sinteznih metodah kalcinacije in zgorevalne sinteze razlikuje. Pri zgorevalni sintezi lantanov kromit nastane v reakciji razpada lantanovega kromata. Ta je tudi v vzorcu, pripravljenem s kalcinacijo po segrevanju pri 600 °C, kar kaže na to, da lantanov kromit nastaja po dveh mehanizmih. Pri prvem nastaja v reakciji faze, bogate z lantanom (La_2CrO_6), s kromovim oksidom, pri drugem pa z razpadom LaCrO_4 . Navadno pri rekacijeh hidroksidov z oksidi prevladuje prvi mehanizem.

5 LITERATURA

- ¹ A. Shiryaev, M. D. Nevsasyan, N. Q. Ming, D. Luss, *Thermodinamic feasibility of SHS of SOFC materials*, J. Mater Synth. and Process, 7 (1999), 83–90
- ² S. Bilger, G. Blass and R. Forthmann, *Sol-gel Synthesis of Lanthanum Chromite Powder*, J. Eur. Ceram. Soc., 17 (1997) 1027–1031
- ³ M. R. De Guire, S. E. Dorris, R. B. Poeppel, S. Morissette, U. Balachandran, *Coprecipitation synthesis of doped lanthanum chromite*, J. Mater. Res., 8 (1993), 2327–2335
- ⁴ K. Vidyasagar, J. Gopalkrishnan, N. Rao, A convenient route for the synthesis of complex metal oxides employing solid solutions precursors, Inor. Chem., 23 (1984), 1206–1210
- ⁵ Y Zhang, G. C. Stangle, Preparation of fine multicomponent oxide ceramic powder by a combustion synthesis process, J. Mater. Res., 9 (1994) 1997–2004
- ⁶ R. Sukumar, A. Das Sharma, S. N. Roy, H. S. Maiti, *Synthesis of $\text{YBa}_2\text{Cu}_3\text{O}_{7-x}$ powder by autoignition of citrate-nitrate gel*, J. Mater. Res., 8 (1993), 2761–2766
- ⁷ A. Neumann, D. Walter, The thermal transformation from lanthanum hydroxide to lanthanum hydroxide oxide, Thermochimica Acta, 445 (2006), 200–204
- ⁸ T. Kikkawa, M. Yoshinava, K. Hirota and O. Yamaguchi, *Synthesis of LaCrO_3 by the Hydrazine Method*, J. Mater. Sci. Lett., 14 (1995), 1071–1073
- ⁹ K. Zupan, D. Kolar, Študij citratno-nitratnih gelov za pripravo keramike na osnovi LaCrO_3 , Kovine zlit. tehnol., 32 (1998), 355–358
- ¹⁰ K. Zupan, S. Pejovnik, J. Maček, Synthesis of nanometer crystalline lanthanum chromite powders by the citrate-nitrate autoignition reaction, Acta Chim. Slov., 48 (2001), 137–145

DINAMIČNE MEHANIČNE LASTNOSTI ELASTOMERNIH KOMPOZITOV S POLNILI NANOVELIKOSTI

DYNAMIC MECHANICAL PROPERTIES OF ELASTOMERIC COMPOSITES WITH NANO-SCALE FILLERS

Zoran Šušterič, Tomaž Kos, Marija Šuštar

Savatech, d. o. o., Razvojni institut, Škofjeloška 6, 4502 Kranj, Slovenija
zoran.susteric@sava.si

Prejem rokopisa – received: 2006-09-18; sprejem za objavo – accepted for publication: 2006-10-12

V delu je prikazan način preučevanja reoloških lastnosti elastomernih kompozitov z organsko modificirano montmorillonitno glino kot nanopolnilom z uporabo deformacijskih, temperaturnih in količinskih odvisnosti njihovih dinamičnih mehaničnih funkcij, tj. dinamičnega prožnostnega modula in modula izgub. Pri tem je uporabljen teoretični model, ki poleg razlage vedenja dinamičnih funkcij omogoča tudi določitev značilnih energij za deformacijski in toplotni razpad notranje sekundarne strukture teh nanokompozitov.

Ključne besede: elastomer, glina, nanokompozit, reološke lastnosti

The work presents an approach of studying rheological properties of elastomeric composites with organically modified Montmorillonite clay, as nanofiller, by deformational, temperature and content dependence of their dynamic mechanical functions, i.e. the storage and loss moduli. Within this frame a theoretical model has been used, which, apart from elucidation of dynamic functions, also enables determination of characteristic energies for deformational and thermal breakdown of the nanocomposite internal secondary structure.

Keywords: elastomer, clay, nanocomposite, rheological properties

1 UVOD

V zadnjih nekaj letih se je zanimanje za uporabo nanopolnil, posebno določenih vrst gline¹ kot ojačevalnih in toplotnostabilizacijskih dodatkov elastomerom močno povečalo. Nanopolnila imajo veliko specifično površino in zato lahko v elastomerih že v razmeroma majhnih količinah učinkovito nadomestijo klasična aktivna polnila, na primer saje ali siliko. Poleg kemijske sestave, zgradbe, velikosti in površinskih značilnosti delcev nanopolnil to dejstvo potrjujejo tudi reološke analize nastalih elastomernih nanokompozitov^{1,2}.

To delo podaja rezultate reološkega preučevanja kompozitov iz naravnega kavčuka in organsko modificirane montmorillonitne gline, dobljenih z mešanjem v talini. S sekundarnimi interakcijami delci gline med seboj in s kavčukovimi molekulami ustvarjajo vezi ter tako sekundarno mrežo. Ker je zaradi površinsko aktivne gline gostota nastalih vezi velika, so prožnostni moduli takšnih mrež pri majhnih deformacijah in zmernih temperaturah visoki. Vendar zaradi šibkosti sekundarnih vezi z večanjem deformacije in/ali temperature začne mreža razpadati v energijsko disipacijskem procesu, kar je reološko možno spremeljati. V ta namen je posebno primerna periodična deformacija z merjenjem kompozitovih dinamičnih mehaničnih funkcij, to je dinamičnega prožnostnega modula in modula izgub, v odvisnosti od deformacije in temperature. Za razumevanje

rezultatov je uporabljen statističnomehanični model^{3,4}, s katerim je omogočena tudi določitev značilnih energij mehaničnega in toplotnega razpada mreže in s tem kvantitativna označba teh nanovelikostnih učinkov v elastomerih.

2 TEORETIČNI DEL

Z interkalacijo elastomernih molekul v glini in eksfoliacijo delcev gline med mešanjem se zaradi medsebojnih elektrostatičnih interakcij v snovi ustvarijo multifunkcionalne vezi in s tem ustrezna tridimensionalna mreža. Ker so tovrstne interakcije kratkega dosega van der Waalsove vrste, so nastale vezi v primerjavi s kovalentnimi ali ionskimi vezmi šibke⁵ z značilnimi energijami v območju 5–50 kJ mol⁻¹. Mehanični in toplotni učinki zato močno vplivajo na stabilnost posledične sekundarne mreže. Že pri majhnih deformacijskih in/ali temperaturnih dvigih začnejo vezi in s tem sekundarna mreža razpadati, kar je jasno razvidno iz poteka dinamičnih mehaničnih funkcij nanokompozita, saj je po teoriji gumene prožnosti prožnostni modul sorazmeren z gostoto vezi⁶, modul izgub pri danih pogojih pa z njeno spremembo. Za takšne mreže pa je pri tem značilno, da se v mirovanju po določenem času reformirajo, kar se sicer pri porušenih mrežah s kovalentno vezavo ne zgodi nikoli.

2.1 Vpliv deformacije

Načelno je vseeno, katere vrste oscilirajoča deformacija se uporabi pri preučevanju odvisnosti dinamičnih mehaničnih funkcij nanokompozitov od njene velikosti. Da bi se izognili določenim teoretičnim in tudi merilnim nerodnostim, zlasti pri velikih deformacijah, je ugoden strig, saj so strižni prožnostni moduli, nasprotno od nateznih ali kompresijskih, dobro definirani v znatno širšem deformacijskem območju⁷.

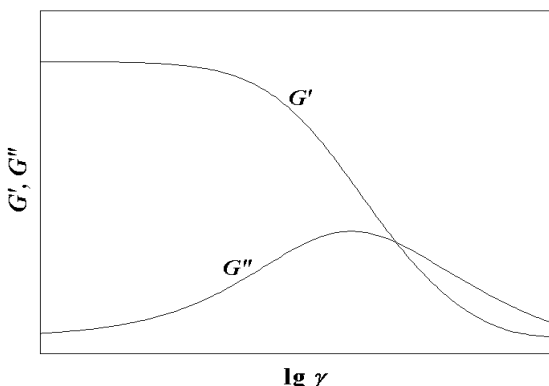
Tako ima pri majhnih (strižnih) deformacijah dinamični (strižni) prožnostni modul kompozita G' visoko vrednost, saj je gostota sekundarnih vezi visoka. Z naraščajočo deformacijo (ker gre za periodično deformiranje, je mišljena amplituda strižne deformacije γ) se zaradi razpadanja vezi njihova gostota manjša in G' monotono pojema z začetne proti nizki končni vrednosti, ko je sekundarna mreža v celoti porušena. Ker je razpad sekundarne mreže disipacijski proces, pa (strižni) modul izgub G'' po drugi strani, z začetne nizke vrednosti naraste in preide maksimum, ko je razpad najmočnejši, ter nato pojema, podobno kot G' . Pri tem pa je treba opozoriti tudi na disipacijo energije zaradi notranjega trenja, ki je močno odvisna od frekvence in vpliva na vrednost G'' , zlasti pri majhnih deformacijah. Deformacijski potek dinamičnih mehaničnih funkcij pri razpadu sekundarne mreže je shematično prikazan na sliki 1.

S statistično mehaniko verigastih molekul in statistiko razpada sekundarne mreže je možno priti do naslednjih analitičnih izrazov deformacijske odvisnosti dinamičnih mehaničnih funkcij $G'(\gamma)$ in $G''(\gamma)$ ^{3,4}:

$$G'(\gamma) = G'(0) (1 + W_r \gamma / RT) \exp(-W_r \gamma / RT) \quad (1)$$

$$G''(\gamma) = G''(\gamma_{\max}) (W_r \gamma / RT) \exp(1 - W_r \gamma / RT) \quad (2)$$

kjer sta $G'(0)$ in $G''(\gamma_{\max})$ maksimalni vrednosti dinamičnih strižnih modulov, R plinska konstanta, T temperatura in W_r značilna energija za deformacijski razpad sekundarne mreže, ki jo je možno določiti iz enačb (1) in (2) ter meritev $G'(\gamma)$ in $G''(\gamma)$. Energija W_r je odvisna



Slika 1: Deformacijska odvisnost dinamičnih mehaničnih funkcij nanokompozitov

Figure 1: Deformational dependence of nanocomposites' dynamic mechanical functions

še od vsebnosti polnila in temperature, vendar je deformacijsko neodvisna pri majhnih deformacijah. Z večanjem deformacije postane odvisna tudi od slednje $W_r = W_r(\gamma)$:

$$W_r(\gamma) = W_r(\infty) + \{1/[W_r(0) - W_r(\infty)] + \gamma/3RT\}^{-1} \quad (3)$$

kjer sta $W_r(0)$ in $W_r(\infty)$ za dano sekundarno mrežo od deformacije neodvisni konstanti s pričakovanimi vrednostmi v območju, značilnem za energije sekundarnih interakcij.

Enačbi (1) in (2) napovedujeta asimptotično deformacijsko pojemanje strižnih modulov proti ničli, namesto proti nizkima, vendar končnima vrednostima $G'(\infty)$ in $G''(\infty)$. Strogo vzeto bi bilo to treba upoštevati, v resnici pa je nebistveno, ker sta ti vrednosti zelo majhni in praviloma doseženi zunaj merilnega območja praktičnega pomena.

2.2 Vpliv temperature

Pri dani temperaturi sekundarne vezi nastajajo in razpadajo v dinamičnem ravnovesju, tako da njihova povprečna gostota ostane konstantna. S sprememboto temperature se gostota ustali pri drugi vrednosti, nižji, če je temperatura višja, saj je med sprememboto zaradi močnejšega termičnega gibanja molekul razpad vezi verjetnejši od nastanka. Za takšno dogajanje statistična mehanika napoveduje termično aktivacijsko temperaturno odvisnost gostote vezi $n(T)$ Arrheniusove oblike: $n(T) \propto \exp(E_a/RT)$, kjer je E_a aktivacijska energija za toplotni razpad sekundarne mreže.

Po drugi strani teorija gumene prožnosti napoveduje premo sorazmernost prožnostnega modula z gostoto vezi in temperaturo⁶ $G' \propto nT$. Z upoštevanjem $n(T)$ za temperaturno odvisnost modula izhaja⁴:

$$G'(T) \propto T \exp(E_a/RT) \quad (4)$$

Izkaže se, da ta zveza drži z visoko natančnostjo. Vrednosti aktivacijske energije za toplotni razpad mreže E_a so prav tako v območju, značilnem za energije sekundarnih interakcij. Podobna temperaturna odvisnost velja tudi za G'' , le da ima aktivacijska energija zaradi notranjega trenja nekoliko drugačno vrednost.

2.3 Vpliv vsebnosti polnila

Glina kot nanopolnilo v elastomeru deluje ojačevalno, tako zaradi nastanka sekundarnih vezi kot tudi zaradi povečanega notranjega trenja. Delovanje je obenem toplotno stabilizacijsko, saj vezi omejujejo molekulsko gibljivost. Podrobna analiza pokaže, da je za ne prevelike koncentracije polnila ojačevalni učinek, izrazen z odvisnostjo dinamičnega prožnostnega modula kompozita od volumenskega deleža gline ϕ_v , naslednji⁴:

$$G'(\phi_v) \approx G'(0) \exp(\kappa \phi_v) \quad (5)$$

kjer je κ snovna konstanta, značilna za sistem elastomer/nanopolnilo.

3 EKSPERIMENTALNI DEL

Eksperimentalni del zajema pripravo vzorcev nanokompozitov in merjenje dinamičnih mehaničnih funkcij v različnih odvisnostih.

3.1 Snovi in priprava vzorcev

Vzorci so bili pripravljeni z mešanjem elastomerne taline z organsko modificirano montmorillonitno glino in premreževalnim sistemom v gnetilnem mešalniku (Brabender Plastograph) 10 min ob začetni temperaturi glave mešalnika 60 °C in hitrosti 60 r/min, pri čemer so bile uporabljene naslednje snovi:

- naravni kavčuk SMR 10 z viskoznostjo po Mooneyu (ML (1+4) 100 °C) 89
- kemijsko modificirana montmorillonitna glina (Dellite 67G)
- nemodificirana glina (Dellite LVF)
- premreževalni sistem (žveplo, cinkov oksid, stearinska kislina, TBBS)

Tako so bili narejeni kompoziti z 10, 25 in 35 masnimi deli gline na 100 delov kavčuka, količinska sestava premreževalnega sistema pa je bila v skladu s standardom ISO 1659. Za odpravo morebitnih notranjih napetosti, nastalih med mešanjem, so vzorci počivali najmanj 24 h pred preskušanjem.

3.2 Merjenje

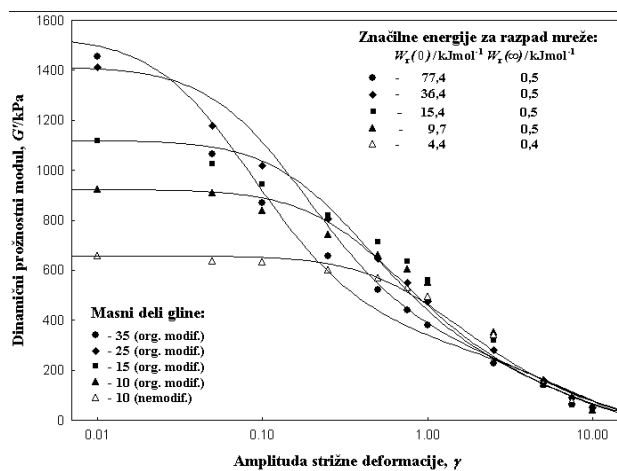
Merjenje dinamičnih mehaničnih funkcij je bilo izvedeno z instrumentom Rubber Process Analyser RPA 2000 (Alpha Technologies) v območju amplitud strižne deformacije 0,01–10 ter v temperaturnem območju 40–100 °C, vse pri frekvenci 0,3 Hz. Ta frekvenca je dovolj nizka, da lahko med meritvijo molekulski deli med topološko sosednjimi vezmi nemoteno spremenijo svoje konformacije, s čimer je zagotovljena varnost pred neželenimi pojavi, na primer elastičnim izbruhom⁸.

Predhodno premreženje (vulkanizacija) vzorcev je bilo izvedeno z istim instrumentom pri temperaturi 160 °C v trajanju do dosega 90-odstotne stopnje premreženja (t_{90}).

4 REZULTATI IN DISKUSIJA

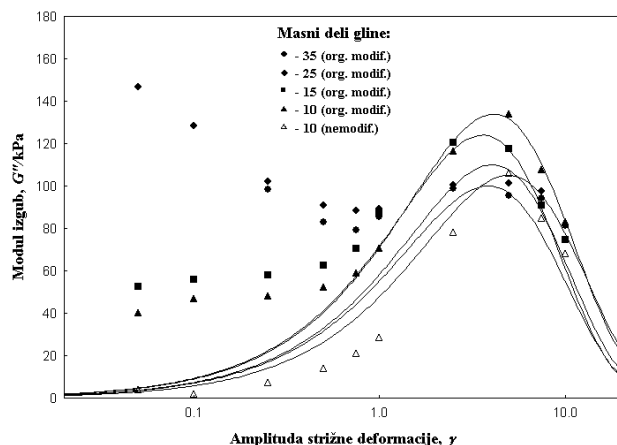
4.1 Vpliv deformacije

Na slikah 2 in 3 sta prikazani dinamični mehanični funkciji $G'(\gamma)$ in $G''(\gamma)$ kovalentno premreženih nanokompozitov z različnimi vsebnostmi gline, pri čemer so točke dobljene eksperimentalno, krivulje pa so izračunane z enačbama (1) in (2). Razmeroma dobro ujemanje modela z eksperimentom je doseženo v primeru $G'(\gamma)$, ujemanje $G''(\gamma)$ pa je slabše, in pri nizkih deformacijah ga sploh ni. Razlog je v tem, da model ne zajema notranjega trenja, ki je pri nizkih deformacijah znatno, pri visokih pa se manjša. Zaradi tega je ujemanje izračunanega $G''(\gamma)$ z izmerjenim nekoliko boljše pri višjih deformacijah.



Slika 2: Deformacijska odvisnost dinamičnega prožnostnega modula elastomernih nanokompozitov z različnimi vsebnostmi gline pri frekvenci 0,3 Hz in temperaturi 40 °C

Figure 2: Deformational dependence of storage modulus for elastomeric nanocomposites of different clay contents at frequency of 0.3 Hz and temperature of 40 °C



Slika 3: Deformacijska odvisnost modula izgub elastomernih nanokompozitov z različnimi vsebnostmi gline pri frekvenci 0,3 Hz in temperaturi 40 °C

Figure 3: Deformational dependence of loss modulus for elastomeric nanocomposites of different clay contents at frequency of 0.3 Hz and temperature of 40 °C

Slike 2 je razviden močan vpliv vsebnosti gline na $G'(\gamma)$ pri nizkih deformacijah. Poleg ojačevalnega učinka, ki je sicer eksplisitno opisan z enačbo (5), je opazno hitrejše pojemanje G' pri deformirajujočem kompozitu z višjimi vsebnostmi gline. To je posledica gostejše sekundarne mreže, v kateri je povprečna razdalja med vezmi krajša, porazdelitev razdalj pa ožja kot pri redkejših mrežah. Zato začne gostejša mreža razpadati pri nižjih deformacijah in hitreje. To se izraža tudi v velikostih za mehanični razpad značilnih energij $W_r(0)$ (slika 2). Odvisnost od vsebnosti gline pa se z naraščajočo deformacijo manjša in pri velikih deformacijah popolnoma izgine. To je razumljivo, saj je v tem deformacijskem stanju mreža praktično porušena in

nizke vrednosti značilne energije $W_r(\infty)$ so za različne vsebnosti gline enake.

Z vidika aktivnih polnil v elastomerih so nekoliko presenetljivi poteki $G''(\gamma)$, predvsem vrednosti $G''(\gamma_{\max})$, glede na vsebnost gline. Pri kompozitih s sajami ali siliko $G''(\gamma_{\max})$ z vsebnostjo narašča, tako zaradi razpada vezi kot zaradi notranjega trenja. Pri kompozitih z organsko modificirano gline pa velike gostote nastalih sekundarnih vezi očitno tako omejijo notranje trenje, da so $G''(\gamma_{\max})$ kompozitov z večjimi vsebnostmi gline, kljub obsežnejšemu deformacijskemu razpadanju vezi in s tem ustrezni energijski disipaciji, nižji od $G''(\gamma_{\max})$ manjših vsebnosti. Takšno vedenje je še ena reološka posebnost elastomernih nanokompozitov.

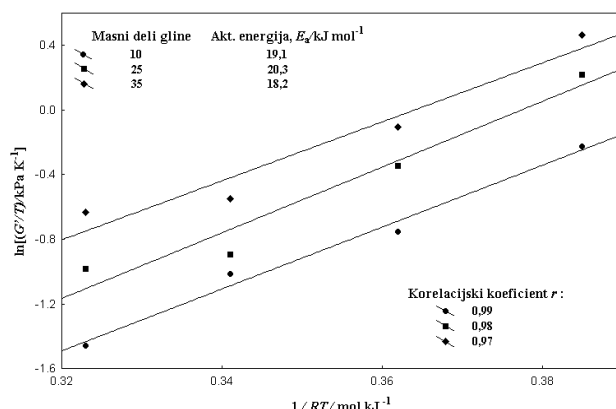
4.2 Vpliv temperature

Na sliki 4 je predstavljena temperaturna odvisnost dinamičnega prožnostnega modula elastomernih kompozitov z različnimi vsebnostmi gline. Glede na sorazmerje (4) je odvisnost podana v obliki $\ln[G'(T)/T]$ kot funkcija $1/RT$, pri čemer so za G' vzete začetne deformacijske vrednosti, tj. pri $\gamma = 0$.

Kot prikazuje slika, je eksperimentalno ujemanje s sorazmerjem (4) dobro, z visoko korelacijo. Aktivacijske energije, podane na sliki, so v značilnem območju energij vezi van der Waalsove vrste, dobro ujemanje pa obenem potrjuje napoved, da je topotna porušitev sekundarne mreže termično aktiviran proces. Pri tem podobne vrednosti aktivacijske energije za kompozite različnih vsebnosti gline pomenijo, da vsebnost nanopolnila bistveno ne vpliva na kinetiko topotnega razpada.

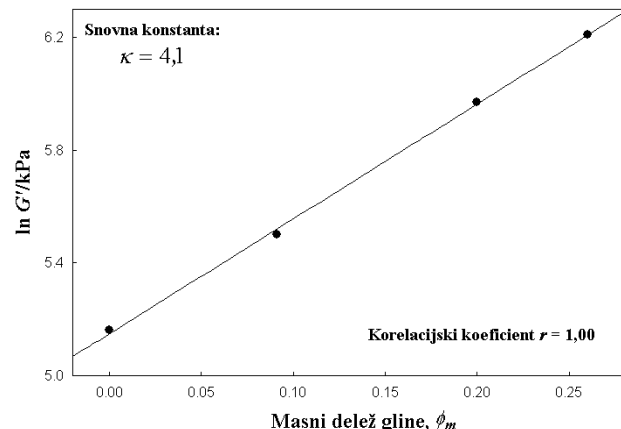
4.3 Vpliv vsebnosti polnila

Ojačevalni učinek gline v elastomeru je podan v obliki eksponentne odvisnosti dinamičnega prožnostnega



Slika 4: Temperaturna odvisnost dinamičnega prožnostnega modula elastomernih kompozitov z različnimi vsebnostmi gline pri frekvenci 0,3 Hz

Figure 4: Temperature dependence of storage modulus for elastomeric composites of different clay contents at zero strain amplitude and frequency of 0.3 Hz



Slika 5: Odvisnost dinamičnega prožnostnega modula elastomernih kompozitov od vsebnosti gline pri amplitudi deformacije nič in frekvenci 0,3 Hz

Figure 5: Dependence of storage modulus for elastomeric composites on clay content at zero strain amplitude and frequency of 0.3 Hz

modula G' od volumenskega deleža gline ϕ_v z enačbo (5). V sistemih elastomer/polnilo je volumenske deleže polnila težko določiti z merjenjem, enostavno pa jih je izračunati z masnim deležem ϕ_v in gostoto. Vendar, ker se gostote kompozitov z različnimi vsebnostmi gline med seboj le malo razlikujejo, je razlika med ϕ_v in ϕ_m dovolj majhna, da je ϕ_v možno nadomestiti z ϕ_m . Zato je na sliki 5 odvisnost G' (vrednosti pri $\gamma = 0$) od vsebnosti gline podana kar z napovedano (z enačbo 5) linearno zvezo $\ln G' - \phi_m$, pri čemer naklon podaja za dan sistem elastomer/glinu značilno konstanto κ .

Slike je razvidno, da je napoved potrjena z visoko korelacijo, kar je dodatni pokazatelj ustreznosti modela za obravnavo reoloških lastnosti mrež s sekundarno vezavo.

5 SKLEP

Način reološkega preučevanja nanokompozitov elastomer/glini z dinamičnima mehaničnima funkcijama, tj. z dinamičnim prožnostnim modulom in modulom izgub, se je pokazal kot primeren. Vsaka spremembva v sekundarni tridimenzionalni mreži, ki jo z van der Waalsovo vezavo gline ustvarja z elastomernimi molekulami in ki je glavni nosilec obremenitev nanokompozita, se izraža v vedenju dinamičnih funkcij, kar je eksperimentalno možno učinkovito spremljati.

Za razumevanje dogajanja na nanoravnini je pri tem prav tako učinkovita uporaba teoretičnega modela deformacijskega in topotnega razpada sekundarnih mrež v elastomernih sistemih z nanopolnilom, saj razmeroma dobro ujemanje njegovih napovedi z izmerjenimi dinamičnimi mehaničnimi funkcijami, posebno v primeru dinamičnega prožnostnega modula, potrjuje ne le obstoj takšnih mrež, temveč tudi verodostojnost samega modela. Vsekakor pa je ob tem najpomembnejše, da model, sprejet z navedenimi pokazatelji kot prepričljiv, omogoča zanesljivo določitev dveh energij, ki kvanti-

tativno označujeta sekundarne mreže: značilne energije za mehanični razpad in aktivacijske energije za topotno porušitev mreže. Njune vrednosti so v območju, značilnem za energije sekundarnih interakcij.

Končno, izkazalo se je, da je z uporabljenim modelom možna tudi kvantitativna karakterizacija tovrstnih nanokompozitov z ozirom na vsebnost gline, kar lahko neposredno koristi pri načrtovanju uporabe.

6 LITERATURA

- ¹R. Krishnamoorti, A. S. Silva in Polymer-clay nanocomposites (T. J. Pinnavaia and G. W. Beall Eds.), Wiley, New York, 2000, Chap. 15
- ²L. H. Sperling, Introduction to physical polymer science, Wiley, New York, 2006, Chap. 13.
- ³Z. Susteric et al., *Acta Chim. Slov.* 46 (1999), 69
- ⁴Z. Susteric, I. Dimitrijević, *Int. J. Polym. Materials* 52 (2003), 527
- ⁵D. Frenkel in Soft and fragile matter (M. E. Cates, M. R. Evans Eds.), SUSSP Publications and Institute of Physics Publishing, Edinburg, London, 2000, 115
- ⁶I. M. Ward, J. Sweeney, An introduction to the mechanical properties of solid polymers, Wiley, New York, 2004, Chap. 3
- ⁷C. W. Macosko, Rheology: principles, measurements and applications, Wiley, New York, 1994, Chap. 1
- ⁸M. Kralj Novak et al., *Kovine zlit. tehnol.* 29 (1995), 251

FRACTURE TOUGHNESS OF A HIGH-STRENGTH LOW-ALLOY STEEL WELDMENT

ŽILAVOST LOMA ZVARA VISOKOTRDNEGA MALOLEGIRANEGA JEKLA

Jelena Tuma¹, Nenad Gubeljak², Borivoj Šuštaršič¹, Borut Bundara³

¹Institute of Metals and Technology, Lepi pot 11, 1000 Ljubljana, Slovenia

²University of Maribor, Faculty of Mechanical Engineering, Smetanova 17, 2000 Maribor, Slovenia

³Institute of Metals Constructions, Mencingerjeva 7, 1000 Ljubljana, Slovenia
jelena.tuma@imt.si

Prejem rokopisa – received: 2006-05-17; sprejem za objavo – accepted for publication: 2006-11-15

The use of high-strength low-alloy steels for high-performance structures, e.g., pressure vessels and pipelines, requires often high-strength consumables to produce an overmatched welded joint. This globally overmatched welded joint contains local mis-matched regions, which can affect the unstable fracture behaviour of the welded joint and the welded structure itself. If local mis-matched regions are present in the vicinity of a crack tip, then the fracture toughness of the weld metal can be significantly lower than that of the base metal. In this paper, the influence of the weld-metal microstructure on the fracture behaviour is estimated enabling an evaluation of the resistance to stable crack growth through different microstructures. The lower bound of the fracture toughness for different microstructures was evaluated using a modified Weibull distribution. The results, obtained using specimens with a through thickness crack front, indicated a low fracture toughness, caused by the strength mis-matching interaction along the crack front. In the case of through-the-thickness specimens, at least one local brittle zone (LBZ) or a local soft region is incorporated into the process zone in the vicinity of the crack tip. Hence, an unstable fracture occurred with small stable crack propagation, or without it. Despite the fact that the differences between the impact toughness of the weld metal and the base metal can be insignificant, the fracture toughness of a weld metal can be significantly lower.

Key words: fracture mechanics, welded joint, crack-tip opening displacement, resistance curves

Uporaba visokotrdnih malolegiranih jekel za zelo obremenjene strukture, npr. posode pod pritiskom in cevovode, zahteva uporabo varilnega materiala, ki ustvari zvar z večjo trdnostjo. Taki zvari vsebujejo lokalna področja z mešano trdnostjo, ki lahko vplivajo na nestabilno lomno vedenje zvara in zvarjene strukture. Če mešana področja ležijo v bližini vrha razpoke, je lahko žilavost loma pomembno manjša kot pri osnovnem materialu. V tem delu je ocenjen vpliv mikrostrukture zvara na vedenje pri lomu, kar omogoča oceno odpornosti proti stabilnemu širjenju razpoke skozi različne mikrostrukture. Nižja vrednost žilavosti loma je bila ocenjena za različne mikrostrukture z modificirano Weibullovo porazdelitvijo. Rezultati, ki so bili dosegzeni pri vzorcih z razpoko preko debeline, so pokazali nizko žilavost loma zaradi različne trdnosti vzdolž čela razpoke. V primeru vzorcev z razpoko preko debeline je vsaj eno lokalno krhko področje (LBZ) ali lokalno mehko področje vključeno v procesno področje v bližini vrha razpoke. Zato se je stabilna propagacija razpoke izvršila z majhnim stabilnim širjenjem ali brez njega. Čeprav so majhne razlike med udarno žilavostjo zvara in osnovnega materiala, je lahko žilavost loma zvara pomembno manjša.

Ključne besede: mehanika loma, zvarni spoj, premik vrha odprtja razpoke, krivulje odpornosti

1 INTRODUCTION

Strength-overmatched welded joints are designed to ensure the safe service of a welded structure by keeping the flaws, e.g., planar defects, in an elastic weld metal, while the base metal starts to yield. Such an approach ensures that a welded structure can sustain local plastic deformation, important when temporary overloading or geometrical changes occur. These changes can be caused by temperature variations during a structures service life. The strength-overmatching requirement presents no special problems for steel with yield strength of less than 600 MPa¹, but in case of steels with higher yield strengths, e.g., above 700 MPa, locally undermatched regions can occur. Such an overmatched weld joint is quite sensitive to planar cracks developing from defects. Thus, a higher stress concentration around the planar defects in a weld metal in locally undermatched regions can cause unstable fracture behaviour². In this case a

significant range of experimentally fracture-toughness values is obtained. It is possible, however, to overcome this problem by determining the lower bound fracture toughness, which can ensure the structural integrity and a safe service life. The lower-bound fracture-toughness value represents the value where the crack propagation occurred. If the stress intensity factor (caused by applied load) is lower than the lower-bound fracture toughness, than crack propagation does not appear. This paper presents a procedure for determining the lower-bound fracture toughness of laboratory specimens cut from a critically overmatched weld joint. The influence of the weld-metal microstructure on the fracture behaviour is estimated, enabling an evaluation of the resistance to stable crack growth through different microstructures, as well as an evaluation of the relevant value of the lower bound of the fracture toughness. Reasons for the range of experimentally measured fracture-toughness values are also presented.

2 MATERIALS AND WELDING

The base metal is a high-strength low-alloy steel, corresponding to grade HT80. The steel, with a thickness of 40 mm, was delivered in quenched-and-tempered (Q + T) condition. Different mechanical properties can be obtained for such a steel by using different tempering temperatures (600–700 °C). The microstructure of the steel of tempered martensite and lower bainite provides a high strength and a high impact toughness. The welding was done on plate samples (500 × 250 × 40) mm and (1000 × 250 × 40) mm using the flux-cored arc-welding (FCAW) process. The edge preparation was X-shaped, **Figure 1**, as is usual for the welding of steel plates with a thickness of 40 mm. The consumables were filled wires (ϕ 1.2 mm), suitable for welding with mixed-gas shielding (82 % Ar and 18 % CO₂). The cooling times from 800 °C to 500 °C ($\Delta t_{8/5}$) were approximately of 9 s, with heat inputs of 1.8–2.0 MJ m⁻¹, while the preheating/inter-pass temperature was of 100 °C. The cooling time was chosen because faster cooling rates ($\Delta t_{8/5} = 6$ s) reduce the toughness in the intercritical region, and the slower cooling rates ($\Delta t_{8/5} > 12$ s) reduce the toughness due to the formation of a martensite-austenite constituent³. The welding parameters are given in **Table 1**. The first passes of the welded joint were made using preheating at 120 °C⁴.

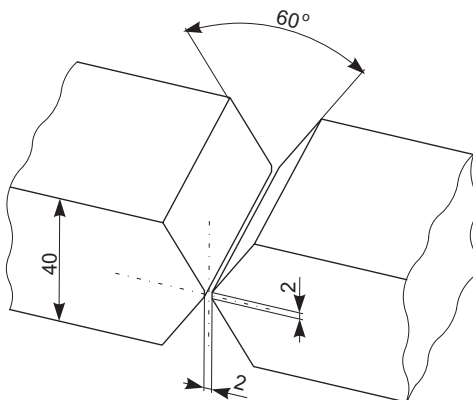


Figure 1: The "X" shaped groove used in this investigation
Slika 1: Žleb z X-obliko, uporabljen pri tej raziskavi

The chemical compositions of the base metal (BM) and the different weld regions are listed in **Table 2**. These compositions indicate a more pronounced alloying effect from the BM in the root region than in the filler regions. Local tempering or quenching caused by reheating and cooling during the deposition of subsequent passes is also present in the root and filler weld regions. This is the main reason why the local mis-matching through the weld thickness varied, even in the case of a homogeneous weld.

Table 1: Welding parameters for each weld pass
Tabela 1: Varilni parametri za vsak varek

Welding pass	Current A	Voltage V	Speed of welding cm/min	Interpass temperature °C	Heat input kJ/cm	$\Delta t_{8/5}$ s	Weld joint region
1	155	24.5	11.5	120	19.813	10.61	
2	185	23.5	13.7	135	19.040	10.82	root
3	250	24	16.0	30	22.500	8.78	
4	250	24	15.0	65	24.000	10.47	
5	240	23	10.5	105	31.543	15.65	
6	240	23	11.1	120	29.784	15.66	
7	220	23	15.9	65	19.130	8.43	
8	220	23.5	14.6	85	21.203	9.96	filler
9	210	23	14.2	120	20.481	10.95	part
10	220	23	13.9	125	21.763	11.83	
11	210	24	15.4	80	19.662	9.11	
12	250	24	14.8	110	24.342	12.43	
13	220	25	15.8	95	20.899	10.18	
14	230	25	19.5	125	17.692	9.70	
average	210	24	14.0	88	21.338	10.17	root
average	226	24	15.0	103	22.648	11.39	filler

Table 2: Chemical composition of the base metal, the pure weld metal and the actual weld metal of the filler and the root regions
Tabela 2: Kemična sestava osnovnega materiala, čistega vara, realnega vara v območju polnitve in korena v masnih deležih w/%

Material	C w/%	Si w/%	Mn w/%	P w/%	S w/%	Cr w/%	Ni w/%	Mo w/%	CE w/%
Base metal	0.09	0.27	0.25	0.015	0.004	1.12	2.63	0.25	0.366
Weld metal (pure)	0.06	0.35	1.43	0.011	0.008	0.86	3.01	0.56	0.448
WM _{fill} (filler part)	0.07	0.33	1.27	0.008	0.006	0.86	2.21	0.47	0.404
WM _{root}	0.08	0.32	0.78	0.012	0.007	0.99	2.50	0.35	0.388

The content of carbon is very low in the base metal and the weld metals and the temperature of martensite transformation is higher. Thus, the time interval for self-tempering from the temperature of martensite transformation up to room temperature is larger. In this case a brittle hard microstructure does not appear. This is the reason for the high toughness of the microstructure. **Table 2** presents the change of the carbon equivalent (CE) during the welding process. The low CE and the low strength hinder the hydrogen-assisted cold cracking. The mechanical properties of the welds were determined using round tensile specimens (ϕ 5 mm) extracted from the root and the cap region of the X-groove welds in longitudinal direction. The tensile tests were performed at room temperature and at the fracture-toughness testing temperature, i.e., -10°C . The results are listed in **Table 3**, with the data in brackets representing the designed values (theoretical) of the mis-matching factor, which do not correspond to the real welds. The differences between the designed values and real mis-matching factors are a consequence of the weld-pool dilution/alloying by molten BM (see chemical compositions in **Table 2**). It should also be pointed out that the cooling rate in these experiments ($\Delta t_{8/5} \approx 9$ s) was obviously different from that used during the all-weld metal sample preparation by the consumable producer.

Table 3: Average mechanical property values of the base metal and the weld metal

Tabela 3: Povprečne mehanske lastnosti osnovnega materiala in varja

Material	Temp. $^{\circ}\text{C}$	E GPa	$R_{p0.2}$ MPa	R_m MPa	A_t %	C_V^+ J	M
Base	20°	201	711	838	19.6	54 ₋₄₀ °C	—
metal	-10°	209	712	846	19	85 ₋₁₀ °C	—
WM	20°	210*	770	845	16	56 ₋₁₀ °C	(1.08)
WM _{fill}	20°	205	861	951	11.7	56 ₋₁₀ °C	1.21
	-10°	211	873	1041	10.8	33 ₋₄₀ °C	1.22
WM _{root}	20°	221	807	905	15.3	61 ₋₁₀ °C	1.14
	-10°	212	824	902	16.5	50 ₋₄₀ °C	1.16

+ mean value of three Charpy-V notched impact-toughness specimens

* value has been estimated because an accurate experimental value was not available

The impact-toughness V-notch specimens and the single-edge notch bend SE(B) specimens were also extracted from the welded joints. Different testing temperatures were used to evaluate the impact toughness. It can be concluded that the impact toughness corresponds to the brittle-to-ductile transition region of the weld joint, see **Table 3**. In spite of higher dilution/alloying by the molten BM in the root region, a better impact toughness is achieved in that region than in the filler part of the WM.

The mis-match factor M is defined as:

$$M = \frac{\sigma_{y,WM}}{\sigma_{y,BM}} \quad (1)$$

The mechanical properties listed in **Table 3** are the average values of the region from where the tensile specimens were taken. Hence, an empirical relationship was used to obtain the local mis-matching values of mechanical properties.

3 METALLOGRAPHIC INVESTIGATION

The cross-sections of the welded joints were polished and etched (3 % nital) to reveal the microstructure⁵, shown in **Figure 2**. Previously performed fracture-toughness testing^{6,7} showed that in the case of unstable crack propagation, the fracture-toughness value depended on the microstructure of the crack-tip region. Hence, a fracture-toughness analysis of unstable crack propagation requires the classification of the fracture toughness data connected to the microstructures at the crack tip.

Figure 3 shows a welded joint cross-section indicating two different regions inside a weld pass – one region, with a dendritic structure ('as-welded'), and the other one showing evidence of being re-heated at the subsequent welding pass. The darkened regions in the weld metal correspond to the partially transformed

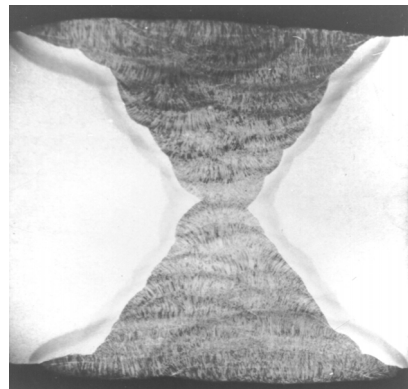


Figure 2: Macrograph of the cross-section of the welded joint, $\times 1.5$
Slika 2: Makroposnetek prereza zvara, povečano 1,5-krat

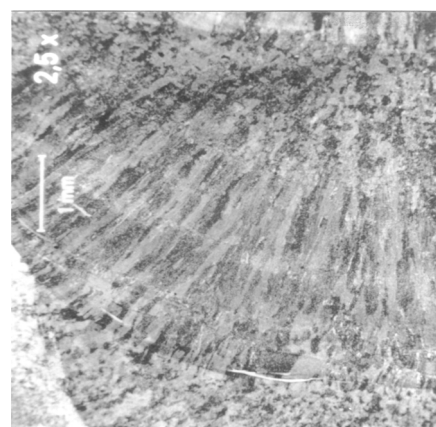


Figure 3: The re-heated and as-welded region within a welded pass, $\times 20$
Slika 3: Pogreto in kot varjeno področje v varku, povečano 20-krat

regions, re-heated above Ac_1 . The temperature of the subsequent weld pass was between Ac_1 and the self-tempering temperature.

4 FRACTURE-TOUGHNESS TESTING

Specimen and Location of Machined Notch

The critical crack-tip opening displacement ($CTOD$) value in the case of unstable crack propagation strongly depends on the microstructures at the crack tip. Different microstructures are formed in the weld metal, depending on the thermal cycles and the chemical composition. For this reason, the notch positioning in the welded joint is very important. The effect of different microstructure on the fracture behaviour was assessed by testing $CTOD$ $B \times 2B$ specimens (thickness $B = 36$ mm) with a through-the-thickness notch tip in the weld metal. The $CTOD$ $B \times B$ specimens, with the surface notch in the weld metal, were used to assess the effect of different microstructures on the fracture behaviour of the welded joint.

Crack-tip opening displacement testing

The fatigue pre-cracking of the specimens was performed according to the step-wise high-ratio R "SHR" technique⁸. The $CTOD$ testing was performed on the fracture-toughness specimen in accordance with the BS 7448 standard⁹. The testing temperature was of -10°C , according to the recommendations of the Offshore Mechanics and Arctic Engineering (OMAE)¹⁰. A single-specimen method was used with the DC potential-drop technique applied to monitor the stable crack growth¹¹. The specimens were loaded using a constant cross-head velocity of 1 mm/min, i.e., in displacement control. Base-metal $B \times B$ specimens with a shallow crack ($a/W = 0.1$) and a deep crack ($a/W = 0.5$) were also tested. In both cases the maximum $CTOD_m$ values were observed: $CTOD_m = 1.08$ mm (for $a/W = 0.1$) and $CTOD_m = 0.604$ mm (for $a/W = 0.5$).

5 ANALYSIS OF THE FRACTURE-TOUGHNESS RESULTS

Figure 4 shows the resistance curves for almost the same crack lengths ($a/W = 0.27$), but with a different microstructure at the crack tip. The critical value of the $CTOD$ during crack-growth initiation is lower for the 'as-welded' microstructure, denoted WM(B), than for the 're-heated' microstructure, denoted WM(A). The stable crack growth through WM(B) is characterised by a low slope of the resistance curve and thus by a low resistance to stable crack growth. The shallow-cracked specimen with a shorter crack ($a/W = 0.28$) exhibited a higher value of $CTOD$ initiation than in the case of the longer crack ($a/W = 0.4$). In the latter case, local instability occurred ('pop-in') during crack-tip blunting, followed by crack arrest in the WM(A). The same slope

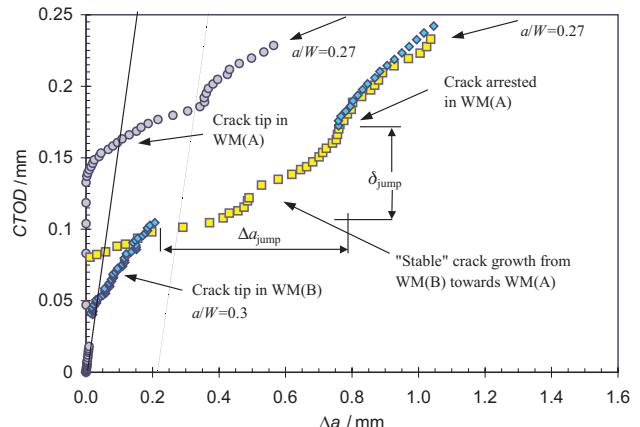


Figure 4: $CTOD$ resistance curves of $B \times B$ specimens with the crack tip in different microstructure

Slika 4: $CTOD$ odpornostne krivulje za $B \times B$ vzorce s konico razpoke v različni mikrostrukturi

for the resistance curves obtained from the two specimens with different crack lengths ($a/W = 0.27$ and $a/W = 0.4$) indicates to a stable crack growth through the same WM(A) microstructure.

Figure 5 shows the values of the $CTOD$ as a fracture-toughness parameter for both series of specimens, $B \times 2B$ and $B \times B$, with the notch in the weld metal and the base metal. Significant differences between the fracture-toughness values of the base metal and weld metal were observed. Also, all critical values for the $B \times 2B$ specimens were within the same interval. This is a consequence from the incorporation of at least one local brittle zone (LBZ) or local soft region in the process zone in the vicinity of the crack tip.

The results for the critical $CTOD$, obtained using $B \times B$ specimens, are classified according to the microstructure, WM(A) and WM(B), depending on the position of the fatigue crack tip at the beginning of the $CTOD$ testing. Since, the higher critical $CTOD$ values were measured for the specimens with a crack tip in the WM(A), it is clear that the critical $CTOD$ values for the specimens with a crack tip in the WM(B) can be divided

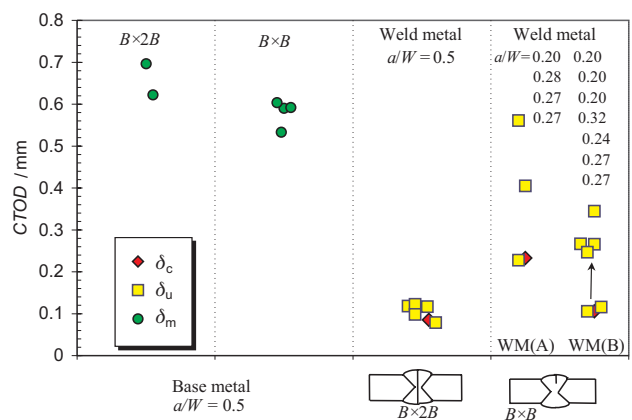


Figure 5: Compilation of the critical $CTOD$ values
Slika 5: Pregled kritičnih vrednosti $CTOD$

into two groups, depending on the crack depth. Obviously, the scatter of the critical $CTOD$ values and the relatively small amount of data prevented a more reliable estimation of the fracture-toughness lower-bound value for different microstructures.

A modified Weibull distribution was used for the statistical interpretation of the measured and corrected critical $CTOD$ values. Zerbst et al.¹² proposed a modified Weibull distribution for estimating the lower-bound fracture toughness in terms of the J-integral¹³. The distribution function referring to this is given by:

$$P_f = \begin{cases} \frac{\sqrt{\ln 2}}{J_0} (J_c - J_{l.b.}), & P_f \leq 0.5 \\ 1 - \exp \left\{ - \left[\frac{J_c}{J_0} \right]^2 \right\}, & P_f \geq 0.5 \end{cases} \quad (2)$$

with the lower bound, $J_{l.b.}$, as the toughness for a failure probability of zero.

The term J can be replaced with $CTOD = \delta$ by using the relation between δ and J ¹⁴:

$$\begin{aligned} d &= \frac{J}{m \cdot \sigma_{ys}} \\ m &= -0.111 + 0.817 \frac{a}{W} + 1.36 \cdot R^*; \\ R^* &= \left(\frac{500 \cdot n}{2.718} \right)^n \quad \text{or} \quad R^* = \frac{\sigma_m}{\sigma_y} \end{aligned} \quad (3)$$

The terms m and R^* were introduced by Kirk and co-workers [14] on the basis of finite-element analysis results. The lower bound fracture toughness can be derived by considering the condition of continuity for P_f . As a result, the lower bound is simply obtained from the mean value by the expression:

$$\begin{aligned} \delta_{l.b.} &= 0.26 \cdot \beta \cdot \delta_{c,mean} \\ \text{with } \beta &= 1 + 2.737p - 2.327p^2 + 12.580p^3 \end{aligned} \quad (4)$$

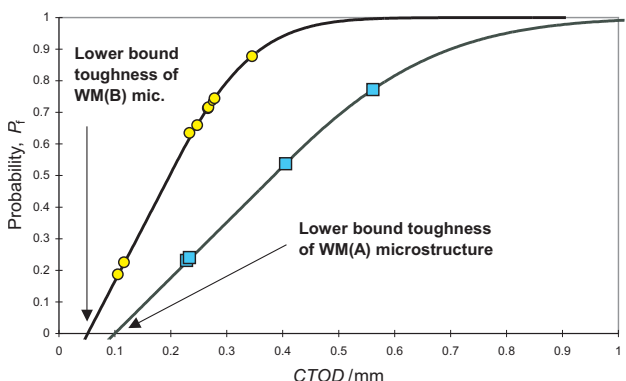


Figure 6: Failure probability with lower bound values classified by microstructures WM(A) and WM(B)

Slika 6: Verjetnost preloma pri spodnji vrednosti za mikrostrukture WM(A) in WM(B)

where p is the fraction of data that is rejected by the size criterion.

The results of this analysis are two curves of Weibull distribution that are in good agreement with the experimental results for each individual microstructure, as shown in Figure 6. The lower-bound fracture-toughness value is represented by the $CTOD$ value at the intersection point of the Weibull distribution curve with the x -axis. Although the Weibull distribution curves are for different microstructures, it is worth pointing out that the fracture-toughness lower-bound value is low for both of them 7.

6 CONCLUSION

In spite of the fact that the differences between the impact toughness of the weld metal and the base metal are insignificant, the fracture toughness of the weld metal can be significantly lower. The overmatched weld metal exhibited unstable crack propagation, while the base metal is ductile at the same test temperature. From the analysis performed on the B x B specimen it can be concluded that the critical value of the fracture toughness and the fracture behaviour of the weldment as a whole, depend on the crack depth and the microstructure at the crack tip, and also on the microstructure toward which the crack is growing. The influence of these parameters is reflected in pronounced differences in the experimentally obtained values. The higher reliability for estimating the fracture-toughness lower bound was achieved by using a modified Weibull distribution with the $CTOD$ parameter. The B x 2B specimens also indicated low critical $CTOD$ values, but with lower scatter. The reason for this is the increased constraint, since the ligament profile is of square shape, and also the fact that the stress state at the crack tip causes an interaction between strength-mis-matched microstructures, which are inevitably crossed by the crack front. In the case of through-the-thickness specimens at least one local brittle zone (LBZ) or a local soft region is incorporated in the process zone in the vicinity of the crack tip. Hence, the unstable fracture occurred with small stable crack propagation, or without. The statistically determined lower-bound fracture toughness takes account of this effect, which causes an increased scatter of experimental results. Therefore, for structural integrity procedures, it is possible to use the present approach to determine relevant fracture-toughness values.

7 REFERENCES

- Vojvodić Tuma J.: Low-temperature tensile properties, notch and fracture toughness of steels for use in nuclear power plants, Nuclear Engineering Design, (2002) 211, 105–119
- Gubeljak N.: The fracture behaviour of specimens with a notch tip partly in the base metal of strength mis-matched welded joints, Int. J. Fract., 100 (1999) 2, 169–181

- ³ Matsuda, F., Fukada, Y., Okada, H., Shoga, C., Ikeuchi, K., Horii Y., Shiaku, T., Suzuki, S.: Review of mechanical and metallurgical investigations of martensite-austenite constituent in welded joints in Japan, Welding in the World, 37 (1996) 3, 134–154
- ⁴ Duren C.: Evaluation of large diameter pipe steel weldability by means of the carbon equivalent, Duisburg 1982
- ⁵ Compendium of weld metal microstructures and properties (Submerged-arc welds in ferritic steel), Prepared for Commission IX of the International Institute of Welding by Sub-Commission IXJ, The Welding Institute Abington Hall, Cambridge UK 1985
- ⁶ Machida, S., Miyata, T., Toyosada, M., Hagiwara, Y.: Study of methods for CTOD testing of weldments, fatigue and fracture testing of weldments, ASTM STP 1058, H. I. McHenry, J. M. Potter, Eds., American Society for Testing and Materials, Philadelphia, 1990, 142–156
- ⁷ Fairchild, D. P.: Fracture toughness testing of weld heat-affected zones in structural steel, fatigue and fracture testing of weldments, ASTM STP 1058, H. I. McHenry, J. M. Potter, Eds., American Society for Testing and Materials, Philadelphia, 1990, 117–142
- ⁸ Koçak M., Seifert, Yao S., Lampe H.: Comparison of fatigue precracking methods for fracture toughness testing of weldments: Local compression and step-wise high ratio, Conference Welding-90
- ⁹ BS 7448 (1997): Fracture mechanics toughness tests, Part 2. Method for determination of K_I , critical CTOD and critical J values of welds in metallic materials, British Standards Institution, London
- ¹⁰ Fairchild, D. P., Theisen, J. D., Royer, C. P.: Philosophy and technique for assessing HAZ toughness of structural steels prior to steel production, Paper OMAE-88-910, Seventh International Conference on Offshore Mechanics and Arctic Engineering, Houston, TX, February 1988
- ¹¹ Johnson, H. H.: Calibrating the electric potential method for study slow crack growth, Materials Research and Standards, (1965) 5, 442–445
- ¹² Zerbst, U., Heerens, J., Puff, M., Wittkowsky, B. U., Schwalbe, K.-H.: Engineering estimation of the lower bound toughness in the transition regime of ferritic steels, Fatigue & Fracture of engineering materials & Structures, (1998) 21, 1273–1278
- ¹³ Anderson, T. L.: Fracture mechanics fundamentals and applications, Second edition, 1994
- ¹⁴ Kirk, M. T., Dodds, R. H.: J and CTOD estimation equations for shallow cracks in single edge notch bend specimens, J. of Testing and Evaluation, 21 (1993) 4

SOLIDIFICATION AND FRACTURE OF AN AS-CAST Ni ALLOY

STRJEVANJE IN PRELOM LITE NIKLJEVE ZLITINE

Matjaž Torkar

Institute of Metals and Technology, Lepi pot 11, 1000 Ljubljana, Slovenia
matjaz.torkar@imt.si

Prejem rokopisa – received: 2006-05-17; sprejem za objavo – accepted for publication: 2006-11-06

The investigation was carried out on samples cut from 20-kg as-cast ingots of a Ni alloy. The as-cast microstructures were examined, the intensity of the segregations were determined, and the fracture surfaces of the specimens, cooled in liquid nitrogen, were examined. It was found that with slow solidification, carbide particles precipitate on the grain boundaries, diminishing the grain-to-grain cohesion and influencing the morphology of fracture. In the areas of columnar solidification the fracture propagates along the dendrite boundaries.

Key words: Ni alloy, solidification structure, segregation intensity, fracture surface

Izceje v zlitini z lito strukturo poslabšujejo preoblikovalnost v vročem. Za preiskavo so bili odrezani vzorci iz litih ingotov zlitine na osnovi niklja z maso 20 kg. Preiskana je bila strjevalna struktura in določena intenziteta izcej. Vzorci so bili prelomljeni v hladnem in preiskana je bila morfologija površine preloma. Med počasnim strjevanjem nastajajo po mejah zrn karbidni delci, ki zmanjšujejo kohezijo med zrni in vplivajo na morfologijo preloma. Na vrsto preloma vplivajo stebrasta strjevalna zrna zaradi poti preloma vzdolž mej dendritov.

Ključne besede: nikljeva zlิตina, strjevalna struktura, intenziteta izcej, površina preloma

1 INTRODUCTION

Most as-cast Ni-based superalloys have a low hot workability¹. The hot-workability window depends on the microstructural characteristics, the yield strength², the deformation rate and the dynamic and static recrystallization. The Ni-based alloy with about 75 % Ni, 20 % Cr, 2.5 % Ti, 1.4 % Al and 0.08 % C is strengthened by sub-micron precipitates of γ' phase (Ni_3Al) and, with a sufficient content of carbon, also by carbide precipitates. During solidification, primary carbide and carbo-nitride particles of the M(C,N) type are formed, while the secondary carbides, M_7C_3 and $M_{23}C_6$, precipitate at dendrite boundaries during the cooling of the solid alloy, because of the decreased solubility of carbon in austenite with decreasing temperature. The presence of carbides and the intermetallic precipitates greatly increases the creep resistance of the alloy, which depends on the size, quantity and distribution of the precipitates. The basic mechanism of hot deformation consists of the gliding and climbing of dislocations. The resulting strain hardening is decreased by dynamic recovery and recrystallization, which also affect the kinetics of precipitation and the temperature of phase transformation. With a higher content of alloying elements, the yield strength of the alloy and the activation energy, E_a , for recrystallization are greater. The yield strength of the alloy also depends on the deformation rate, according to the Zener-Hollomon equation³.

For this reason the intercrystalline hollows and segregations decrease the workability until the moment

when the microstructure is modified by recrystallization. Sufficient dynamic recrystallization also stops the propagation of the microcracks formed on non-deformable inclusions and on the triple points of the grains. If a grain-boundary crack is oriented orthogonally to the flow of the metal it propagates until a grain boundary of a very different orientation is met, at which point the propagation of the crack is arrested⁴.

To obtain the optimal properties for Ni-based superalloys a heat treatment, specific to the particular alloy⁵, is necessary. During the heat treatment two essential operations are included:

- The solution of the γ' phase and most of the carbide particles. The solution of the γ' occurs in the range 960–980 °C. This range of temperature increases with the increasing content of Ti in the alloy. $M_{23}C_6$ precipitates are dissolved in the temperature range 1040–1095 °C and M_7C_3 particles in the range 1095–1150 °C.
- The controlled precipitation of γ' and carbide particles during cooling from the solution temperature and during holding at 700 °C.

The two-step heat treatment produces an over saturation of the matrix of the alloy with carbon, which increases the tensile strength at lower temperatures, but leads, however, to a more unstable microstructure at higher temperatures.

The grain size of nickel superalloys also affects the proper relation between the tensile strength and the low-cycle fatigue. The resistance to low-cycle fatigue requires a small grain size (forged material), while the

resistance to creep requires a coarse grain size (as-cast material). For this reason, modern turbine blades are mostly produced by casting⁶. As a compromise, a thermo-mechanical treatment giving a "necklace" structure⁷ has been developed. This structure consists of coarse, slightly elongated grains, surrounded by small grains, and ensures the best balance of properties.

As-cast Ni alloys usually have a microstructure of coarse, columnar grains, which requires careful starting reductions during the hot-working process. During dendritic solidification, strong segregations of elements are formed in the interdendritic pockets. The intensity of the segregations and the size of the dendrites depend on the rate of solidification: the slower the cooling rate, the coarser are the dendrites and the greater are the segregations.

The aim of this work was to characterise the as-cast microstructure of a Ni-based alloy.

2 EXPERIMENTAL PROCEDURE

The alloy was prepared by melting in air in an induction furnace and casting into 20-kg ingots. The ingots were forged, and during the forging a great number of cracks were formed. Specimens were cut from several places in the ingot and areas containing segregations were assessed by using a scanning electron microscope (SEM) equipped with a wavelength-dispersive spectrometer (WDS). The microstructures were also examined using optical microscopy. The coefficient of segregation was calculated from the difference in the content of elements within the grain and in the interdendritic region. Prior to fracturing the samples were cooled in liquid nitrogen. In addition, the resulting fracture surfaces were examined in the SEM.

3 RESULTS AND DISCUSSION

From the solidification microstructure (**Figure 1**), with coarse, columnar grains near the surface and equiaxed crystal grains in the middle of the ingot, the content of Cr, Co, Al and Ti was determined in the region of the equiaxed grains with point analysis within the grain and in the interdendritic region. The contents of

Table 1: Concentration of elements in and between the solidification grains

Tabela 1: Masni delež elementov v strjevalnih zrnih in med njimi

Element	Concentration, w/%		Coef. of segregation $K = c_{\max}/c_{\min}$
	In the grain	In the inter-dendritic pocket	
Cr	20.08	26.04	1.29
Co	1.14	1.39	1.21
Ni	69.88	69.72	-
Al	0.43	0.46	1.06
Ti	2.03	4.45	2.19
Fe	1.12	1.29	1.15

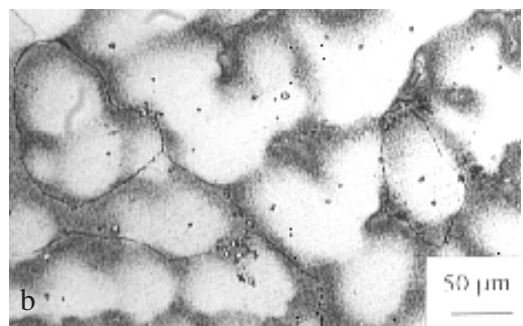
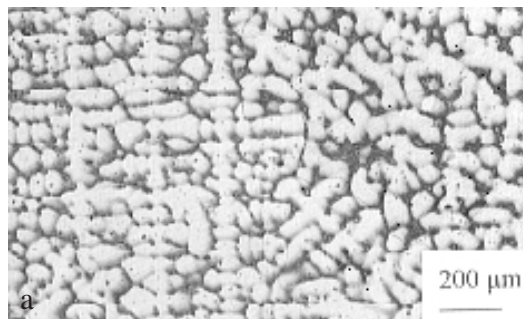


Figure 1: Dendrites and interdendritic segregations of as-cast Ni-based alloy. Etched with Marble's reagent.
Slika 1: Dendriti in meddendritne izceje v liti nikljevi zlitini; jedkano z Marblovim jedkalom

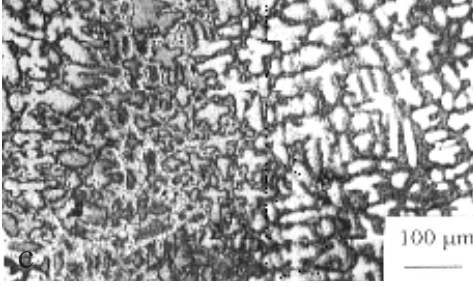


Figure 2: Columnar and equiaxed grains with dendrites in as-cast Ni-based alloy. Etched with Marble's reagent.
Slika 2: Stebrasta in enakoosna zrna z dendriti v liti nikljevi zlitini; jedkano z Marblovim jedkalom

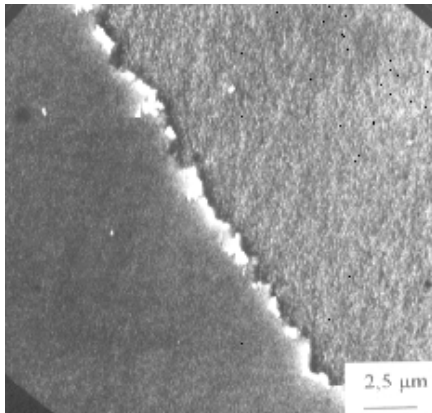


Figure 3: Stringer of carbide particles on the grain boundary in as-cast ingot (SEM)

Slika 3: Niz karbidnih delcev na meji zrn v ingotu z lito strukturo

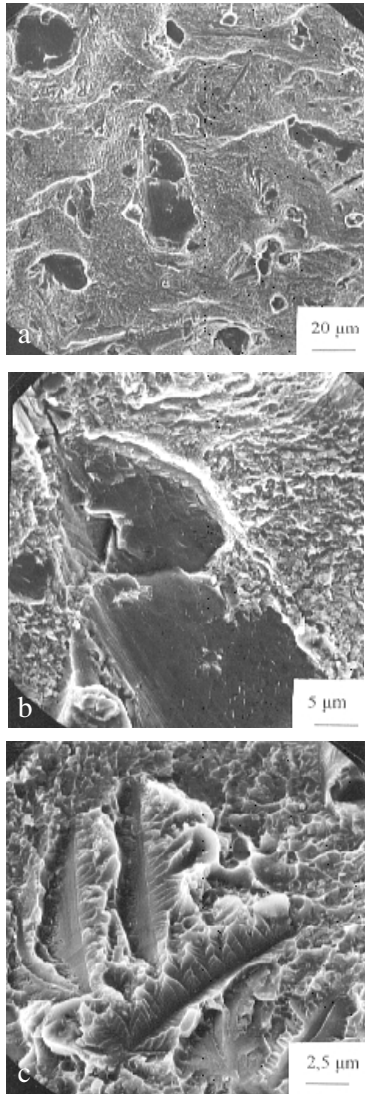


Figure 4: Ductile and brittle fracture of as-cast sample in the region of equiaxed grains (SEM)

Slika 4: Duktilen in krhek prelom v item vzorcu v območju enakoosnih zrn (SEM)

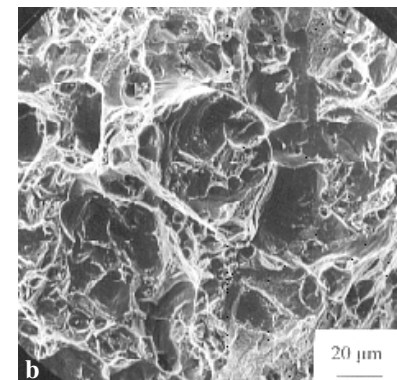
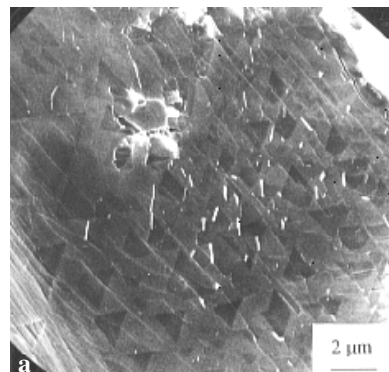


Figure 5: Detail of brittle-fracture surface with triangles and tetrahedra and a mixture of brittle and ductile fracture with dimples (SEM)

Sliki 5: Detajl krhke površine preloma s trikotniki in tetaedri ter duktilni prelom z jamicami (SEM)

analysed elements and the calculated segregation coefficients in **Table 1** confirm the expected strong segregation.

The segregation intensity increases from iron to cobalt to chromium, and it is much greater for titanium. The segregations make the alloy chemically inhomogeneous and cause a difference in the hot deformability.

The morphology of the as-cast microstructure depends on the cooling rate; however, it is also related to the segregation intensity. Several samples were cut from the as-cast ingots and the microstructures were examined

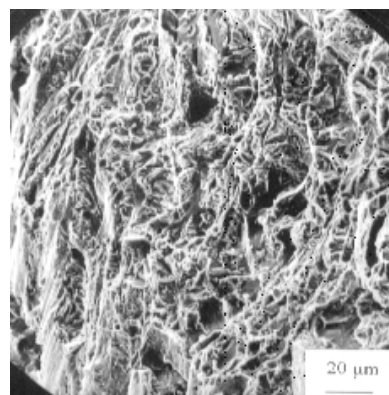


Figure 6: Fracture along the columnar grains

Slika 6: Prelom vzdolž stebrostih zrn

using optical microscopy. The as-cast microstructure reveals a dendritic solidification (**Figure 1**) with coarse, columnar and equiaxed grains (**Figure 2**), with interdendritic segregations and stringers of carbide particles on the grain boundaries (**Figure 3**).

The examination of the cold fracture of the as-cast alloy (**Figures 4, 5**) revealed a mixed fracture surface, with both ductile- and brittle-fracture areas being present. Since the alloy is very tough, the fracture was obtained by bending samples that were cooled in liquid nitrogen. As shown in **Figure 5**, on the relatively smooth surface of the brittle fracture, triangles or tetrahedra were observed, indicating that the fracture occurred on the {111} lattice plane. The stacking-fault tetrahedra are special forms of point-defect agglomerates⁸. They are formed by dissociated glide or climb and the aggregation of vacancies. In face-centred cubic metals and alloys the vacancies can group in three-dimensional faults in the form of stacking faults on four {111} planes with six edges of the tetrahedron.

On the fracture surface a ductile area with transcrystalline dimples prevails (**Figures 4, 5**), with carbide particles at the bottom of the dimples. The fracture along the boundaries of the columnar grains is similar. The mixture of ductile and brittle fracture is shown in **Figures 4b, c and 5b**. The fractures are mostly transcrystalline. In some areas a quasi-ductile and quasi-brittle micromorphology was observed, which does not permit a proper interpretation of the prevailing fracturing process.

4 CONCLUSIONS

The Ni alloy had a poor hot workability and a large number of hot cracks appeared during the hot forging. The metallography revealed dendritic solidification with coarse, columnar grains near the surface, equiaxed grains in the centre of the ingot and interdendritic segregation of the alloyed elements and carbide particles on the grain boundaries.

The stringers of the carbide particles are the main reason for the poor grain-to-grain cohesion and represent an easy path for crack propagation during the hot working. They also affect the fracture propagation during cold fracture. The precipitation of carbide particles at the grain boundaries occurs during the slow cooling after solidification or during a too-low soaking temperature prior to hot working.

The examination of the cold fractures revealed quasi-ductile and quasi-brittle areas, partly transcrystalline and partly intercrystalline. On the brittle-fracture surfaces triangles and tetrahedra were observed, suggesting a fracture on the {111} lattice planes.

For improved hot workability of the alloy it is necessary to decrease the grain size and the amount of segregation and to avoid the precipitation of carbide particles on the grain boundaries.

ACKNOWLEDGEMENT

The Ministry of Higher Education, Science and Technology of the Republic of Slovenia sponsored this research.

5 REFERENCES

- ¹ Schindler, I., Macháček, J., Spittel, M., *Intermetallics* 7 (1999), 83–87
- ² Torkar, M., Šuštaršič, B., Vodopivec, F., Kovine, zlit., tehnol., 27 (1993) 4, 289–294
- ³ Long, Z., Zhuang, J., Lin, P., Zhong, Z., Advanced Technologies for Superalloy Affordability, ed. K. M. Chan, S. K. Srivastava, D. U. Furrer, K. R. Bain, The Minerals, Metals&Materials Society, 2000, 187–196
- ⁴ Ryan, N. D., McQueen, H. J. *J. of Mech. Work. Technol.*, 12 (1986), 279–296
- ⁵ Mc Queen, H. J., Bourell, D. L. *J. of Metals*, (1987), Sept., 28–35
- ⁶ Ryan, N. D., McQueen, H. J. *J. of Mech. Work. Technol.*, 12 (1986), 323–349
- ⁷ Wright, D. C., Smith D. J. *Mat. Sci. And Technol.*, (1986) 2, 742–747
- ⁸ Matsukawa, Y., Zinkle S.J., Dynamic observation of the collapse process of a stacking fault tetrahedron by moving dislocations, *Journal of Nuclear Materials*, 329–333 (2004), 919–923

LABORATORY ACCREDITATION – CONFIDENCE IN THE ACTIVITIES OF CONFORMITY ASSESSMENT OF PRODUCTS

LABORATORIJSKA AKREDITACIJA- ZAUPANJE V AKTIVNOST OCENE USTREZNOSTI PROIZVODOV

Azemina Klobodanović, Mirsada Oruč

Institute of Metallurgy "Kemal Kapetanović", Travnička cesta 7, 72000 Zenica, Bosnia and Herzegovina
miz@miz.ba

Prejem rokopisa – received: 2005-08-29; sprejem za objavo – accepted for publication: 2006-10-19

The role of accredited laboratories is to verify the quality of products. This is particularly important for those products intended for export. The activities of the laboratories of the Institute of Metallurgy and their significance for industrial activity in Bosnia and Herzegovina are presented.

Key words: accreditation, products quality control, quality management

Naloga akreditiranih laboratorijskih je preverjanje kakovosti proizvodov. To je posebno pomembno za izdelke, namenjene za izvoz. Predstavljena je aktivnost laboratorijskih na Institutu za metalurgijo in njegov pomen za industrijsko dejavnost v Bosni in Hercegovini.

Ključne besede: akreditacija, kontrola kakovosti proizvodov, upravljanje kakovosti

1 INTRODUCTION

The prime task of Central and East European Countries is to achieve the required level of quality for products and services that are exported to the countries of the European Union. A considerable amount of work and knowledge are needed to bring the quality of products to a higher level, and much effort is necessary to improve the quality and responsibility of the work of all the people involved in the processes of production, control and quality assurance. The first difficulty to overcome is the barriers related to the conformity of the national legal framework, metrology, standardisation and of quality assessment with EU regulations. This is a major and complex task, since it involves the adoption of rules and processes prescribed in about 200 legal directives and about 7000 European standards related to metrology systems, methods of testing and certification, all necessary in order to have a comparable and transparent system of quality and procedures in all the involved countries, and which are easy to supervise¹.

Also, for the placement of products in EU markets in the non-obligatory area of certification, serious barriers exist. First of all, certificates for the quality-management system in accordance with the standard ISO 9001:2000 and for the environmental management systems in accordance with ISO 14000 must be obtained, with the aim to ensure that certificates, accreditations, test and calibration reports are accepted throughout Europe. This means that products intended for export must be tested in accredited laboratories that have a certified system of quality control.

Quality is a characteristic confirming that the product is manufactured according to an approved procedure and that the properties are in agreement with a standard or

with a prescription accepted by the manufacturer and the purchaser. The word quality has also a more general significance that may not be defined by a document in the case when it is related to a specific activity, a process or an organisation. With the quality system for companies and laboratories, the rules of behaviour in business are established, and reciprocal relations, tasks and responsibilities of the quality management are put in place. Therefore, good quality control for companies is one of the attributes for survival in a competitive market.

2 QUALITY – A NEW APPROACH TO BUSINESS

Quality is a global requirement valued in developed countries and becoming of essential importance for different industrial companies in Bosnia and Herzegovina, too. The market success of a number of products is more and more dependent on the purchaser's satisfaction and the price of the product. Because of the competition, which may offer the same quality for a lower price or an improved quality for an unchanged price, the quality determines the competitiveness in the market place for companies too³.

For this reason, the concept of quality has radically changed, and at present it is completely oriented towards the purchaser, his or her needs, expectations and preferences. It is not enough for the supplier to have high-quality products/services, it is also necessary to be ready to offer an acceptable price for an increasing level of quality. Therefore, only continuous improvements enable the producer to stay at the front of the general development and to be continuously competitive in the market.

At the beginning of the industrial revolution the sellers controlled the market, and because of the limited range of goods on offer, the purchaser was frequently forced to accept products of insufficient quality. The primary task of manufacturing was to ensure an increasing quantity of goods on the market. The saturation of the market set up the balance between supply and demand and asserted the quality and reliability as being significant for the market value of products. The increased number of suppliers of goods on the market is the cause of decreasing prices for goods of increasing quality. Success in competitive markets forces the producers to ensure not only that their products conform to standards, but also to improve the extent and reliability of the control of quality, including also non-standardised requirements.

The increased market competition and the strengthening of the role of the purchaser led to the development of a quality system involving the control of the quality of products and the inclusion of preventive actions to provide a constant supervision of the manufacturing process as well as the provision of an acceptable level of interference of this process with the environment. All the people involved in the production process have to take part in the activities related in a broad sense to the quality control. This understanding of the broad significance of quality control led to the development of the principles of the system of quality assurance for products.

Rapid changes in the market for products put the producers into a position in which even permanent improvement of the product quality, process and quality system were not sufficient to ensure success. This was the reason for the evolution of quality with new methods of integration and harmonization to predict the customer's behaviour. The processes inside an organization based on standards and internal producer rules were combined with continuous research and development and led to the system of Total Quality Management (TQM).

3 THE IMPORTANCE AND PARTICIPATION OF ACCREDITED LABORATORIES

Frequently, in the business sections of journals in Bosnia and Herzegovina there are reports on the successful operation of companies that have obtained certificates in accordance with standards from the ISO 9000 and ISO 9001 series. However, very rarely, if ever, is the reader informed about organizations with accredited testing and calibration laboratories, in spite of the fact that these organisations are competitive with different services in their domain of activity in accordance with the European standard EN 45001 and the ISO/IEC 17025 standard⁴. The value of the accreditations according to these two standards is equal to the value of the ISO 9000 certificates. The quality of the system involving standards, internal company rules

and metrology and the assessment of the conformity of products depends also on the quality of some basic elements of the country's infrastructure, since the rules, standardization, and metrology for the assessment of the conformity of products and services according to standards are base elements of the infrastructural quality of the country.

The differences in principles and the level of development of the quality of the infrastructure between different countries set up barriers and limited the growth rate of trade on the European and world markets. It is, for this reason, of primary importance that the level of development of the infrastructure, especially in less-developed countries, becomes very fast relative to those in countries that are potential markets for products.

Testing and calibration are base elements for the assessment of conformity and are applied widely for a large range of products and their results are a reliable basis for the inspection and certification of products. In building up the EU market, it was necessary to develop conditions for the acceptance of goods produced in one country to be accepted in other countries without retesting. It was, therefore, necessary to define requirements which can be fulfilled in every certified European laboratory for testing and calibration and make the results of the testing and calibration acceptable in all the countries of the EU². The approach is based on the European standard EN 45001. On the other hand, the countries' governments have a responsibility towards consumers in terms of health, safety, the environment and legal regulations. This requires that all of the testing is carried out in accredited laboratories.

The rules in the standards of the EN 45000 series have been satisfactory for Europe; however, accredited bodies have come to the conclusion that trade is a worldwide process and many countries cannot accept the EU's standards. This was one of the reasons for the development of the new ISO/IEC 17025 standard. This standard includes previous requirements defined in the EN 45001 standard, but also others, which have to be accepted by the testing and calibration laboratories, if these laboratories want their services to be accepted internationally.

It is the policy of the EU to remove trade barriers; one of the basic conditions for a successful functioning of the common market, "a new approach to technical harmonization and standards" is defined. Part of this policy, related to the conformity of assessment, is the goal to abolish technical trade barriers and establish a mutual confidence in producer competence and in the competence of the body for the assessment of conformity (**Figure 1**).

This confidence should be ensured in obligatory and in non-obligatory areas with harmonized standards, with the application of quality assurance methods, with the testing, inspection and certification of products as well as with the introduction of a modern and independent

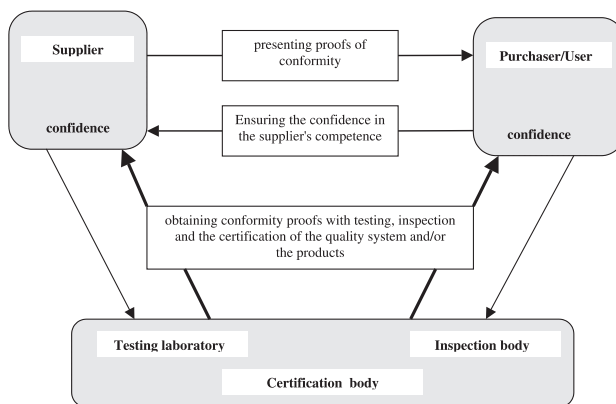


Figure 1: Procedure for ensuring confidence in supplier's competence
Slika 1: Procedura za zagotovitev zaupanja v kompetenco dobavitelja

organization for cooperation in testing, certification and accreditation at the European level.

The basic task is to support the establishment of agreements on the mutual recognition of tests in the non-obligatory area.

If accreditation bodies certify and announce that services from bodies they have accredited are based on the same rules and, for this reason, to be trusted and accepted, then all services will be acceptable in all countries that have signed the document of agreement. In this way, it is possible to build up the "pyramid of confidence", an example of which is shown for the EU in **Figure 2**.

Accreditation is, indeed, the basis for establishing the mutual confidence between the conformity-assessment bodies. It ensures the transparency of the activity of accreditation bodies at national and regional levels.

4 ACCREDITED LABORATORIES OF THE METALLURGICAL INSTITUTE

"Kemal Kapetanović", d.o.o., ZENICA

The metallurgical Institute "Kemal Kapetanović", d.o.o., Zenica (formerly "Hasan Brkić") has been active in Bosnia and Herzegovina for almost 45 years, and it is, for this field of activity, the only organization in the country.

Several institute laboratories served initially as a testing and analytical base for scientific investigations; later they also provided services to outside customers, sometimes with a smaller participation in the scientific analysis of the experimental data. During more than 40 years a great deal of experience in laboratory work was gained and many testing methods have been developed, e.g., mechanical testing of different materials (metallic and non-metallic), metallography, chemical, ceramic and mineralogical analysis, calibration methods for force, hardness, torque, temperature and pressure. In the time of war, the market required laboratory services, and priority was given to this activity and to continuous

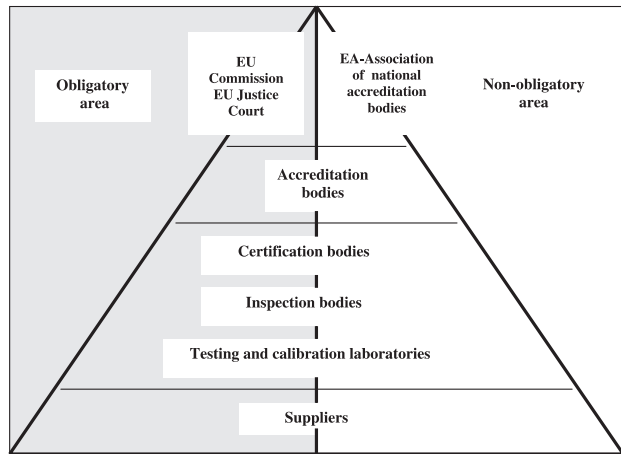


Figure 2: Example of the pyramid of confidence for the EU
Slika 2: Primer piramide zaupanja za EU

efforts to work in accordance with European and international standards.

In accordance with the available recourses, it was decided to further improve the quality system. This began with the laboratories and inspection bodies, and to ensure an efficient and transparent operation at all levels of the institute, taking care that the interest of the customers is considered.

The laboratories were the first accredited laboratories in Bosnia and Herzegovina in 1998. The accreditation was carried out by the National Department for Standardization, Metrology and Patents BiH (now the Institute for Accreditation BiH) in accordance with the EN 45001 standard. Later, the laboratories were reaccredited according to the ISO/IEC 17025 standard, and the institute has the following accreditations:

- **LK - 02-01** (calibration scope: calibration of equipment for force, torque and hardness);
- **LI - 02-02** (testing scope: mechanical testing of metallic materials);
- **LI - 02-03** (testing scope: metallographic testing of metallic materials);
- **LI - 02-04** (testing scope: chemical analysis of metallic materials and petroleum products, physical and mechanical testing of construction materials, including refractories);
- **LK - 02-05** (calibration scope: calibration of measuring instruments for temperature and pressure).

5 CONCLUSION

From the experience of countries in transition, it is known that a very important part of the agreement for all the candidate countries for inclusion in the EU is the chapter related to the free exchange of products. This requires the conforming of the technical legislature, the reciprocal recognition of results of assessment of conformity and the establishment of mechanisms for the

removal of trade barriers. For this reason, the competence of laboratories for testing materials and products is very important, since it determines which test results will be the basis for the assessment of the conformity of products to standards. The mutual confidence in the competence is the condition for the acceptance of the global principle: "once tested and once certificated", based on accreditations that are themselves based on multi-national agreements of recognition of the equality of results of national conformity assessments.

The Metallurgical Institute "Kemal Kapetanović" Zenica has the possibility to perform, together with the accredited laboratories, an important role in this area in Bosnia and Herzegovina, having already gained sufficient experience, satisfactory resources and the confidence of customers/users of services resulting from many years of cooperation. In recent years, the laboratories were certified by the Croatian Register of

Shipping and Metallurgical Institute "Kemal Kapetanović" Zenica has got opportunity to be in the list of approval service suppliers in the important areas for conformity assessment.

6 REFERENCES

- ¹ D. Ujević.: Planning and introduction of a quality system into the manufacturing process following the ISO 9000 standards, Proceedings – 1st Symposium, Revitalization and modernization of metal industry of Bosnia and Herzegovina, Bihać, 1997
- ² A. Mešanović: Accreditation – instrument for acquisition of confidence in the other activities to conformity assessment, Glasnik No. 3 – Department for standardization, metrology and patents B&H, 1999
- ³ Mirsad Begić: Quality – New philosophy of business, NIP "Economic newspaper" d.d., Sarajevo, 2001
- ⁴ A. Klobodanović: Importance of laboratory's accreditation, Business newspaper No 1113/1114, Sarajevo, 2003



Letnik / Volume 40 2006

ISSN 1580-2949

MATERIALI IN TEHNOLOGIJE / MATERIALS AND TECHNOLOGY**VSEBINA / CONTENTS
LETNIK / VOLUME 40, 2006/1, 2, 3, 4, 5, 6****2006/1****Inhibition of the pitting corrosion of grey cast iron using carbonate**

Raziskave inhibiranja jamičaste korozije sivih litin z uporabo karbonatne mešanice

A. Kocjan, M. Jenko 3

The characterization of polymer composites by thermogravimetry

Termogravimetrična karakterizacija polimernih kompozitov

I. G. Popović, L. Katsikas 7

The influence of copper on the decarburization and recrystallization of Fe-Si-Al alloys

Vpliv bakra na razogličenje in rekristalizacijo zlitin Fe-Si-Al

D. Steiner Petrovič, M. Jenko, V. Doleček 13

Improving the corrosion resistance of components made from structural steels

Povečanje korozijske odpornosti delov iz konstrukcijskih jekel

P. Jurčič, P. Stolař 17

Evolucija globularne mikrostrukture pri postopku Rheo-light

Evolution of globular microstructure at the Rheo-light process

M. Torkar, M. Godec 23

Poslovanje družb z dejavnostjo proizvodnje kovin v Sloveniji v obdobju od leta 1992 do 2004

Operation of metal producing companies in Slovenia in the period from 1992 to 2004

V. Pirih 27

2006/2**Segregation and oxidation**

Segregacija in oksidacija

H. J. Grabke 39

Small-punch testing of a weld's heat-affected zones

Testiranje lezenja topotno vplivanih področij varja z uporabo majhnega bata

R. Šturm, Y. Li 49

Degradation of VOC'S by a two stage thermal and high frequency DBDC system

Degradiacija VOC z dvostopenjskim termičnim in visokofrekvenčnim DBDC-sistemom

O. G. Godoy-Cabrera, A. Mercado-Cabrera, R. López-Callejas, R. Valencia A., S. R. Barocio, A. E. Muñoz-Castro, R. Peña-Eguiluz, A. de la Piedad-Beneitez 55

Determination of the deformational energy during slab-width rolling on an edger mill

Določanje deformacijske energije pri valjanju slabov na krčilnem ogrodju

F. Vode, A. Jaklič, R. Robič, A. Košir, F. Perko, J. Novak 61

B₂O₃ and CaO in the magnesium oxide from seawaterB₂O₃ in CaO v magnezijevem oksidu iz morske vode

V. Martinac, M. Labor, N. Petric 65

Preparation of NiO/YSZ powders using a pechini-type method

Priprava NiO/YSZ prahov s prilagojeno pechini metodo

T. Razpotnik, V. Francetič, J. Maček 69

Microstructure evaluation of an NRC-processed automotive component

Ocena mikrostrukture avtomobilске komponente, izdelane po postopku NRC

M. Torkar, B. Breskvar, M. Godec, P. Giordano, G. Chiarmetta 73

Properties and microstructure of very pure CrNiV steel

Lastnosti in mikrostruktura zelo čistih jekel CrNi

S. Němeček, P. Motyčka 79

2006/3**Mechanical and corrosion properties of AA8011 sheets and foils**

Mehansko vedenje in korozijske lastnosti trakov in folij AA8011

K. Delijić, V. Asanović, D. Radonjić 83

Flame temperature as a function of the combustion conditions of gaseous fuels	
Temperatura plamena v odvisnosti od pogojev zgorevanja plinastih goriv	
M. Lalovic, Z. Radovic, N. Jaukovic	89
Študij mikrostrukture tiskanih slojev YSZ na podlagi Ni-YSZ	
Microstructure characterisation of screen-printed layers of YSZ on Ni-YSZ substrate	
M. Marinšek, B. Kapun, A. Zupančič Valant, K. Zupan, G. Kapun, J. Maček	93
Supramolekularni poliuretani z azobenzenskimi skupinami	
Supramolecular azobenzene polyurethanes	
G. Ambrožič, M. Žigon	99
Mehanske lastnosti kavčukovih zmesi na osnovi NBR	
Mechanical properties of NBR based compounds	
H. Šubic ml., Z. Šušterič, M. Žumer	107
Influence of micro-alloying on the phase transformations in cast manganese steels	
Vpliv mikrolegiranja na fazne premene vitem manganovem jeklu	
P. Motyčka, J. Drnek, L. Kraus	111
2006/4	
A crack growth analysis in critical structural components	
Analiza rasti razpoke v kritičnih komponentah naprav	
D. Semenski, Ž. Božič, H. Wolf	123
Hot ductility of austenite stainless steel with a solidification structure	
Vroča preoblikovalnost avstenitnega nerjavnega jekla s strjevalno strukturo	
F. Tehovnik, F. Vodopivec, L. Kosec, M. Godec	129
The extraction of raw materials for the cement industry and nature conservation	
Zagotavljanje primernih materialov za cementno industrijo s ciljem ohranjanja narave	
Ž. Pogačnik, M. Stupar	139
Vacuum teaching for undergraduate students at the University of Coimbra	
Učenje vakuuma za študente na Univerzi Coimbra	
J.M.F. dos Santos	145
Isothermal decomposition of the β' phase in Cu-Zn-Al shape-memory alloys	
Izotermska razgradnja β' -faze v zlitinah s spominom Cu-Zn-Al	
V. Asanović, K. Deljić, N. Jauković	153
Estimation of the fatigue threshold values for a crack propagating through a bi-material interface taking into account residual stresses	
Ocena utrujenostnega praga za razpoko, ki napreduje skozi vmesno ploskev med dvema materialoma z upoštevanjem rezidualnih napetosti	
L. Náhlík	157
Karakterizacija kopolimerov SEC in SEC-MALS asparaginske kisline in laktida	
SEC and SEC-MALS characterization of copolymers of aspartic acid and lactide	
M. Gričar, E. Žagar, A. Kržan, M. Žigon	161
2006/5	
Fatigue behaviour of a cast nickel-based superalloy Inconel 792-5A at 700 °C	
Utrjanje lite nikljeve superzlitine Inconel 792-5A pri 700 °C	
M. Petrenec, K. Obrtlík, J. Polák, T. Kruml	175
The application of linear elastic fracture mechanics to optimize the vacuum heat treatment and nitriding of hot-work tool steels	
Uporaba linearne elastomehanike loma pri optimiraju vakuumske toplotne obdelave in nitriranju orodnih jekel za delo v vročem	
V. Leskovšek, B. Šuštaršič, D. Nolan	179
The influence of long-term service exposure on the structure and properties of high-temperature steels and alloys	
Vpliv dolgotrajnega obratovanja pri visokih temperaturah na lastnosti jekel in zlitin, namenjenih uporabi v energetskih napravah	
A. Rybníkov, L. Getsov, G. Pigrova, N. Dashunin, E. Manilova, N. Mozaiskaja	185
The influence of mim and sintering-process parameters on the mechanical properties of 316L SS	
Vpliv procesnih parametrov brizganja in sintranja na mehanske lastnosti nerjavnega jekla 316L	
B. Berginc, Z. Kampuš, B. Šuštaršič	193
Behaviour and optimisation of multi-directional laminate specimens under delamination by bending	
Vedenje in optimizacija večsmernih vzorcev laminatov pri upogibu z delaminacijo	
N. Ouali, A. Ahmed-Benyahia, A. Laksimi, T. Boukharouba	199

LETNO KAZALO – INDEX

The behavior of fatigue-crack growth in shipbuilding steel using the ESACRACK approach Modeliranje rasti utrujenostne razpoke jekla za ladijske pločevine po postopku ESACRACK M. Shehu, P. Huebner, M. Cukalla	207
Ocena odpornosti proti zmrzovanju gradbene keramike na podlagi direktnih in indirektnih metod Frost resistance evaluation of building ceramics by indirect and direct methods T. Kopar, J. Ranogajec, M. Radeka, R. Marinković-Nedučin, V. Ducman	211
2006/6	
Plazemska sterilizacija bakterij s kisikovo plazmo Oxygen plasma sterilization of bacteria D. Vujošević, Z. Vranica, A. Vesel, U. Cvelbar, M. Mozetič, A. Drenik, T. Mozetič, M. Klanjšek-Gunde, N. Hauptman	227
A comparison of experimental results and computations for cracked tubes subjected to internal pressure Primerjava eksperimentalnih rezultatov in izračuna za cevi z razpoko, ki so obremenjeni z notranjo razpoko J. Capelle, I. Dmytrakh, J. Gilgert, Ph. Jodin, G. Pluviniage	233
Fatigue problems of transmission belts: a viscoelastic analysis of the strain-accumulation process Problem utrujanja pogonskih jermenov: viskoelastična analiza procesa akumuliranja deformacije I. Emri, J. Kramar, A. Nikonorov, U. Florjančič, A. Hribar	239
A micro-macro analysis of the tool damage in precision forming Mikro-makroanaliza poškodb orodja za natančno kovanje T. Rodič, J. Korelc, A. Pristovšek	243
The stability of cast alloys and CVD coatings in a simulated biomass-combustion atmosphere Stabilnost zlitin v CVD-prevlek v simulirani atmosferi zgorevanja biomas D. A. Skobir, M. Spiegel	247
Nastanek LaCrO₃ med zgorevalno sintezo LaCrO ₃ formation during combustion synthesis K. Zupan, M. Marinšek, S. Pejovnik, T. Hrobart	253
Dinamične mehanične lastnosti elastomernih kompozitov s polnili nanovelikosti Dynamic mechanical properties of elastomeric composites with nano-scale fillers Z. Šušterič, T. Kos, M. Šuštar	257
Fracture toughness of a high-strength low-alloy steel weldment Žilavost loma zvara visokotrdnega malolegoranega jekla J. Tuma, N. Gubeljak, B. Šuštaršič, B. Bundara	263
Solidification and fracture of an as-cast Ni alloy Strjevanje in prelom lite nikljeve zlitine M. Torkar	269
Laboratory accreditation – confidence in the activities of conformity assessment of products Laboratorijska akreditacija- zaupanje v aktivnost ocene ustreznosti proizvodov A. Klobodanović, M. Oruč	273

MATERIALI IN TEHNOLOGIJE / MATERIALS AND TECHNOLOGY**AVTORSKO KAZALO / AUTHOR INDEX****LETNIK / VOLUME 40, 2006, A–Ž**

A	Hrobat T. 253	Mozetič T. 227
Ahmed-Benyahia A. 199	Huebner P. 207	Muñoz-Castro A. E. 55
Ambrožič G. 99		
Asanović V. 83, 153		
B		N
Barocio S. R. 55	Jaklič A. 61	Náhlík L. 157
Berginc B. 193	Jauković N. 89, 153	Němeček S. 79
Božić Ž. 123	Jenko M. 3, 13	Nikonov A. 239
Boukharouba T. 199	Jodin Ph. 233	Nolan D. 179
Breskvar B. 73	Jurči P. 17	Novak J. 61
Bundara B. 263		
C		O
Capelle J. 233	Kampuš Z. 193	Obrlík K. 175
Chiarmetta G. 73	Kapun B. 93	Oruč M. 273
Cukalla M. 207	Kapun G. 93	Ouali N. 199
Cvelbar U. 227	Katsikas L. 7	
D	Klanjšek-Gunde M. 227	
Dashunin N. 185	Klobodanović A. 273	
Delijić K. 83, 153	Košir A. 61	
Dmytrakh I. 233	Kocijan A. 3	
Doleček V. 13	Kopar T. 211	
Drenik A. 227	Korelc J. 243	
Drnek J. 111	Kos T. 257	
Ducman V. 211	Kosec L. 129	
E	Kržan A. 161	
Emri I. 239	Kramar J. 239	
F	Kraus L. 111	
Florjančič U. 239	Kruml T. 175	
Francetić V. 69		
G	L	R
Getsov L. 185	Labor M. 65	Radeka M. 211
Gilgert J. 233	Laksimi A. 199	Radonjić D. 83
Giordano P. 73	Lalovic M. 89	Radovic Z. 89
Godec M. 23, 73, 129	Leskovšek V. 179	Ranogajec J. 211
Godoy-Cabrera O. G. 55	Li Y. 49	Razpotnik T. 69
Grabke H. J. 39	López-Callejas R. 55	Robič R. 61
Gričar M. 161		Rodič T. 243
Gubeljak N. 263	M	Rybnikov A. 185
H	Maček J. 69, 93	
Hauptman N. 227	Manilova E. 185	
Hribar A. 239	Marinšek M. 93, 253	
	Marinković-Nedučin R. 211	S
	Martinac V. 65	Santos dos J. M. F. 145
	Mercado-Cabrera A. 55	Semenski D. 123
	Motyčka P. 79, 111	Shehu M. 207
	Mozaiskaja N. 185	Skobir D. A. 247
	Mozetič M. 227	Spiegel M. 247
		Steiner Petrovič D. 13

LETNO KAZALO – INDEX

Stolař P. 17
Stupar M. 139

Š

Šturm R. 49
Šuštar M. 257
Šuštaršič B. 179, 193, 263
Šušterič Z. 107, 257
Šubic ml. H. 107

T

Tehovnik F. 129

Torkar M. 23, 73, 269
Tuma J. 263

V

Valencia A. R. 55
Vesel A. 227
Vode F. 61
Vodopivec F. 129
Vranica Z. 227
Vujošević D. 227

W

Wolf H. 123

Z

Zupan K. 93, 253
Zupančič Valant A. 93
Ž
Žagar E. 161
Žigon M. 99, 161
Žumer M. 107

MATERIALI IN TEHNOLOGIJE / MATERIALS AND TECHNOLOGY**VSEBINSKO KAZALO / SUBJECT INDEX****LETNIK / VOLUME 40, 2006****Kovinski materiali – Metallic materials**

Inhibition of the pitting corrosion of grey cast iron using carbonate Raziskave inhibiranja jamičaste korozije sivih litin z uporabo karbonatne mešanice A. Kocijan, M. Jenko	3
The influence of copper on the decarburization and recrystallization of Fe-Si-Al alloys Vpliv bakra na razogljicanje in rekristalizacijo zlitin Fe-Si-Al D. Steiner Petrovič, M. Jenko, V. Doleček	13
Improving the corrosion resistance of components made from structural steels Povečanje korozjske odpornosti delov iz konstrukcijskih jekel P. Jurčič, P. Stolař	17
Evolucija globularne mikrostrukture pri postopku Rheo-light Evolution of globular microstructure at the Rheo-light process M. Torkar, M. Godec	23
Poslovanje družb z dejavnostjo proizvodnje kovin v Sloveniji v obdobju od leta 1992 do 2004 Operation of metal producing companies in Slovenia in the period from 1992 to 2004 V. Pirih	27
Segregation and oxidation Segregacija in oksidacija H. J. Grabke	39
Small-punch testing of a weld's heat-affected zones Testiranje lezenja topotno vplivanih področij vara z uporabo majhnega bata R. Šturm, Y. Li	49
Degradation of VOC'S by a two stage thermal and high frequency DBDC system Degradiacija VOC z dvostopenjskim termičnim in visokofrekvenčnim DBDC-sistemom O. G. Godoy-Cabrera, A. Mercado-Cabrera, R. López-Callejas, R. Valencia A., S. R. Barocio, A. E. Muñoz-Castro, R. Peña-Eguiluz, A. de la Piedad-Beneitez	55
Determination of the deformational energy during slab-width rolling on an edger mill Določanje deformacijske energije pri valjanju slabov na krčilnem ogrodju F. Vode, A. Jaklič, R. Robič, A. Košir, F. Perko, J. Novak	61
Microstructure evaluation of an NRC-processed automotive component Ocena mikrostrukture avtomobilske komponente, izdelane po postopku NRC M. Torkar, B. Breskvar, M. Godec, P. Giordano, G. Chiarmetta	73
Properties and microstructure of very pure CrNiV steel Lastnosti in mikrostruktura zelo čistih jekel CrNi S. Němeček, P. Motyčka	79
Mechanical and corrosion properties of AA8011 sheets and foils Mehansko vedenje in korozjske lastnosti trakov in folij AA8011 K. Delijić, V. Asanović, D. Radonjić	83
Flame temperature as a function of the combustion conditions of gaseous fuels Temperatura plamena v odvisnosti od pogojev zgorevanja plinastih goriv M. Lalovic, Z. Radovic, N. Jaukovic	89
Influence of micro-alloying on the phase transformations in cast manganese steels Vpliv mikrolegiranja na fazne premene vitem manganovem jeklu P. Motyčka, J. Drnek, L. Kraus	111
A crack growth analysis in critical structural components Analiza rasti razpoke v kritičnih komponentah naprav D. Semenski, Ž. Božić, H. Wolf	123
Hot ductility of austenite stainless steel with a solidification structure Vroča preoblikovalnost avstenitnega nerjavnega jekla s strjevalno strukturo F. Tehovnik, F. Vodopivec, L. Kosec, M. Godec	129

LETNO KAZALO – INDEX

Isothermal decomposition of the β' phase in Cu-Zn-Al shape-memory alloys Izotermina razgradnja β' -faze v zlitinah s spominom Cu-Zn-Al V. Asanović, K. Delić, N. Jauković	153
Estimation of the fatigue threshold values for a crack propagating through a bi-material interface taking into account residual stresses Ocena utrujenostnega praga za razpoko, ki napreduje skozi vmesno ploskev med dvema materialoma z upoštevanjem rezidualnih napetosti L. Náhlík	157
Fatigue behaviour of a cast nickel-based superalloy Inconel 792-5A at 700 °C Utrjanje lite nikljeve superzlitine Inconel 792-5A pri 700 °C M. Petrenec, K. Obřtisk, J. Polák, T. Kruml	175
The application of linear elastic fracture mechanics to optimize the vacuum heat treatment and nitriding of hot-work tool steels Uporaba linearne elastomehanike loma pri optimiranju vakuumske topotne obdelave in nitriranju orodnih jekel za delo v vročem V. Leskovšek, B. Šuštaršič, D. Nolan	179
The influence of long-term service exposure on the structure and properties of high-temperature steels and alloys Vpliv dolgotrajnega obratovanja pri visokih temperaturah na lastnosti jekel in zlitin, namenjenih uporabi v energetskih napravah A. Rybníkov, L. Getsov, G. Pigrova, N. Dashunin, E. Manilova, N. Mozaiskaja	185
The influence of mim and sintering-process parameters on the mechanical properties of 316L SS Vpliv procesnih parametrov brizganja in sintranja na mehanske lastnosti nerjavnega jekla 316L B. Berginc, Z. Kampuš, B. Šuštaršič	193
The behavior of fatigue-crack growth in shipbuilding steel using the ESACRACK approach Modeliranje rasti utrujenostne razpoke jekla za ladjske pločevine po postopku ESACRACK M. Shehu, P. Huebner, M. Cukalla	207
A comparison of experimental results and computations for cracked tubes subjected to internal pressure Primerjava eksperimentalnih rezultatov in izračuna za cevi z razpoko, ki so obremenjeni z notranjo razpoko J. Capelle, I. Dmytrakh, J. Gilgert, Ph. Jodin, G. Pluviniage	233
Fatigue problems of transmission belts: a viscoelastic analysis of the strain-accumulation process Problem utrujanja pogonskih jermenov: viskoelastična analiza procesa akumuliranja deformacije I. Emri, J. Kramar, A. Nikonor, U. Florjančič, A. Hribar	239
A micro-macro analysis of the tool damage in precision forming Mikro-makroanaliza poškodb orodja za natančno kovanje T. Rodič, J. Korelc, A. Pristovšek	243
The stability of cast alloys and CVD coatings in a simulated biomass-combustion atmosphere Stabilnost zlitin in CVD-prevlek v simulirani atmosferi zgorevanja biomasa D. A. Skobir, M. Spiegel	247
Fracture toughness of a high-strength low-alloy steel weldment Žilavost loma zvara visokotrdnega malolegoranega jekla J. Tuma, N. Gubeljak, B. Šuštaršič, B. Bundara	263
Solidification and fracture of an as-cast Ni alloy Strjevanje in prelom lite nikljeve zlitine M. Torkar	269
Laboratory's accreditation – confidence in the activities of conformity assessment of products Laboratorijska akreditacija- zaupanje v aktivnost ocene ustreznosti proizvodov A. Klobodanović, M. Oruč	273

Anorganski materiali – Inorganic materials

B₂O₃ and CaO in the magnesium oxide from seawater B ₂ O ₃ in CaO v magnezijevem oksidu iz morske vode V. Martinac, M. Labor, N. Petrić	65
Preparation of NiO/YSZ powders using a pechini-type method Priprava NiO/YSZ prahov s prilagojeno pechini metodo T. Razpotnik, V. Francetič, J. Maček	69
Študij mikrostrukture tiskanih slojev YSZ na podlagi Ni-YSZ Microstructure characterisation of screen-printed layers of YSZ on Ni-YSZ substrate M. Marinšek, B. Kapun, A. Zupančič Valant, K. Zupan, G. Kapun, J. Maček	93

Nastanek LaCrO₃ med zgorevalno sintezo LaCrO ₃ formation during combustion synthesis K. Zupan, M. Marinšek, S. Pejovnik, T. Hrobat	253
---------------------------------------------------------------------------------------------------------------------------------------------------------------------------------	-----

Polimeri – Polymers

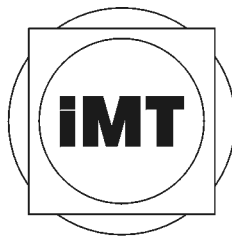
The characterization of polymer composites by thermogravimetry Termogravimetrična karakterizacija polimernih kompozitov I. G. Popović, L. Katsikas	7
Supramolekularni poliuretani z azobenzenskimi skupinami Supramolecular azobenzene polyurethanes G. Ambrožič, M. Žigon	99
Mehanske lastnosti kavčukovih zmesi na osnovi NBR Mechanical properties of NBR based compounds H. Šubic ml., Z. Šušterič, M. Žumer	107
Karakterizacija kopolimerov SEC in SEC-MALS asparaginske kisline in laktida SEC and SEC-MALS characterization of copolymers of aspartic acid and lactide M. Gričar, E. Žagar, A. Kržan, M. Žigon	161
Behaviour and optimisation of multi-directional laminate specimens under delamination by bending Vedenje in optimizacija večsmernih vzorcev laminatov pri upogibu z delaminacijo N. Ouali, A. Ahmed-Benyahia, A. Laksimi, T. Boukharouba	199
Dinamične mehanične lastnosti elastomernih kompozitov s polnili nanovelikosti Dynamic mechanical properties of elastomeric composites with nano-scale fillers Z. Šušterič, T. Kos, M. Šuštar	257

Vakuumska tehnika – Vacuum technique

Vacuum teaching for undergraduate students at the University of Coimbra Učenje vakuuma za študente na Univerzi Coimbra J.M.F. dos Santos	145
Plazemska sterilizacija bakterij s kisikovo plazmo Oxygen plasma sterilization of bacteria D. Vujošević, Z. Vranica, A. Vesel, U. Cvelbar, M. Mozetič, A. Drenik, T. Mozetič, M. Klanjšek-Gunde, N. Hauptman	227

Gradbeni materiali – Materials in civil engineering

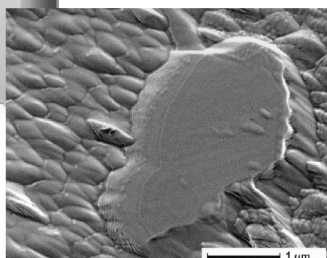
The extraction of raw materials for the cement industry and nature conservation Zagotavljanje primerih materialov za cementno industrijo s ciljem ohranjanja narave Ž. Pogačnik, M. Stupar	139
Ocena odpornosti proti zmrzovanju gradbene keramike na podlagi direktnih in indirektnih metod Frost resistance evaluation of building ceramics by indirect and direct methods T. Kopar, J. Ranogajec, M. Radeka, R. Marinković-Nedučin, V. Ducman	211



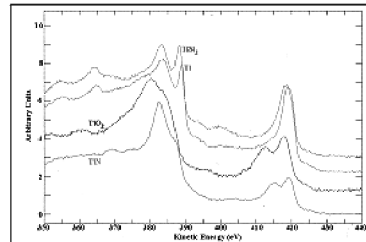
INŠITUT ZA KOVINSKE MATERIALE IN TEHNOLOGIJE



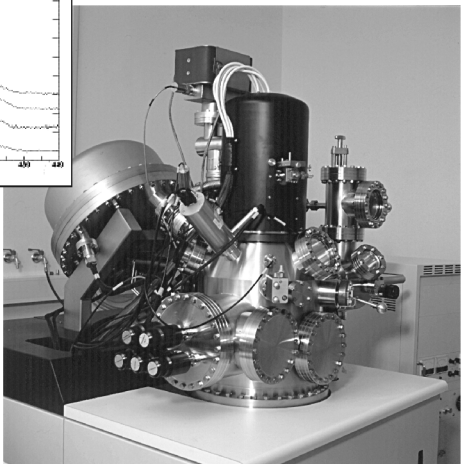
Elektronski mikroskop Jeol JSM-6500F opremljen z ED, WD in EBSD



Zrno kromovega karbida (desno)



AES spekter štirih različnih kemijskih stanj titana (levo)



Elektronski spektrometer Microlab 310-F za HRAES, SAM, SEM in XPS analize površin

Naslov:
IMT, Lepi pot 11,
SI-1000 Ljubljana,
Slovenia
Tel.: +386 1 4701 800,
Faks: +386 1 4701 939
<http://www.imt.si>,
e-pošta: imt@imt.si



Tlačna tehnička RUSKA 2465A za kalibracije merilnikov tlaka



Akreditacijska listina L-030



Vakuumska peč VTTC-324R za topotno obdelavo kovinskih materialov



METAPLAS IONON HZW 600/1000 peč za nitriranje v pulzirajoči plazmi



INŠITUT ZA KOVINSKE MATERIALE IN TEHNOLOGIJE
INSTITUTE OF METALS AND TECHNOLOGY

Lepi pot 11 • POB 431 • 1000 Ljubljana • Slovenia
tel.: +386 1 4701 800 • fax: +386 1 4701 939
www.imt.si • e-mail: imt@imt.si

VACUUM HEAT TREATMENT LABORATORY

Vacuum Brazing

Universally accepted as the most versatile method of joining metals. Vacuum Brazing is a precision metal joining technique suitable for many component configurations in a wide range of materials.

ADVANTAGES

- Flux free process yields clean, high integrity joints
- Reproducible quality
- Components of dissimilar geometry or material type may be joined
- Uniform heating & cooling rates minimise distortion
- Fluxless brazing alloys ensure strong defect free joints
- Bright surface that dispense with expensive post cleaning operations
- Cost effective

Over five years of Vacuum Brazing expertise at **IMT** has created an unrivalled reputation for excellence and quality.

Our experience in value engineering will often lead to the use of Vacuum Brazing as a cost effective solution to modern technical problems in joining.

INDUSTRIES

- | | | |
|---------------|--------------|--------------|
| • Aerospace | • Hydraulics | • Nuclear |
| • Mechanical | • Pneumatics | • Automotive |
| • Electronics | • Marine | |

QUALITY ASSURANCE

Quality is fundamental to the **IMT** philosophy. The choice of process, all processing operations and process control are continuously monitored by **IMT Quality Control Department**.

The high level of quality resulting from this tightly organised activity is recognised by government authorities, industry and International companies.



INŠITUT ZA KOVINSKE MATERIALE IN TEHNOLOGIJE
INSTITUTE OF METALS AND TECHNOLOGY

Lepi pot 11 • POB 431 • 1000 Ljubljana • Slovenia
tel.: +386 1 4701 800 • fax: +386 1 4701 939
www.imt.si • e-mail: imt@imt.si

VACUUM HEAT TREATMENT LABORATORY

Vacuum Heat Treatment

Vacuum Heat Treatment is recognised as a high quality cost effective and ultra clean method for processing a wide range of components and materials currently in use in today's industry. The range of our equipment enables us to heat treat most sizes of load, from small batches to work up to 350 mm diameter, 910 mm high, and weight up to 380 kg.

ADVANTAGES

- Clean, bright surface finish
- Minimal distortion
- Minimal post treatment operations, e.g., grinding or polishing

Five years of continual investment has ensured that **VHTL** maintains its position as market leader in the field of high quality sub-contract metal processing.

We operate the latest generation of IPSEN VTTC furnace capable of processing components up to 350 mm in diameter, which in addition to our high pressure, rapid quenching facilities increases the range of materials suitable for Vacuum Heat Treatment.

TYPICAL APPLICATIONS

- | | |
|-------------------------------------------------------------------------------------------------------------------------------------------------------------------------------------------------------|------------------------------------------------------------------------------------------------------------------------------------------|
| <ul style="list-style-type: none">• Bright Annealing• Bright Stress Relieving• Hardening/Tempering• Brazing/Hardening/Tempering• Solution Treatment | <ul style="list-style-type: none">• Demagnetisation• Degassing• Diffusion Treatments• Sintering |
|-------------------------------------------------------------------------------------------------------------------------------------------------------------------------------------------------------|------------------------------------------------------------------------------------------------------------------------------------------|

QUALITY ASSURANCE

Quality is fundamental to the **IMT** philosophy. The choice of process, all processing operations and process control are continuously monitored by **IMT Quality Control Department**.

The high level of quality resulting from this tightly organised activity is recognised by government authorities, industry and International companies.



Zavod za gradbeništvo Slovenije

Slovenian National Building and Civil Engineering Institute

Dimičeva 12, 1000 Ljubljana, SLOVENIJA, Telefon: + 386 1/280 42 50, Telefaks: + 386 1/280 44 84

Elektronska pošta: info@zag.si, WWW: <http://www.zag.si/>

- temeljne in uporabne raziskave
- preskušanje v akreditiranih laboratorijih (SA, SWEDAC, PTB-DKD), potrjevanje skladnosti in certificiranje gradbenih materialov, proizvodov in izvedenih del
- predkonkurenčni razvoj na področju gradbeništva
- razvoj novih metod preskušanja in meritev
- študije, preiskave, meritve, pregledi in opazovanja,
- ekspertno svetovanje in sodelovanje pri revizijah ter analize stanja: gradbenih objektov, transportnih naprav, prometnic, naravnega in bivalnega okolja
- kalibriranje in overjanje meril, etalonov in referenčnih materialov

Materiali

mineralna veziva in malte

kamen in agregat

beton in betonski izdelki

kovine, korozija in protikorozjska zaščita

keramika in ognjevzdržni materiali

polimeri

asfalti, bitumen in bitumenski proizvodi



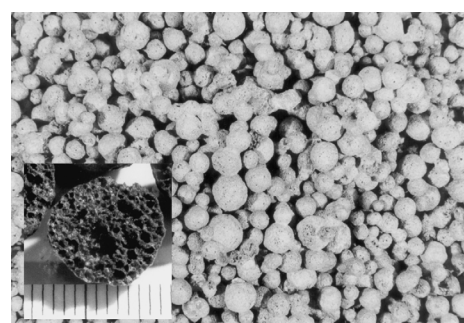
Določitev dinamičnih karakteristik nevezanih materialov s triosnim cikličnim aparatom



Določanje tlačne trdnosti na preizkušancu iz kamna



Mineraloške preiskave naravnih in umetnih nekovinskih materialov



Penjeni stekleni agregat: topotno izolacijski material, izdelan iz odpadnega stekla

Gradbena fizika

akustika

toplota zaščita

požarna preskušanja

požarno inženirstvo

Konstrukcije

stavbe in mostovi

kovinske konstrukcije in transportne naprave

lesene konstrukcije

potresno inženirstvo

dinamika konstrukcij

Geotehnika in prometnice

geomehanika in geotehnika okolja

vzdrževanje in gospodarjenje s cestami

geotehnično opazovanje

inženirska geologija in mehanika hribin

Metrologija



aluminijска industriја

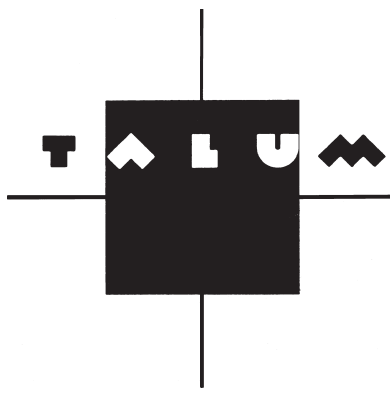
1825-2000

IMPOL d.d.
Partizanska 38
2310 Slovenska Bistrica
SLOVENIJA

tel: +386-2-8453 100
fax:+386-2-8181 219
e-mail: info@impol.si
<http://www.impol.si>

IZDELKI IZ ALUMINIJA: palice in cevi, profili, pločevine, folije





Lahkota prihodnosti

TALUM, d.d., KIDRIČEVO

Tovarniška ulica 10
2325 Kidričeve, Slovenia
Telephone: +386 2 799 51 00
Telefax: +386 2 799 51 03

FIZIKALNA METALURGIJA REŠENE NALOGE

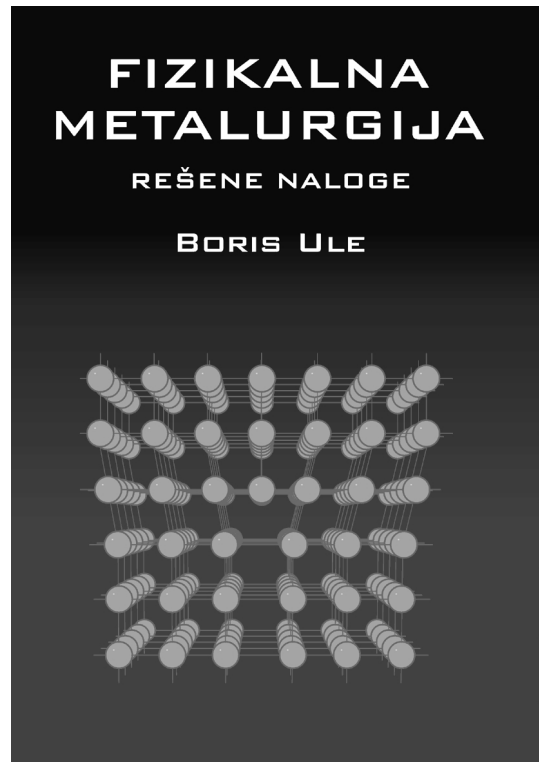
Izdal: Inštitut za kovinske materiale in tehnologije, Ljubljana
Avtor: Boris Ule

NOVO!

PRVA ZBIRKA REŠENIH NALOG IZ FIZIKALNE METALURGIJE

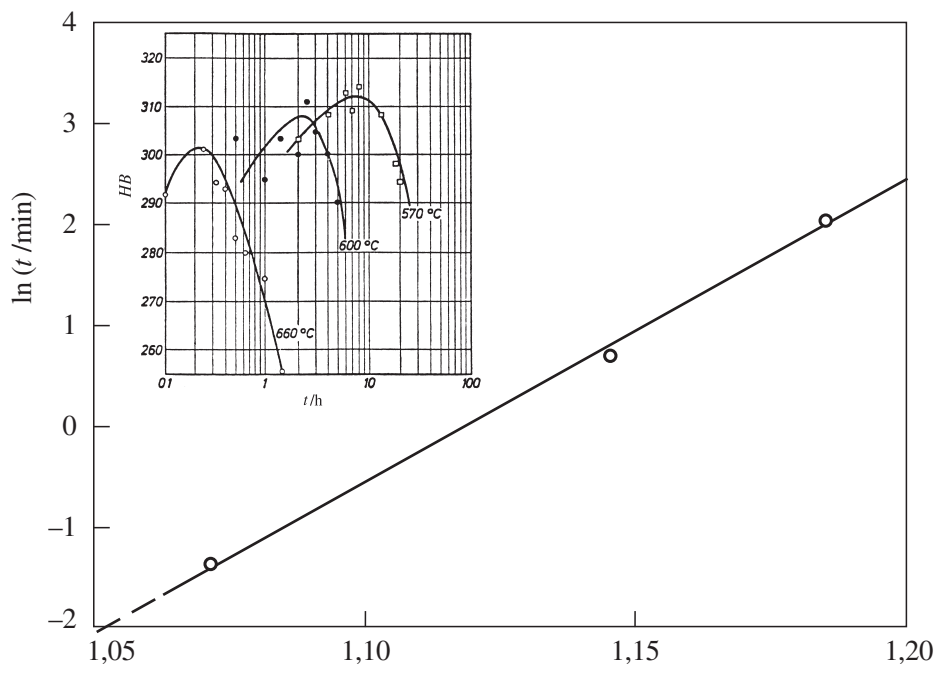
Delo je nekje vmes med zbirko rešenih nalog in učbenikom fizikalne metalurgije. Naloge v knjigi so rešene v vseh podrobnostih, večino rešitev pa uvodoma dopoljuje nekaj teoretične razlage. Pri vsaki nalogi so navedeni vsi potrebeni podatki, da uporabnik pri samostojnem reševanju ne bo potreboval še kakšnih drugih virov. Če pa že, so ti navedeni med tekstrom, nekaj najboljših del s področja fizikalne metalurgije pa je naštetih v popisu literature na koncu knjige.

Pri pripravi knjige je bilo uporabljeno običajno didaktično načelo, po katerem se vsako poglavje prične z lažjimi, konča pa z zahtevnejšimi nalogami. Nekatere izmed nalog so zastavljene kot teoretične, spet drugim pa je avtor skušal pridati še praktično uporabnost. V zbirko so zato vključene tudi naloge, ki so pomembne za vsakdanjo inženirsko prakso. Takšne naloge na primer obravnavajo nekatera vprašanja toplotne obdelave ali pa dobo trajanja obremenjenih kovinskih materialov.



Knjiga vsebuje devet poglavij:

- (1) Kristalna zgradba kovin
- (2) Točkaste napake
- (3) Difuzija
- (4) Strjevanje
- (5) Dislo-kacije
- (6) Mejne površine
- (7) Utrjevanje kovin
- (8) Fazne premene
- (9) Lom, utrujanje in lezenje



Marec 2005

500 strani, 191 nalog, 221 slik in diagramov

ISBN 961-91448-1-3

$10^3 T^{-1} / K^{-1}$

Temeljne informacije o najnovejših tehnologijah in zlitinah

KOVINE IN ZLITINE

kristalna zgradba, mikrostruktura, procesi, sestava in lastnosti

Izdal: Inštitut za kovinske materiale in tehnologije, Ljubljana

Avtor: Franc Vodopivec

PRVA SLOVENSKA ZNANSTVENA MONOGRAFIJA O TEMELJNIH ZNANJIH ZGRADBE KOVIN IN ZLITIN

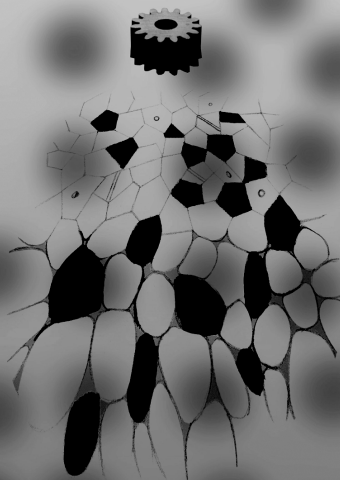
Delo povzema temeljna znanja o zgradbi kovin in zlitin na treh redih velikosti, od atoma in kristalne mreže do lastnosti pri uporabi in povezavi med njihovimi lastnostmi, mikrostrukturo in kemijsko sestavo. Dokumentirano je tudi z izsledki iz slovenskih raziskovalnih ustanov in iz industrije, ki proizvaja ali uporablja kovine in zlitine v Sloveniji.

Knjiga prinaša temeljne informacije o najnovejših tehnologijah in zlitinah, vse do amorfnih in nanokristalnih zlitin.

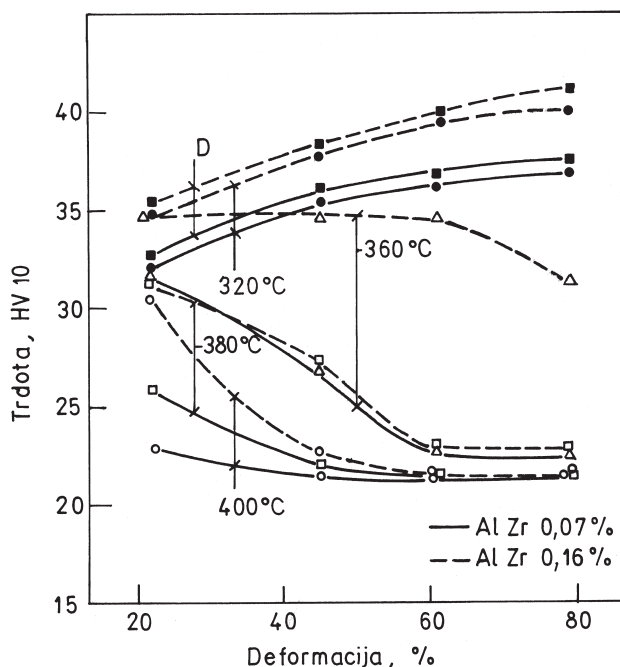
Za pripravo knjige je uporabljen nad 30 monografij in nad 250 člankov iz številnih najbolj kakovostnih inozemskih strokovnih in znanstvenih revij iz let 1980 do 2001. Opremljena je z 271 slikami in diagrami ter 167 analitičnimi odvisnostmi, ki opisujejo ravnotežna stanja in kinetiko procesov. V knjigi je citirano več kot 900 avtorjev, med njimi več kot 100 slovenskih. Vsebuje avtorsko in vsebinsko kazalo. Knjiga bo dosegljiva tudi na CD plošču.

KOVINE IN ZLITINE

kristalna zgradba, mikrostruktura, procesi, sestava in lastnosti



Franc Vodopivec



September 2002,
474 str., 271 slik, diagramov
ISBN 961-238-084-8

VSEBINA

Kristalna zgradba in procesi

Kristalna mreža • točkaste in linijske napake • deformacija, utrjevanje in sproščanje, deformacijske energije • termično aktivirana plastična deformacija • trdne raztopine, razgradnja in utrjevanje • kristalizacija taline • fazne premene • difuzija v trdnem • utrujenost • prelom • struktura in lastnosti površin • absorpcija in segregacije • električna prevodnost • magnetizem • korozija in pasivnost • površinska in notranja oksidacija.

Mikrostruktura in procesi

Ravnotežni fazni diagrami • strjevanje inženirskeih zlitin; segregacije in homogenizacija • vroča in hladna predelava jekla in aluminijevih zlitin • topotna obdelava jekel in zlitin • utrjevanje površine s termokemičnimi in fizikalnimi postopki • kovinski kompoziti • kovinska stekla • mehansko legiranje • nanozlitine • intermetalne spojine.

Sestava in lastnosti kovinskih zlitin

Temeljne značilnosti inženirskeih zlitin • obremenitve pri uporabi • metode karakterizacije • jekla • sive litine • aluminij in zlitine • baker in zlitine • titan in zlitine • magnezij in zlitine • cink, kositer in svinec ter zlitine • nikelj in kobalt ter zlitine • kovine in zlitine z visokim tališčem • plemenite kovine in zlitine • mehko in trdomagnetne zlitine • zlitine za električne upore in kontakte • cermeti in trde kovine • biokompatibilne zlitine.

NAVODILA AVTORJEM

BESEDILO ČLANKA (ROKOPIS IN ELEKTRONSKA OBLIKA)

Glavnemu uredniku je treba predložiti dve kopiji rokopisa članka, skupaj s povzetkom, ključnimi besedami in z ilustracijami. Prispevki morajo biti napisani v slovenskem ali angleškem jeziku; izvlečki, ključne besede, podpisi k slikam in naslovi tabel pa v obeh jezikih.

Glavni urednik bo poskrbel za strokovno oceno članka. Avtorji imajo pravico navesti imena (naslove in telefonske številke) treh ali štirih oseb, ki so usposobljene strokovno oceniti njihov prispevek. Izbrani recenzent ni nujno, da je iz predloženega seznama avtorja. Nepopolni podatki o predloženih recenzentih lahko upočasnijo objavo rokopisa. Rokopis bo vrnjen avtorju skupaj s pripombami recenzenta.

Če je članek sprejet (po recenzentovem in lektorjevem pregledu), avtor vrne popravljen članek uredništvu (izpis na papirju, elektronska oblika, originalne slike) v enem od bolj razširjenih urejevalnikov besedil: Word for Windows ali Word Perfect. Če avtor uporablja kakšen drug urejevalnik, naj ga posname ali konvertira končni izdelek v navaden ASCII-format.

Priprava rokopisa

- Besedilo naj bo napisano na listih A4 z dvojnim presledkom med vrsticami, ob levi strani s 3 cm širokim robom (da je mogoče vnašati popravke lektorjev) na oštevilčenih straneh.
- Formule so lahko v datoteki samo naznačene, na izpisu pa ročno izpisane.
- Članek v elektronski obliki lahko avtor posreduje tudi po e-pošti: mit@imt.si.

Opomba: V vseh primerih si izdajatelj pridržuje pravico odločanja, ali bo članek sprejet za objavo ali ne.

Avtor prevzema vso odgovornost za svoj prispevek. Predloženi prispevek ne sme biti v postopku za objavo v kaki drugi publikaciji in avtor ne sme kršiti pravic kopiranja. Ko je prispevek sprejet za objavo, preidejo avtorske pravice kopiranja na izdajatelja. Ta prenos avtorskih pravic na izdajatelja zagotavlja najširše reproduciranje.

Celoten rokopis članka obsega:

- naslov članka (v slovenskem in angleškem jeziku)
- podatke o avtorjih
- izvleček (v slovenskem in angleškem jeziku)
- ključne besede (v slovenskem in angleškem jeziku)
- besedilo članka (v slovenskem ali angleškem jeziku)
- preglednice, tabele (glava tabele v slovenskem in angleškem jeziku)
- slike (risbe, fotografije)
- podnapise k slikam (v slovenskem in angleškem jeziku)
- pregled literature (v angleškem jeziku)

Članek naj bi bil čim krajši in naj ne bi presegal 4–6 tiskanih strani, pregledni članek 12 tiskanih strani, prispevek s posvetovanj pa 2–4 tiskane strani.

Prva stran članka

Naslov članka naj bo natančen toda tudi informativen ter ne sme presegati ene vrstice teksta. Besede iz naslova naj bodo primerne za indeksiranje in iskanje.

Sledijo podatki o avtorju(-jih), imenu in naslovu institucije oz. laboratorija, kjer je delo nastalo.

Podatki o avtorju: ime (celo ime, ne samo začetnica), priimek, akademski naslov in poklic, e-pošta, faks.

Izvleček

Članek mora vsebovati izvleček, ki naj vsebuje bistveno in kratko vsebino, skelepe članka ter opozorilo na kakršnokoli novo informacijo, ki je predstavljena v članku. Izvleček mora biti razumljiv kot samostojna oblika. Napisan naj bo v preteklem času, ker se nanaša na delo, ki je bilo že opravljeno. Sklicevanje na formule, enačbe in vire literature v tekstu ni dovoljeno. Izogibati se je treba manj znamenitih izrazom, kraticam in okrajšavam.

Dolžina izvlečka naj bi bila do 250 besed.

Ključne besede

Avtor določi do šest ključnih besed po lastni presoji, s katerimi natančno določi vsebino članka in ki so primerne za indeksiranje in iskanje.

Merske enote, enačbe

Obvezna je raba merskih enot, ki jih določa Odredba o merskih enotah (Ur. L. RS št. 26/01), tj. enot mednarodnega sistema SI. Uporaba in pisava morata biti po tej odredbi skladni s standardi SIST ISO 2955, serije SIST ISO 31 in SIST ISO 1000.

Enačbe se označujejo ob desni strani besedila s tekočo številko v okroglih oklepajih.

Preglednice (tabele)

Preglednice (tabele) naj bodo napisane na ločenih listih in ne med besedilom, označene s primerno glavo tabele.

V preglednicah in diagramih se ne uporabljajo izpisana imena veličin, ampak ustrezni simboli v skladu z ISO 31. (Glavne smernice so v prispevku P. Glavič, *Mednarodni standardi – veličine in enote, Materiali in tehnologije*, 37 (2003) 1–2, 79–84.)

Preglednice (tabele) morajo biti jasno citirane v besedilu z arabskimi številkami.

Preglednica (tabela) mora imeti naslov (v slovenskem in angleškem jeziku), da je njen pomen razumljiv tudi brez citiranja v besedilu.

Ilustracije

Ilustracije (risbe, diagrami, fotografije) morajo biti oštevilčene, priložene posebej in ne vstavljenе (ali nalepljene) med besedilom.

Diagrami in fotografije morajo biti izdelani od 1,5- do 3-krat večji od velikosti tiskanega diagrama in morajo biti natančno označeni. Navadno so tiskani v širini enega stolca (7,9 cm), razen v posebnih primerih (maks. širina ≈16 cm). Neprimerena velikost črk na diagramu omogoča pomanjšavo le do optimalne čitljivosti. Črkovne oznake na diagramu naj bodo take velikosti, da je po pomanjšavi velikost številk in (velikih) črk od 1,2 mm do 2,4 mm. Pogosto so črte na diagramih pretanke v primerjavi s celotnim diagramom.

Za vse slike po fotografskih posnetkih je treba priložiti izvirne fotografije, ki so ostre, kontrastne in primereno velike. Pomembno je, da fotografije niso že skenirane. Če je treba, naj bo označeno na hrbtni strani slik, kje je njihov zgornji rob. Priporočljivo je primereno pomanjšanje slike, če ni jasno, kateri njen detajl je pomemben.

Diagrami in slike naj bodo narisani in posneti v formatih BMP, TIF, JPG. Za risanje naj bo po možnosti uporabljen program CorelDraw.

Vsi podpisi k slikam (v slovenskem in angleškem jeziku) naj bodo zbrani na ločenem listu in ne med besedilom.

Izdajatelj zahteva kvalitetne slike, ki omogočajo tudi kvalitetno tiskanje. Izdajatelj praviloma ne sprejema kopij slik in diagramov.

Ilustracije so lahko tiskane barvno, če uredništvo presodi, da je to bistvenega pomena pri objavi. Izdajatelj in avtor nosita vsak del dodatnih stroškov. Nadaljnje informacije o barvnih ilustracijah in stroških avtorjev so dosegljive pri izdajatelju.

Na avtorjevo željo uredništvo vrne diagrame in slike, ko je članek objavljen.

Literatura

Literurni viri so zbrani na koncu članka in so oštevilčeni po vrstnem redu, kakor se pojavitjo v članku.

Vsek vir mora biti opremljen s podatki, ki omogočajo bralcu, da ga lahko poišče.

Vsek literturni vir mora biti popoln, in tako okrajšave ibid., idem., et al., etc., niso dovoljene.

Literurni viri, ki se nanašajo na še neobjavljena ali nesprejeta dela, naj se ne citirajo. Avtorjem pripomočamo, da ne navajajo večjega števila samocitatov.

Bibliografske navedbe naj bodo dosledno pripravljene v angleškem jeziku.

Knjige, periodične publikacije, deli knjig, članki v periodičnih publikacijah, patenti, elektronske monografije, članki in drugi prispevki v elektronski obliki morajo biti citirani kot npr.:

1. Monografije

Zgled: H. Ibach, H. Luth, Solid state physics, 2nd ed., Springer, Berlin 1991, 245

2. Članki v periodičnih publikacijah

Zgled: H. J. Grabke, Kovine zlitine tehnologije, 27 (1993), 1–2, 9

3. Periodične publikacije

Zgled: Kovine zlitine tehnologije. IMT Ljubljana, 1992–1999. Ljubljana: IMT, 1998. Text in Slovene and English. ISSN 1318-0010

4. Prispevki v zbornikih posvetovanj

Zgled: I. Rak, M. Kocak, V. Gliha, N. Gubeljak: Fracture behaviour of over-matched high strength steel welds containing soft root layers, Proc. of the 2nd Inter. Symp. on Mis-Matching of Interfaces and Welds, Reinsford, 1997, 627–641

5. Članki in drugi prispevki v elektronski obliki

Zgled: M. P. Wnuk: Principles of fracture mechanics for space applications. Kovine zlitine tehnologije [online]. 34, 1999, 6, 505–508 [cited 2000-01-30]. Available from World Wide Web:
<http://www.imt.si/materiali-tehnologije/>

AVTORSKI PREGLED ČLANKA

Avtorji prejmejo tiskan članek v avtorski pregled. Uredništvu ga morajo vrniti v dveh dneh, sicer si uredništvo pridržuje pravico, da objavi članek brez avtorskega pregleda.

SEPARATI

Avtorji prejmejo brezplačno 20 izvodov separatov objavljenega članka. Dodatne izvode lahko avtor naroči po ceniku, ki ga dobí v uredništvu.

AVTORSKE PRAVICE

Avtor mora predložiti izjavo, da je besedilo njegovo izvirno delo in ni bilo v taki obliki še nikoli objavljeno. Predloženi prispevek ne sme biti v postopku za objavo v kaki drugi publikaciji. Deli člankov so lahko že bili predstavljeni kot referati. Z objavo preidejo avtorske pravice na izdajatelja. Pri morebitnih kasnejših objavah, mora biti periodična publikacija Materiali in tehnologije navedena kot vir.

Uredništvo periodične publikacije Materiali in tehnologije:

- odloča o sprejemu člankov za objavo
- poskrbi za strokovne ocene in morebitne predloge za krašjanje ali izpopolnitve prispevka
- poskrbi za jezikovne popravke

Rokopisi člankov ostanejo v arhivu uredništva periodične publikacije Materiali in tehnologije.

DODATEK: ZGLED ZA UVELJAVLJEN NAČIN PISANJA ČLANKA

NASLOV ČLANKA

Pravilen in dober *naslov* članka vsebuje kar najmanj možnih besed, ki najbolj ustrezeno opišejo vsebino prispevka.

Naslov mora

- biti natančen in ne sme presegati ene vrstice teksta.

Naslova ne smemo

- pričenjati z nepotrebnimi oz. odvečnimi besedami, kot so "Študij" ali "Preiskava"
- oblikovati v vprašalni obliki.

IZVLEČEK

Izvleček naj bo skrajšana oblika članka, dolžina ne sme presegati 250 besed.

Napisan naj bo v preteklem času, ker se nanaša na delo, ki je bilo že opravljeno.

Izvleček mora

- opisati glavni predmet in cilj preiskave
- povzeti rezultate
- oblikovati glavne sklepe

Izvleček ne sme

- posredovati informacije ali sklepov, ki niso del članka
- citirati literature

1 UVOD

Namen pisanja *uvoda* je podati zadosti predhodnih informacij, da bi bralec članka lahko pravilno razumel in ocenil rezultate študije. Kratko in jasno naj bo podan namen pisanja prispevka.

Uvod naj bo napisan v sedanjem času, ker se nanaša na problem in osvojeno znanje problema na začetku preiskave.

Uvod mora

- jasno opisati naravo in obseg problema, ki ga raziskuje avtor
- podati pregled najnovejše literature, da bi pravilno usmeril bralca
- podati uporabljeno metodo preiskave, in če je treba tudi razloge za izbor določene metode

2 EKSPERIMENTALNI DEL

Eksperimentalni del prispevka mora podati vse podrobnosti eksperimentalnih naprav in metod, ki so bile uporabljeni, da je avtor dosegel navedene rezultate.

Napisan naj bo v preteklem času, pasivna oblika.

Eksperimentalni del mora

- vsebovati podrobnosti, ki se nanašajo na opremo in uporabljene materiale, njihovo količino, temperature, čase itd.
- zagotoviti zadostno informacijo, ki bo omogočala raziskovalcu istega znanstvenega področja, da preizkus lahko ponovi.

Eksperimentalni del ne sme

- navajati nobenih doseženih rezultatov preiskave.

3 REZULTATI

Ta del mora podati celotno sliko vseh preizkusov, ne da bi se ponavljale posamezne podrobnosti iz eksperimentalnega dela. Podatki morajo biti jasni in natančni. Avtor lahko uporabi diagrame in tabele, če je to potrebno.

Ta del naj bo napisan v preteklem času.

Rezultati ne smejo

- opisovati in navajati eksperimentalnih metod
- vsebovati diskusije o doseženih rezultatih (Zaradi narave nekaterih člankov je možno združiti rezultate in diskusijo v eno poglavje, da bi bil članek bralcu bolj jasan in lažje razumljiv.)
- vsebovati rezultatov ali podatkov, ki niso del diskusije.

4 DISKUSIJA

Namen *diskusije* je podati načela, odnose in pospol-ševanja, ki so bili prikazani v *rezultatih*.

Diskusija mora razjasniti pomen rezultatov in primerjati sedanja dognanja s prej objavljenimi deli.

Diskusija naj bo napisana v sedanjem ali preteklem času.

Diskusija mora

- razložiti rezultate in jih ne sme samo ponoviti

Diskusija se ne sme

- izogibati komentiranju rezultatov, ki niso povsem ustrezni.

5 SKLEPI

Sklepi morajo biti kratki. Vsebujejo naj enega ali dva sklepa, povzeta iz rezultatov in *diskusije* rezultatov.

Če je treba, naj bodo sklepi oblikovani po točkah.

Sklepi morajo

- biti natančni in bralcu jasno razumljivi

Sklepi ne smejo

- biti ponovitev rezultatov
- biti enaki izvlečku.

6 LITERATURA

INSTRUCTIONS FOR AUTHORS

SUBMISSION OF PAPERS (MANUSCRIPT + ELECTRONIC TEXT ON DISKETTE)

Two duplicate copies of the original manuscript complete with abstract, key words and illustrations should be submitted to the Editor-in-chief.

All contributions should be written in Slovene or English, with title, abstract, key words and figure captions in both languages. The Editor-in-chief will take care of the review process.

Authors are encouraged to list the names, addresses and telephone numbers of three or four individuals who are qualified to serve as referees for their paper, however, the referees selected by the Editor will not necessarily be from the list suggested by the author. Failure to provide information on several possible referees may delay processing of the manuscript.

The manuscript will be returned to the author together with the notes of the referees.

If the paper is accepted the author will be asked to amend the manuscript in accordance with the referees' comments (for both language and technical content) and return it to the Editorial Board (hard copy plus electronic form with original illustrations) in one of the widely used word-processing programs such as Word for Windows or Word Perfect. If the author wishes to use any other word-processing program the final product should be converted into normal ASCII (text).

Preparation of the manuscript

- Manuscripts should be typed on A4 paper, double-spaced, with 3 cm margins (for corrections) on numbered pages.
- Contributions in electronic form can also be submitted by e-mail: mit@imt.si.

Note: In all cases the Publisher reserves the right to decide whether to accept the paper for publication.

The author should obtain all the necessary authority for publication. Submission of an article implies it is not under consideration for publication elsewhere and that the author is satisfied that no copyright will be infringed. Upon acceptance of an article, the copyright is transferred to the publisher. This transfer will ensure the widest possible dissemination of the article.

Style of manuscript:

- title of the paper (in Slovene and English)
- authors' full names with affiliations
- abstract (in Slovene and English)
- key words (in Slovene and English)
- text of the paper (in Slovene or English)
- tables (table titles in Slovene and English)
- illustrations (drawings or photographs)
- captions to figures (in Slovene and English)
- references (in English)

The paper should be as short as possible and should not exceed 4–6 print pages. Review papers may be up to

12 printed pages, papers presented at conferences should be restricted to 2–4 printed pages.

Title page

Papers should be headed by a concise but informative title which should not exceed one line, words from the title should be suitable for indexing and searching.

The title should be followed by the name(s) of the author(s) and by the name and address of the institution(s) or laboratory(ies) where the work was carried out. Telephone and fax numbers as well as an e-mail address for a contact author should also be supplied.

Abstract

Papers must include an abstract. This summary should present a brief and factual account of the content and conclusions of the paper and an indication of any new information presented in the paper. The abstract should be understandable in isolation. The abstract should be written in the past tense, because it refers to work which was already done. References to formulae, equations and references that appear in the text is not allowed. Uncommon expressions and abbreviations should be avoided.

The length of the abstract should not exceed 250 words.

Key words

The author may supply up to six key words, that describe the content of the article and are suitable for indexing and searching.

Symbols, equations (units of measurement)

Units of measurement should comply with the Law of Units of Measurement and Measures (Official Gazette of the Republic of Slovenia 2001/26) i.e. international SI units. Equations should be marked on the right-hand side of the text with numbers in round brackets.

Tables

Tables should be typed on separate sheets.

Written names of quantities should not be used in tables and diagrams, only the corresponding symbols, according to ISO 2955, series ISO 31 and ISO 1000.

Tables should be clearly referred to in the text using Arabic numerals.

Each table should have a title which makes the general meaning understandable without reference to the text.

Illustrations

Illustrations (drawings, diagrams, photographs) should be numbered and provided separately, not inserted in the text.

The drawings or gloss prints for the line pictures should be 1.5–3 times larger than the printed size of the figures and should contain carefully applied lettering. Figures are reduced to a single-column width (7.9 cm) except in special cases (max. printed size ≈16 cm).

Inappropriately sized lettering on a figure may prevent its reduction to the size optimum for its information content.

The lettering used on a figure should be chosen so that after reduction the height of numbers and capital letters falls within the range (1.2–2.4) mm.

Lines and arrows should also be of sufficient thickness so as to remain clear after the reduction process.

The photographs supplied for reproduction should be original, sharp, with good contrast and of appropriate size. It is important that the photographs supplied are not already screened. When necessary, the top side of a photograph should be marked on the back. A reduction factor should be recommended for a photo when it is not obvious what detail in the photo is of interest.

Diagrams and figures should be drawn and saved in any supported format, e.g. BMP, GIF, JPG. Use Corel Draw if available, since figures can be saved as vector images.

Figure captions (in Slovene and English) should be listed together at the end of the manuscript and not inserted in the text.

The publisher requires a set of good quality drawings and photographs to ensure good quality printing. Photo copies cannot be accepted.

Illustrations can be printed in colour when they are judged by the Editor to be essential to the presentation. The publisher and the author will each bear part of the extra costs involved. Further information concerning colour illustrations and the costs to the author can be obtained from the publisher.

Upon request original drawings and photographs will be returned after publication of the paper.

References

The references should be collected at the end of the article, and numbered in the order of their appearance in the text.

Each reference should be complete, the use of *ibid.*, *idem.*, *et al.*, etc. is not permitted.

References to unpublished or not readily accessible reports should be avoided.

References should be cited in English.

We recommend the authors to avoid self-citing in the references.

In the list of references monographs, articles in journals, journals, contributions to conference proceedings, patent documents, electronic monographs, articles and other electronic documents should be cited in accordance with the following examples:

1. *Monographs*

Example: H. Ibach, H. Luth, Solid State physics, 2nd ed., Springer, Berlin 1991, 245

2. *Articles in journals*

Example: H. J. Grabke, Kovine zlitine tehnologije, 27 (1993), 1–2, 9

3. *Journals*

Example: Kovine zlitine tehnologije, IMT Ljubljana, 1992–1999, Ljubljana, IMT, 1998. Text in Slovene and English. ISSN 1318-0010

4. *Contributions to conference proceedings*

Examples: I. Rak, M. Kocak, V. Gliha, N. Gubeljak: Fracture behaviour of over-matched high strength steel welds containing soft root layers, Proc. of the 2nd Inter. Symp. on Mis-Matching of Interfaces and Welds, Reinsford, 1997, 627–641

5. *Articles and other contributions in electronic form*

Example: M. P. Wnuk: Principles of fracture mechanics for space applications. Kovine zlitine tehnologije [online]. 34, 1999, 6, 505–508 [cited 2000-01-30]. Available from World Wide Web: <http://www.imt.si/materiali-tehnologije>

PROOFS

Authors will receive a set of proofs. They are requested to return the proofs with any corrections within two days. In the case of a delay the Editorial Board reserves the right to publish the article without the author's proofs.

OFFPRINTS

A total of 20 prints of each article will be supplied free of charge to the author(s). Additional offprints can be ordered, prices are available from the Editorial Board.

COPYRIGHT

In addition to the paper, authors must also enclose a written statement that the paper is original work and has not been published in this form anywhere else and that it is not under consideration for publication elsewhere.

Parts of the paper may have been given in the form of reports.

On publication, copyright will pass to the publisher. The Journal of Materials and Technology must be stated as the source in all later publications.

The Editorial Board of the Journal of Materials and Technology:

- decide whether to accept a paper for publication;
- obtain professional reviewers for papers and decide on any proposals to shorten or extend them;
- obtain correct terminology and edit language.

Manuscripts of papers will be kept in the archives of the journal: Materials and Technology.

ADDITION: INSTRUCTIONS FOR AUTHORS

WRITING A TITLE

A good *Title* will have the fewest possible words that adequately describe the contents of the paper.

The *Title* **should**:

- Be concise and not exceed a single line of text.

The *Title* **should not**:

- Begin with the waste words such as "Study of" or "An investigation";
- Be in the form of a question.

PREPARING THE ABSTRACT

The *Abstract* should be viewed as a miniversion of the paper and not exceed 250 words.

The *Abstract* should be written in the past tense, because it refers to work already done.

The *Abstract* **should**:

- State the principal objectives and scope of the investigation;
- Describe the methodology employed;
- Summarize the results;
- State the principal conclusions.

The *Abstract* **should not**:

- Give information or conclusions that are not included in the paper;
- Cite references to the literature.

1 WRITING THE INTRODUCTION

The purpose of the *Introduction* is to supply sufficient background information to allow the reader to understand and evaluate the results of the present study. It should state briefly and clearly the purpose in writing the paper.

Much of the *Introduction* should be written in the present tense, because it relates to the problem and the established knowledge relating to the problem at the start of the work.

The *Introduction* **should**:

- Present as clearly as possible the nature and scope of the problem investigated;
- Review recent literature to orient the reader;
- It should state the method of the investigation, and if necessary the reasons for the choice of a particular method.

2 THE EXPERIMENTAL SECTION

The *Experimental* section of the paper must give full details of the experimental apparatus and the methods used in obtaining the results.

It is recommended that authors use passive language in the past tense.

The *Experimental* section **should**:

- Include accurate details relating to the equipment and materials used, including quantities, temperatures, times etc.
- Provide sufficient information for a colleague in the same field to reproduce the experiment.

The *Experimental* section **should not**:

- Introduce any of the results obtained.

3 WRITING THE RESULTS SECTION

The *Results* section should provide an overall picture of the experiments without repeating any of the details in the Experimental section. The data should be presented clearly and concisely, using graphs and tables where appropriate.

The *Results* section should be written in the past tense, using a mixture of passive and active language.

The *Results* section **should not**:

- Describe any experimental methods;
- Include any discussion of the data obtained (Because of the nature of some papers it may be appropriate to combine the Results and Discussion sections into a single section to improve clarity and make it easier for the reader.);
- Contain results or data which play no part in the Discussion.

4 THE DISCUSSION

The purpose of the *Discussion* is to present the principles, relationships, and generalisations shown by the *Results*.

The *Discussion* must make clear the significance of the *Results* and compare the findings with previously published work.

The *Discussion* should be written using both the present and past tenses. Active and passive language should be used to enhance the readability.

The *Discussion* **should**:

- Discuss the results not simply repeat them.

The *Discussion* **should not**:

- Avoid commenting on results which do not quite fit.

5 THE CONCLUSIONS

The *Conclusion* section should be short. It will present one or more conclusions which have been drawn from the *Results* and the subsequent *Discussion*.

If appropriate, the conclusions should be presented in point form.

The *Conclusions* **should**:

- Be concise and easily understood by the reader.

The *Conclusions* **should not**:

- Be a re-statement of the results;
- Be the same as the *Abstract*.

6 REFERENCES